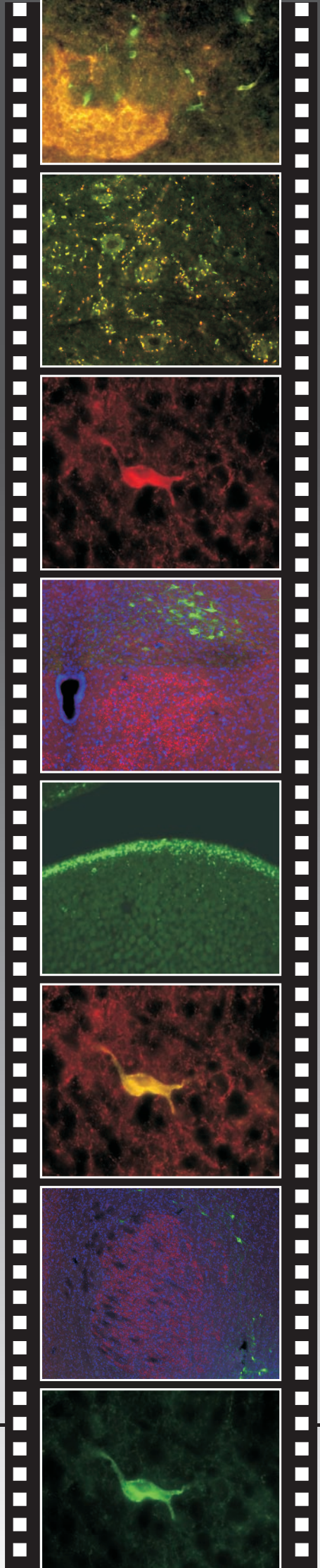

Carla Freire Celedonio Fernandes

Molecular Characterization and Expression of Two New Members of the SLC10 Transporter Family:

SLC10A4 and SLC10A5

Dissertation zur Erlangung des
Doktorgrades der Naturwissenschaften
(Dr. rer. Nat.)
dem Fachbereich Pharmazie der
Philipps-Universität Marburg

édition scientifique
VVB LAUFERSWEILER VERLAG

1. Auflage 2007

1st Edition 2007

VVB LAUFERSWEILER VERLAG
édition scientifique

STAUFENBERGRING 15, D-35396 GIESSEN
Tel: 0641-5599888 Fax: 0641-5599890
email: redaktion@doktorverlag.de

www.doktorverlag.de

Aus dem Institut für Pharmakologie und Toxikologie
der Philipps-Universität Marburg

Betreuer: Prof. Dr. Dr. Joseph Krieglstein

und

dem Institut für Pharmakologie und Toxikologie
der Justus-Liebig-Universität Gießen

Betreuer: Prof. Dr. Ernst Petzinger

Molecular Characterization and Expression of Two New Members of the SLC10 Transporter Family: SLC10A4 and SLC10A5

Dissertation zur
Erlangung des Doktorgrades
der Naturwissenchaften
(Dr. rer. nat.)
dem Fachbereich Pharmazie
der Philipps-Universität Marburg

vorgelegt von

Carla Freire Celedonio Fernandes

Pharmazeutin aus Limoeiro do Norte,
Ceará, Brasilien

Marburg/Lahn 2007

Vom Fachbereich Pharmazie der Philipps-Universität Marburg als Dissertation am 02. November 2007 angenommen.

Erstgutachter: Prof. Dr. Dr. Josef Krieglstein

Zweitgutachter: Prof. Dr. Ernst Petzinger

Tag der mündlichen Prüfung am 14. Dezember 2007

„Denn der Himmel ist der Mensch
und der Mensch ist der Himmel
und alle Menschen ein Himmel
und der Himmel nur ein Mensch.“

Paracelsus

This dissertation is dedicated to my parents Carlos & Ariza, my siblings Carliza & Carlos Júnior, and my husband Cléberson.

Com amor...

ERKLÄRUNG

Ich versichere, dass ich meine Dissertation “ Molecular characterization and expression of two new members of the SLC10 transporter family: SLC10A4 and SLC10A5 „ selbständig ohne unerlaubte Hilfe angefertigt und mich dabei keiner anderen als der von mir ausdrücklich bezeichneten Quellen bedient habe.

Die Dissertation wurde in der jetzigen oder einer ähnlichen Form noch bei keiner anderen Hochschule eingereicht und hat noch keinen sonstigen Prüfungszwecken gedient.

Marburg, den 02 November 2007

Carla Freire Celedonio Fernandes

Contents

Figures

Tables

Abbreviations

%	Per cent
°C	Centigrade
ABC	ATP-Binding-Cassette
ASBT	Apical sodium-dependent bile acid transporter
ATP	Adenosine triphosphate
BLAST	Basic Local Alignment Search Tool
bp	Base pair
BSA	Bovine serum albumin
cDNA	complementary DNA
Chr.	Chromosome
ChAT	Choline acetyl transferase
CHT1	High-affinity choline transporter
C	Cholate
Ci	Curie
cpm	counts per minute
CNS	Central nervous system
cRNA	complementary RNA
Da	Dalton
dATP	Desoxyadenosine triphosphate
dCTP	Desoxycytosine triphosphate
DDBJ	DNA Data Bank of Japan
ddH_2O	Double distilled water
DEPC	Diethylpyrocarbonate
dGTP	Desoxyguanosine triphosphate
DHEAS	Dehydroepiandrosterone sulfate
D-MEM	Dulbecco's Modified Eagle Medium
DNA	Desoxyribonucleic acid
dNTPs	Deoxyribonucleoside triphosphate
dpm	disintegration per minute
dTTP	Desoxythymidine triphosphate
EBI	European Bioinformatics Institute
E. coli	*Escherichia coli*
EDTA	Ethylenediaminetetraacetic acid
EMBL	European Molecular Biology Laboratory
Fig.	Figure
FCS	Fetal calf serum
g	gram
GC	Glycocholate
GCD	Glycodeoxycholate
GCDC	Glycochenodeoxycholate
GUDC	Glycoursodeoxycholate
h	hour
HA	Hemagglutinin
HEK	Human Embryonic Kidney
HEPES	4-(2-hydroxyethyl)-1-piperazineethanesulfonic acid
IPTG	Isopropyl β-D-1-thiogalactopyranoside
IU	International Unit
kb	kilo base
kDa	kilo Dalton
l	Liter
LB	Luria Bertani
LC	Lithocholate

M	Molar (mol/liter)
mA	Milliampere
MCS	Multiple cloning site
MDR	Multidrug-resistance
min	minute
MMLV	Moloney-Murine Leukemia Virus, recombinant
MOPS	3-N(Morpholino) Propane Sulfonic Acid
mRNA	messenger RNA
MRP	Multidrug resistance-associated protein
NT	Neurotransmitter
NTCP	Na^+/taurocholate cotransporting polypeptide
NZY	NZ-amine/yeast extract
OD	Optical density
ORF	Open reading frame
PBS	Phosphate buffered saline
PCR	Polymerase chain reaction
pH	Reverse logarithmic representation of relative hydrogen proton (H^+) concentration
PREGS	Pregnenolone sulfate
RNA	Ribonucleic acid
rpm	rotations per minute
RT	Room temperature
RT-PCR	Reverse transcriptase–PCR
s	second
SDS	Sodium dodecyl sulfate
SLC10	Solute Carrier Family 10
SSC	Sodium chloride – sodium citrat solution
SOAT	Sodium-dependent organic anion transporter
Tab.	Table
TAE	Tris-acetate-EDTA buffer
TBE	Tris-Borate-EDTA buffer
TCD	Taurodeoxycholate
TCDC	Taurochenodeoxycholate
TUDC	Tauroursodeoxycholate
TE	Tris-EDTA buffer
TEMED	N,N,N',N'-Tetramethylethylendiamine
T_m	melting temperature of a primer
TMD	Transmembrane domain
Tris	Trishydroxymethylaminomethane
Triton X-100	Octyl phenol ethoxylate
U	Unit
UV	Ultraviolet
V	Volt
VAChT	Vesicular acetylcholine transporter
X-Gal	5-bromo-4-chloro-3-indolyl- beta-D-galactopyranoside
X. laevis	*Xenopus laevis*

RNA Codon Table

.

1st base		2nd base				3rd base
		U	C	A	G	
	U	UUU Phe F	UCU Ser S	UAU Tyr Y	UGU Cys C	U
		UUC Phe F	UCC Ser S	UAC Tyr Y	UGC Cys C	C
		UUA Leu L	UCA Ser S	UAA Stop	UGA Stop	A
		UUG Leu L	UCG Ser S	UAG Stop	UGG Trp W	G
	C	CUU Leu L	CCU Pro P	CAU His H	CGU Arg R	U
		CUC Leu L	CCC Pro P	CAC His H	CGC Arg R	C
		CUA Leu L	CCA Pro P	CAA Gln Q	CGA Arg R	A
		CUG Leu L	CCG Pro P	CAG Gln Q	CGG Arg R	G
	A	AUU Ile I	ACU Thr T	AAU Asn N	AGU Ser S	U
		AUC Ile I	ACC Thr T	AAC Asn N	AGC Ser S	C
		AUA Ile I	ACA Thr T	AAA Lys K	AGA Arg R	A
		AUG Met* M	ACG Thr T	AAG Lys K	AGG Arg R	G
	G	GUU Val V	GCU Ala A	GAU Asp D	GGU Gly G	U
		GUC Val V	GCC Ala A	GAC Asp D	GGC Gly G	C
		GUA Val V	GCA Ala A	GAA Glu E	GGA Gly G	A
		GUG Val V	GCG Ala A	GAG Glu E	GGG Gly G	G

* *AUG: initiation codon.*

Decimal system

Power	Prefix	Short symbol	Power	Prefix	Short symbol
10^{15}	peta	P	10^{-15}	femto	f
10^{12}	tera	T	10^{-12}	pico	p
10^{9}	giga	G	10^{-9}	nano	n
10^{6}	mega	M	10^{-6}	micro	µ
10^{3}	kilo	k	10^{-3}	milli	m
10^{2}	hecto	h	10^{-2}	centi	c

1. Introduction

1.1 Review of the Literature

1.1.1 Principles of Membrane Transport

Cell membranes of eukaryotic organisms basically consist of a bilayer of phospholipids, steroids, carbohydrates, and peripheral and integral proteins. They form a non-static semipermeable structure that serves as physical barrier to separate the intracellular compartment from the extracellular environment. The hydrophobic character of this barrier permits that only small and non-polar molecules, such as gases (O_2, CO_2, NO, NO_2), inhalation anesthetics, or lipophilic steroid hormones and drugs, can cross this barrier by simple diffusion according to their concentration gradient. In contrast, the uptake or efflux of polar or charged substances, such as sugars, amino acids, peptides, inorganic ions, neurotransmitters, metabolites, and hydrophilic drugs, is controlled by specific transport mechanisms mediated by diverse carrier proteins.

1.1.2 Membrane Transport Systems

Transport systems for organic solutes comprise passive transporters, which permit passive movement of molecules across the plasma membrane down its concentration gradient, and active transporters, which use different energy-coupling mechanisms.

Passive transporters include channel proteins that form hydrophilic pores across the membrane to allow the passage of specific solutes, such as inorganic ions and water molecules, and facilitated transporters, which bind the specific solute that will be carried across the membrane. During the transport cycle, carrier proteins undergo conformational changes similar to catalytic enzymes.

Active transporters couple the transport of solutes to the input of energy. It is divided into two classes: ATP-dependent transporters (primary active transporters) and ion-coupled transporters (secondary active transporters). ATP-dependent carriers include the members of the ATP-binding cassette (ABC) transporter family and ion pumps (ATPases). These transporters utilize energy of ATP hydrolysis to translocate specific substrates and also generate and maintain electrochemical ion gradients across cell membranes. Using these electrochemical ion gradients, ion-coupled transporters drive their solutes across the membrane. In general, these carriers are coupled to the cotransport of H^+, Na^+, and Cl^- or to the countertransport of K^+ and OH^-. Many members of the solute carrier family belong to this class of transporters (Hediger et al. 1994, 2004) (Fig.1).

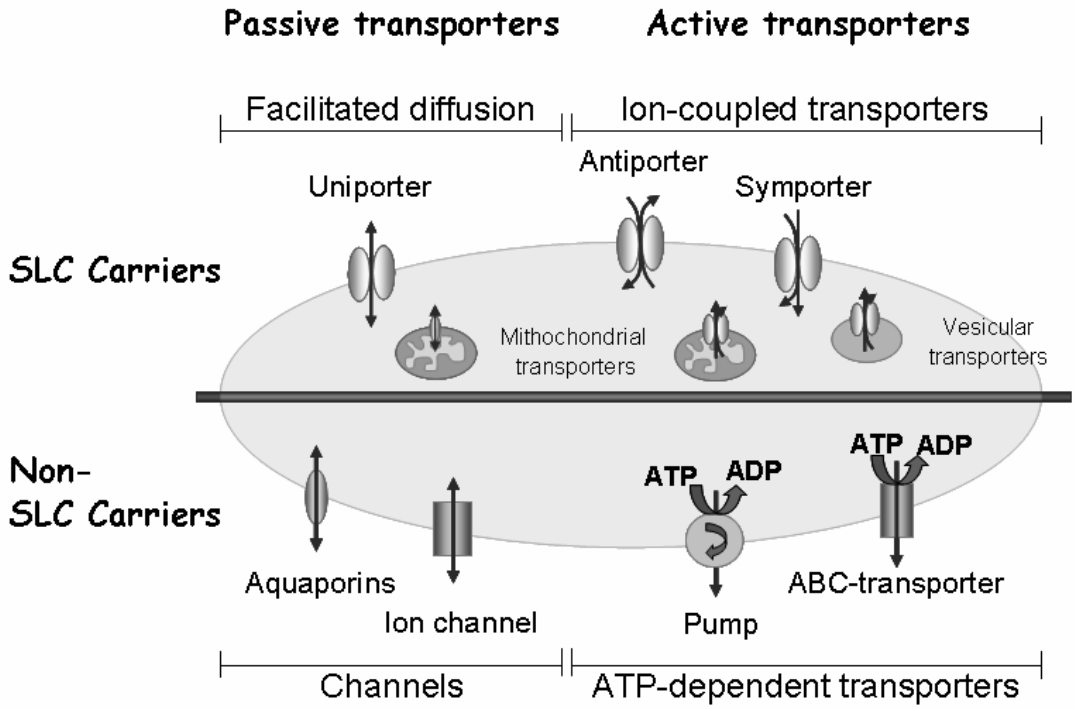

Figure 1: General view of membrane transport systems in a biological cell. Solute Carriers (SLC) and non-SLC transporters are expressed at the plasma membrane or in intracellular compartment membranes. Differences between these transporters concern the necessity of energy input, transport mechanisms, and substrate spectrum. Non-SLC transporters can also be expressed in intracellular compartments. (Modified from Hediger et al. 2004).

1.1.3 The Solute Carrier Superfamily (SLC)

The Human Genome Organization (HUGO) Nomenclature Committee Database classifies all cloned 361 solute carriers genes in 46 families (Hediger et al. 2004) (Tab.1). Around the same number of rat and mouse Slc genes have been identified. This superfamily comprises facilitated transporters, ion-coupled symporters, and antiporters in the plasma membrane and other cellular compartments (Fig. 1). A new carrier has been included in a specific SLC family if it has at least 20-25% amino acid sequence identity to other members of that family. The SLC gene nomenclature is normally elaborated using a numeral after the SLC symbol, the letter A, which divides the numerals, and the number of the individual transporter (e.g., SLC10A4, member 4 of the solute carrier family 10) (Hediger et al. 2004).

A considerable number of human diseases are directly related to SLC transporter gene defects (see chapter 9.4). Alterations in two genes of the electroneutral cation-chloride-coupled cotransporter gene family (SLC12), SLC12A1 and SLC12A3, which transport potassium, sodium, and chloride, result in two types of hypertension: Bartter syndrome and Gitleman's syndrome, respectively (Simon et al. 1996a,b). Mutations in the glucose-6-phosphate carrier (SLC37A4) cause glycogen storage disease (Yang Chou and Mansfield, 1999) and defects in the ferroportin gene (SLC40A1) result in hemochromatosis (Montosi et al. 2001).

As transporters can be employed either as drug targets or as drug delivery systems, some SLC carriers have been used to pharmaceutical objectives. Recently, members of the neurotransmitter transporter family (SLC6) and the bile acid transporter family (SLC10), were established as drug

targets (Kramer et al. 1992; Petzinger et al. 1995; Root et al. 1995; Kramer and Wess 1996; Petzinger et al. 1999; Chen et al. 2004). SLC transporters specifically expressed at the blood-brain barrier have been used as drug delivery system (Hediger et al. 2004).

Table 1: List of solute carrier (SLC) families based on the HUGO databases.

The Solute Carrier Families		Number of Genes
SLC1	The high-affinity glutamate and neutral amino acid transporter family	7
SLC2	The facilitative GLUT transporter family	14
SLC3	The heavy subunits of the heteromeric amino acid transporters	2
SLC4	The bicarbonate transporter family	11
SLC5	The sodium glucose cotransporter family	12
SLC6	The sodium- and chloride-dependent neurotransmitter transporter family	20
SLC7	The cationic amino acid transporter/glycoprotein-associated amino-acid transporter family	14
SLC8	The Na^+/Ca^+ exchanger family	3
SLC9	The Na^+/H^+ exchanger family	11
SLC10	The sodium bile salt cotransport family	7*
SLC11	The proton coupled metal ion transporter family	2
SLC12	The electroneutral cation-Cl cotransporter family	9
SLC13	The human Na^+ -sulfate/carboxylate cotransporter family	5
SLC14	The urea transporter family	2
SLC15	The proton oligopeptide cotransporter family	4
SLC16	The monocarboxylate transporter family	14
SLC17	The vesicular glutamate transporter family	8
SLC18	The vesicular amine transporter family	3
SLC19	The folate/thiamine transporter family	3
SLC20	The type-III Na^+-phosphate cotransporter family	2
SLC21/ SLCO	The organic anion transporting family	20
SLC22	The organic cation/anion/zwitterion transporter family	18
SLC23	The Na^+-dependent ascorbic acid transporter family	4
SLC24	The Na^+-(Ca^{2+}-K^+) exchanger transporter family	6
SLC25	The mitochondrial carrier family	46
SLC26	The multifunctional anion exchanger family	11
SLC27	The fatty acid transporter protein family	6
SLC28	The Na+-coupled nucleoside transport family	3
SLC29	The facilitative nucleoside transporter family	4
SLC30	The zinc efflux family	10
SLC31	The copper transporter family	2
SLC32	The vesicular inhibitory amino acid transporter family	1
SLC33	The acetyl-CoA transporter family	1
SLC34	The type-II Na^+-phosphate cotransporter family	3
SLC35	The nucleoside-sugar transporter family	23
SLC36	The proton-coupled amino-acid transporter family	4
SLC37	The sugar-phosphate/phosphate exchanger family	4
SLC38	The System A and N, sodium-coupled neutral amino acid transporter family	6
SLC39	The metal ion transporter family	14
SLC40	The basolateral iron transporter family	1
SLC41	The MgtE-like magnesium transporter family	3
SLC42	The Rh ammonium transporter family	3
SLC43	The Na+-independent, system-L-like amino acid transporter family	3
SLC44	Choline-like transporter family	5
SLC45	Putative sugar transporter family	4
SLC46	Heme transporter family	3

Modified from Bioparadigms™ (www.bioparadigms.org), originally prepared by the authors of the SLC mini-review series published in *Pflügers Arch – Eur J Physiol (2004) 447:465-812*.

*Based on the results presented in the present study

1.1.4 The Solute Carrier 10 Family

The solute carrier family 10, also known as “sodium bile acid cotransporter family”, comprises two well established carriers, i.e. the Na^+/taurocholate cotransporting polypeptide NTCP (SLC10A1) and the apical sodium-dependent bile acid transporter ASBT (SLC10A2). These carriers are essentially involved in the maintenance of the enterohepatic circulation of bile acids mediating the first step of active bile acid transport through the membrane barriers in the liver (via NTCP) and intestine (via ASBT). Three years ago, four new members of the SLC10 family were identified in our group and referred to as SLC10A3, SLC10A4, SLC10A5, and sodium-dependent organic anion transporter SOAT (SLC10A6) (Geyer et al. 2004; Hagenbuch and Dawson, 2004). Whereas the functional properties of SLC10A3, SLC10A4, and SLC10A5 still remain unclear, SOAT was shown to transport sulfoconjugated steroid hormones and sulfoconjugated bile acids (Geyer et al. 2004, 2007). Recently, an additional member of the the SLC10 family was discovered by us and referred to as SLC10A7 (Godoy et al. 2007). Table 2 gives an overview of the human SLC10 carriers with the respective protein names, tissue expression pattern, substrates, chromosome localization, and GenBank accession numbers.

Table 2: Human members of the SLC10 carrier family

Gene	Protein	Tissue Expression Pattern	Substrate	Gene locus	GenBank Accession
SLC10A1	NTCP	Liver (basolateral membrane) and pancreas (tubuli)	Bile acids, Steroid sulfates	14q24	NM_003049
SLC10A2	ASBT	Ileum (apical membrane), kidney (proximal tubules) and cholangiocytes (apical membrane)	Bile acids	13q33	NM_000452
SLC10A3	P3	Colon, small intestine, ovary, prostate	Unknown	Xq28	NM_019848
SLC10A4	SLC10A4	Brain	Unknown	4p12	NM_152679
SLC10A5	SLC10A5	Fetal brain[§]; liver, kidney	Unknown	8q21	NM_001010893
SLC10A6	SOAT	Testis, placenta, adrenal gland, mammary gland	Steroid sulfates	4q21	NM_197965
SLC10A7	SLC10A7	Heart, kidney, liver, brain, placenta	Unknown	4q31.21	AK075364

[§]: Based on EST data

1.1.4.1 NTCP / Ntcp*

The Na+/taurocholate cotransporting polypeptide, the first member of the SLC10 family, was cloned from rat liver (Hagenbuch et al. 1990, 1991). Subsequently, further orthologs were isolated from human (Hagenbuch and Meier 1994), mouse (Cattori et al. 1999) and rabbit (Kramer et al. 1999). Human NTCP and rat/mouse Ntcps consist of 349 and 362 amino acids, respectively, and show an overall sequence identity of >70%. Additionally, the mouse Ntcp gene encodes a second

*Capital letters devote to the human transporters, whereas lower case names refer to further species.

less abundant splice variant with 317 amino acids and a shorter C-terminal end (Cattori et al. 1999). NTCP/Ntcps are exclusively expressed at the basolateral membrane of hepatocytes (Ananthanarayanan et al. 1994; Stieger et al. 1994; Kullak-Ublick et al. 1997). They mediate sodium-coupled uptake of taurocholate and other bile acids with a Na^+:taurocholate stoichiometry of 2:1 (Hagenbuch and Meier 1996; Weinman 1997). Because more than 80% of hepatic uptake of taurocholate appears in a sodium-dependent manner and Ntcp-specific antisense oligonucleotides blocked the Na^+-dependent taurocholate uptake in rat liver mRNA-injected *Xenopus laevis* oocytes by 95% (Hagenbuch et al. 1996), Ntcp represents the predominant taurocholate uptake systems in hepatocytes (Trauner and Boyer 2003; Kullak-Ublick et al. 2004). More recently, expression of rat Ntcp was also detected in the luminal membrane of pancreatic acinar cells (Kim et al. 2002). Under normal physiological conditions, Ntcp may be involved in the clearance of bile acids that leak to the terminal acini. However, bile acid uptake in the pancreatic acinar cells is associated with cell injury and pancreatic disorders (Kim et al. 2002). NTCP/Ntcp genes are located on chromosomes 14q24, 6q24 and 12 D1 in man, rat and mouse, respectively (Hagenbuch and Meier 1994; Cohn et al. 1995; Green et al. 1998). NTCP/Ntcp expression is regulated by a complex interplay of several ligand-activated receptors (retinoic acid receptor RARα, glucocorticoid receptor) and hepatic transcription factors (hepatocyte nuclear factors HNF1α, HNF3α, and HNF4α and small heterodimer partner SHP1). This regulation is of particular interest under cholestatic conditions, where down regulation of Ntcp contributes to the reduced hepatocellular accumulation of potentially toxic bile acids (Meier and Stieger 2002; Trauner and Boyer 2003; Anwer 2004; Kullak-Ubick et al. 2004).

1.1.4.2 ASBT / Asbt

The apical sodium-dependent bile acid transporter was initially isolated from hamster cDNA library by expression cloning (Wong et al. 1994). Later, human ASBT, as well as the rat Asbt, rabbit Asbt, and mouse Asbt were cloned from the ileum (Wong et al. 1995; Shneider et al. 1995; Kramer et al. 1999; Saeki et al. 1999). These proteins consist of 348 amino acids and show an overall amino acid identity of >80%. Although sequence identity to the hepatic NTCP is relatively low, at 35%, all NTCP/Ntcp and ASBT/Asbt carriers transport conjugated bile acids with high affinity in a sodium-dependent manner (Wong et al. 1994, 1995; Craddock et al. 1998). This transport is electrogenic and shows a 2:1 Na^+: bile acid coupling stoichiometry (Weinman et al. 1998). In contrast to the basolateral localization of Ntcp, Asbt is highly expressed in the apical brush border membrane of enterocytes of the terminal ileum (Shneider et al. 1995). Here, Asbt is associated with 14 kilodalton cytoplasmic ileal lipid-binding protein ILBP, which is the predominant bile acid binder in the cytosol of ileal enterocytes (Stengelin et al. 1996; Kramer et al. 1997, 2001a,b). At lower levels ASBT is also expressed in renal proximal tubules (Craddock et al. 1998). ASBT transports all major species of bile acids. However, it favors trihydroxy- over dihydroxy- bile salts, and conjugated over

unconjugated species. Alterations in the ASBT gene result in primary bile salt malabsorption, a disorder associated with interruption of the enterohepatic circulation of bile salts and fat malabsorption (Oelkers et al. 1997).

Based on observations that reduced bile acid reflux from the intestine is able to increase the expression of hepatic cholesterol 7α-hydroxylase (CYP7A1), the rate-limiting enzyme in the bile acid synthetic pathway (Dietschy et al. 1993; Bjorkhem et al. 1997; Vlahcevic et al. 1999), and that the impairment of ASBT by mutations will increase bile acid synthesis in the liver and thereby lowering plasma cholesterol levels (Oelkers et al. 1997), several specific ASBT inhibitors have been developed as candidates for the treatment of hypercholesterolaemia (Root et al. 1995; Higaki et al. 1998; Ichihashi et al. 1998; West et al. 2002; Li et al. 2004; Tremont et al. 2005) (Fig.2).

1.1.4.3 SLC10A3

Before NTCP and ASBT were discovered, SLC10A3 was isolated from human placenta. This gene is located 40 kb downstream from the human G6PD gene (glucose-6-phosphate dehydrogenase) and has a CpG island in its promoter region (Alcalay and Toniolo 1988). CpG islands are typically associated with housekeeping genes or genes with tissue-specific expression (Gardiner-Garden and Frommer 1987). Further SLC10A3 expression was detected in human T-lymphocytes, HeLa cells, Ca-Ma (human mamary carcinoma cells), PA-1 (human neuroblastoma cells), COS-1 cells and JEG cells (human choriocarcinoma cells) (Alcalay and Toniolo 1988). SLC10A3 is also expressed in murine Melan-a2 melanocytes and its expression is downregulated in BI6FI melanoma cells (Chiu et al. 2007). SLC10A3 comprises two exons, one with 350 bp and the second, which encodes the 477 amino acid P3 protein, with 1806 bp. The P3 protein shows approximately 20% amino acid identity to NTCP and ASBT and, therefore, it was retrospectively classified within the SLC10 family. SLC10A3-related sequences were also detected in the genomes of different animal and yeast species and shown be well conserved during evolution. Because of this aspect and the presence of a CpG island in the SLC10A3 promotor, Alcalay and Toniolo 1988, speculated that SLC10A3 protein may have a housekeeping function. However, still now no functional evidence for SLC10A3 is known.

1.1.4.4 SLC10A4

SLC10A4 represents a recently discovered member with distinctive mRNA expression in the brain (Geyer et al. 2006; Splinter et al. 2006). This high SLC10A4 expression in the brain was totally unexpected, because the two classic representatives of this carrier family are bile acid transporters of hepatic (NTCP) and intestinal (ASBT) origin. Furthermore, SLC10A4 expression was detected in the placenta, pancreas, and cultured cholangiocytes (Splinter et al. 2006). Currently it remains unclear if SLC10A4 is a physiologically relevant solute carrier for the transport of neurosteroids or

other neuroactive molecules, but interestingly, SLC10A4 does not transport bile acids (see chapter 4.1.3) (Geyer et al. 2006, Splinter et al. 2006).

1.1.4.5 SLC10A5

Based on EST sequence data, SLC10A5 is expressed in the fetal brain. SLC10A5/Slc10a5 proteins consist of 434-438 amino acids in man, rat, and mouse and show approximately 34% sequence identity to SLC10A3 (Geyer et al. 2006). No further molecular or functional characterization of SLC10A5 is known. Therefore, apart from SLC10A4 I have analyzed this carrier, too.

1.1.4.6 SOAT / Soat

In 2004, the sodium-dependent organic anion transport was identified and cloned at the Institute of Pharmacology and Toxicology of the Justus Liebig University Giessen. SOAT/Soat genes were isolated from human and rat adrenal gland, and mouse liver (Geyer et al. 2004, 2006, 2007). However, the highest expression of SOAT mRNA in man was detected in testis. Relatively high SOAT expression was also found in placenta and pancreas (Geyer et al. 2007). Further partial orthologue sequences were cloned from dog, cattle, and horse testis (GenBank accession numbers DQ409210, DQ409211, DQ409212, respectively). Human, rat, and mouse SOAT/Soat proteins consist of 377, 370, and 373 amino acids, respectively. SOAT shows 42% sequence identity to ASBT and 33% to NTCP. SOAT exhibits a seven transmembrane domain topology with an outside N-terminal and an inside C-terminal end. It does not transport classical bile acids, such as taurocholate, cholate, and chenodeoxycholate, but it transports the sulfoconjugated bile acid taurolithocholate-3-sulfate in a sodium-dependent manner. Beyond this, SOAT transports sulfoconjugated steroid hormones, such as dehydroepiandrosterone sulfate, estrone-3-sulfate, pregnenolone sulfate, and sulfoconjugated pyrene, indicating that the substrate pattern of SLC10 carriers is not restricted to bile acids. The new carrier SLC10A6 plays an important physiological role in the hormone response of testis and placenta for sulfoconjugated steroid hormones and also in their toxicologic exposure to sulfoconjugated pyrene carcinogens as well as in the placental transport of sulfoconjugated bile acids (Geyer et al. 2007).

1.1.4.7 SLC10A7

SLC10A7 was recently discovered in our group (Godoy et al. 2007). SLC10A7/Slc10a7 mRNAs are broadly expressed in heart, brain, colon, small intestine, lung, liver, testis, and adrenal gland. The SLC10A7 genes comprise 12 coding exons and the encoded proteins consist of 340-343 amino acids in man, rat, mouse, and frog. The SLC10A7 protein showed, in contrast to NTCP, ASBT, and SOAT, a membrane topology of 10 transmembrane domains. A total of six splicing variants were detected for SLC10A7, their physiological relevances, however, remain unclear.

Among the SLC10 family, SLC10A7 proteins have the highest interspecies homology (>94% amino acid sequence identity between mammalian SLC10A7 proteins) and show the closest relationship to bacterial proteins (>20% amino acid sequence identity). Despite detected in the plasma membrane of *Xenopus laevis* oocytes and transfected HEK293 cells, SLC10A7/Slc10a7 proteins revealed no transport activity for bile acids and steroid sulfates (Godoy et al. 2007). Further experiments with the bacterial SLC10A7-related proteins were not performed.

1.1.5 Enterohepatic circulation of bile acids

Splinter et al. (2006) supposed that SLC10A4 is a putative bile acid carrier because of the certain homology to members of the sodium bile acid cotransporter family SLC10. However, in their work the SLC10A4 transport capacity was not demonstrated. Members of the SLC10 family maintain an effective enterohepatic circulation of bile acids. This enterohepatic circulation is an important mechanism to conserve these cholesterol derivatives from the intestine and reduce energy-wasting *de novo* bile acid synthesis in the liver (Fig.2). Two major processes are involved: the secretion of bile acids from the liver and their absorption from the intestine. In the liver, NTCP (SLC10A1) mainly mediates sodium–coupled uptake of physiological bile acids from the portal blood into hepatocytes (Hagenbuch et al. 1991). Carriers of the Organic Anion Transporting Polypeptide (SLCO) carrier family that are also highly expressed at the basolateral membrane of hepatocytes, such as OATP1B1 and OATP1B3 in humans or Oatp1b2 in rats, are also involved in liver uptake of bile acids (König et al. 2000a,b). In contrast to NTCP, these OATP carriers show a sodium-independent transport mechanism. After uptake of bile acids into hepatocytes, bile acids are secreted into the canaliculus via two members of the ATP-binding cassette transporters: the bile acids export pump (BSEP) which carriers monovalent bile acids and multidrug resistance protein (MRP2) that transports divalent sulfated or glucoronidated bile acids (Trauner and Boyer 2003; Arrese and Ananthanarayanan 2004). Under cholestatic conditions, the bile acids are effluxed across the basolateral membrane of hepatocytes via the multidrug resistance proteins (MRP3 and MRP4) in order to protect hepatocytes from the toxic effects of high-dosed bile acids (Soroka et al. 2001; Rius et al. 2003). Through the bile duct, bile acids are delivered to the intestinal lumen and promote the emulsification of dietary lipids and lipid soluble vitamins. Only about 5% of all intestinal bile acids are excreted in the feces. This loss is balanced by hepatic conversion of cholesterol to bile salts, which represents a route for elimination of cholesterol from the body. The majority of bile acids are absorbed from the intestinal lumen via ASBT (SLC10A2) (Wong et al. 1994). Within enterocytes, the bile acids are shuttled to the basolateral compartment by the ileal bile acid binding protein (ILBP), which is normally attached to the cytoplasmatic domain of the ASBT (Kramer et al. 1997, 2001), and their efflux occurs across the Na^+-independent dimeric organic solute transporters (OSTα/OSTβ) (Wang et al. 2001; Seward et al. 2003). Finally, bile acids return to the portal vein finalizing their enterohepatic circulation.

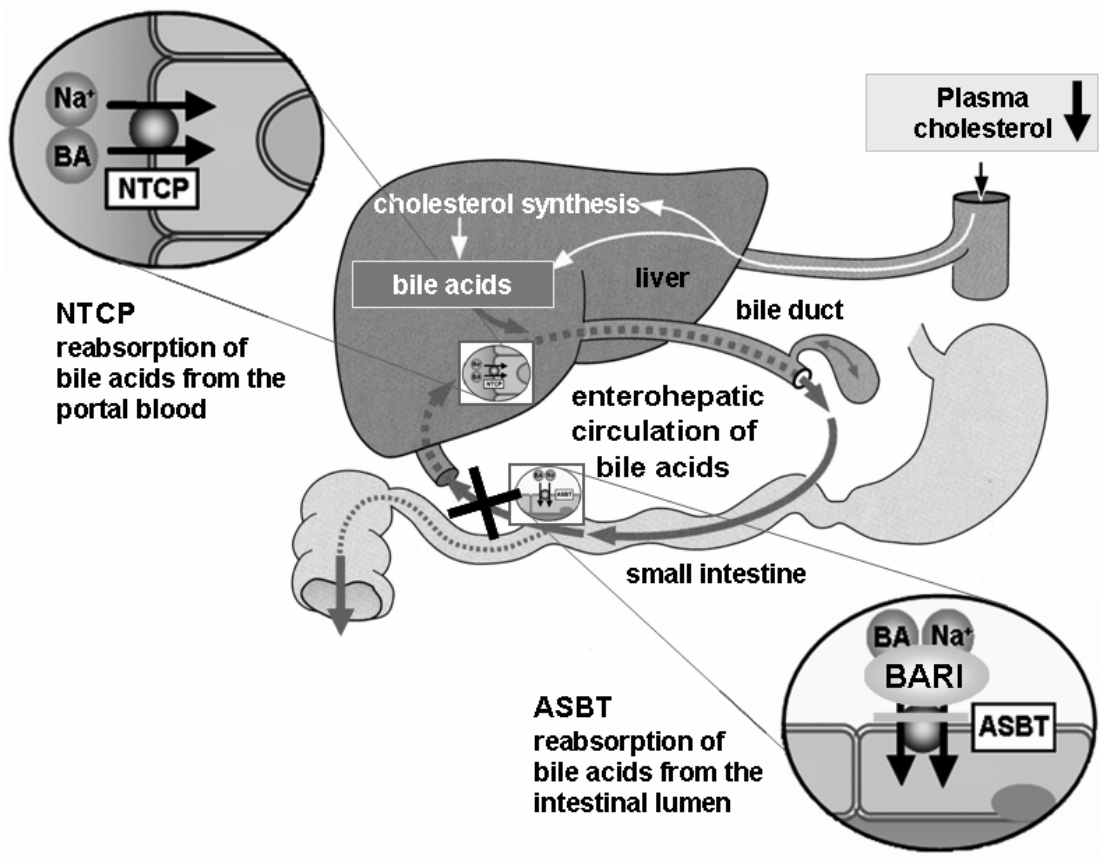

Figure 2: The role of NTCP and ASBT for the maintenance of the enterohepatic circulation of bile acids. Transport proteins are shown as circles. Bile acids are synthesized from cholesterol in the liver and excreted into the bile duct. Intestinal bile acids are efficiently reabsorbed from the terminal ileum by the ASBT and are further extruded into the portal venous circulation. NTCP which is expressed at the basolateral domain of hepatocytes mediates sodium-dependent bile acid reuptake from the portal blood, whereas several hepatic members of the organic anion transporting polypeptide family transport bile acids and also various non-bile acid organic anions in a sodium-independent manner. Bile acid reflow from the intestine is an important regulator of the *de novo* bile acid synthesis in hepatocytes. Several non-systemic inhibitors of the ASBT were developed to block intestinal bile acid reabsorption and interrupt the enterohepatic circulation of bile acids. Several ASBT inhibitors (BARI, bile salt reabsorption inhibitor) are currently tested in clinical trials for cholesterol lowering therapy.

1.1.6 The role of CHT1, VAChT and ChAT in the Cholinergic Synapse

Based on data of the present study, rat Slc10a4 putative carrier is highly expressed in cholinergic neurons of the central nervous system (CNS). In the CNS interneuronal signal transduction *via* synapses often involves the retrieval of the neurotransmitter (NT) from the synaptic cleft and its restorage into presynaptic vesicles (Masson et al. 1999, Gether et al. 2006). NT reuptake across the presynaptic membrane in general represents a sodium-dependent and partially chloride-dependent process mediated by transporter proteins of the solute carrier families SLC1 and SLC6 (e.g. the transporters for dopamine, serotonin, norepinephrine, glutamate, GABA, or glycine)

(Kanai and Hediger 2003; Chen et al. 2004). The high-affinity sodium- and chloride-dependent choline transporter CHT1 (SLC5A7) also belongs to this class of carrier proteins. In cholinergic presynaptic terminals, this protein mediates choline reuptake, which is the rate-limiting step in acetylcholine biosynthesis. CHT1 was initially isolated from *Caenorhabditis elegans* and further orthologs from rat, human, and mouse were cloned (Okuda et al. 2000; Okuda and Haga 2000; Apparsundaram et al. 2000, 2001). The Human CHT1 gene contains 9 exons and is localized on chromosome 2q12. It encodes a protein with 580 amino acids, which exhibits 93% amino acid identity to rat CHT1 and 51% amino acid identity to the respective *C.elegans* protein (cho-1). CHT1 was classified into the SLC5 family (The sodium glucose cotransporter family) based on its amino acid identity with other members of this carrier family. When expressed in *X.laevis* oocytes or COS-7 cells, cho-1 and CHT1 showed K_m values of 2 µM and 1.6 µM for choline transport, respectively. The choline uptake increased with increasing concentrations of choline, Na^+, and Cl^-. Moreover, the CHT1 protein showed to be specifically inhibited by hemicholinium-3 (HC-3) with K_i of 1.3 nM (Okuda and Haga 2000). Expression analyses of rat and human CHT1 mRNA by *in situ* hybridization and northern blot revealed highest expression in the basal forebrain, striatum, brainstem and spinal cord, which are cholinergic regions (Apparsundaram et al. 2000; Okuda et al. 2000; Okuda and Haga 2000). Using a specific antibody against rat CHT1, Misawa et al. (2001) showed high affinity choline transporter-immunoreactive cell bodies in the olfactory tubercle, basal forebrain complex, striatum, mesopontine complex, medial habenula, cranial nerve nuclei, and ventral horn and intermediate zone of spinal cord. Axonal fibers and puncta were visualized in the cerebral cortex, hippocampus, amygdala, striatum, thalamic nuclei, and brainstem. A similar staining pattern was found for CHT1 in the primate central nervous system using a mouse monoclonal antibody raised against a human recombinant CHT1-glutathione-S-transferase fusion protein (Kus et al. 2003).

CHT1 is mainly localized on synaptic vesicles that are also immunopositive for the vesicular acetylcholine transport (VAChT/ SLC18A3) (Ferguson et al. 2003). Only a small fraction of CHT1 is expressed at the plasma membrane. Presynaptic activity-dependent translocation of CHT1 from cytoplasmic pools to the plasma membrane has been suggested to contribute to the regulation of CHT1 capacity (Knnipper et al. 1991; Ferguson et al. 2003; Nakata et al. 2004). Alterations in cholinergic transmission seem to be associated with this CHT1 trafficking (Ferguson et al. 2003; Ferguson and Blakely 2004). Ribeiro et al. (2003) demonstrated that the trafficking of CHT1 between intracellular vesicles and the terminal membrane involves a clathrin-mediated endocytic pathway. Furthermore, CHT1 is a phosphoprotein and its distribution and phosphorylation levels are controlled by neuronal protein kinase C (PKC) and protein phosphatase 1 or 2A (PP1/PP2A) (Gates et al. 2004).

Beyond CHT1, the cholinergic neurotransmission in the central nervous system depends on two other proteins: the choline acetyltransferase (ChAT), which is the enzyme that synthesizes

acetylcholine, and VAChT, which is a proton-dependent transporter that packages acetylcholine synthesized in the cytoplasm into synaptic vesicles. VAChT and ChAT genes are interestingly localized on the same genetic locus, on chromosome 10q11.2. The expression of these two genes has been shown to be co-regulated and together seems to contribute to the normal function of cholinergic transmission (Erickson et al. 1994; Berse and Blusztajn 1995; Berrad et al. 1995). Initially, the UNC-17 gene was isolated from *C.elegans* and was identified as a vesicular acetylcholine transporter. However, no specific acetylcholine transport function was demonstrated (Alfonso et al. 1993). Varoqui et al. (1994) identified a homolog of UNC-17 expressed in the electric organ of the marine ray Torpedo and demonstrated a high affinity binding site for vesamicol, which is a drug that blocks *in vitro* and *in vivo* acetylcholine accumulation in cholinergic synaptic vesicles. Subsequently, the rat and human orthologues were cloned from a PC-12 cell cDNA library and human neuroblastoma cDNA library, respectively (Erickson et al. 1994). The rat VAChT gene encodes a protein with 530 amino acids and twelve putative transmembrane domains with intracellular N- and C-terminals. This protein showed 66% identity to the *C.elegans* and *Torpedo* putative acetylcholine transporters, 94% identity to the human orthologue and 38% identity to members of the vesicular amine transporter family (Slc18). Furthermore, the rat VAChT protein was able to transport acetylcholine, when expressed in a non-neuronal host cell (CV-1) (Erickson et al. 1994). In the rat brain and peripheral nervous system, immunohistochemical analyses using antibodies against the C-terminus of VAChT revealed immunoreactivity exclusively in cholinergic neurons. Its presence in synaptic vesicles was confirmed by electron microscopy (Gilmor et al. 1996; Schäfer et al. 1998a,b). The trafficking of VAChT to these vesicles is apparently mediated by a dileucine motif present in the C-terminus (Colgan et al. 2007). Furthermore, VAChT immunoreactivity was detected in cells that endogenously express this protein, such as in PC12 cells and in primary cultures of spinal motoneurons (Arvidsson et al. 1997). The uptake of acetylcholine mediated by human VAChT-expressing PC-12 cells was ATP-dependent, vesamicol-sensitive, and also dependent on the proton gradient generated by the vesicular H^+-ATPase (Varoqui and Erickson 1996). When expressed in PC12 cells, rat VAChT also showed transport for choline. Bravo et al. (2004) speculated that CHT1 could remove choline from synaptic vesicles, since CHT1 was found in some of the VAChT-containing vesicles. VAChT showed very low substrate selectivity. It is capable to transport diverse small and large organic molecules carrying +1 charge, such as ethidium, tetraphenylphosphonium, N-methylpyridinium-2-aldoxime (Bravo et al. 2005). Although its low selectivity, VAChT appears not to transport its inhibitor vesamicol and monoamine neurotransmitters, although interstingly both compounds carry +1 charge (Clarkson et al. 1993).

Since VAChT (-/-) knockout mice were incompatible with life, new mouse lines with reduced expression of VAChT were recently generated aiming to investigate the role of this protein and acetylcholine in physiological functions and behaviour. It was demonstrated that the decrease of

VAChT expression either affects neurotransmission at the neuromuscular junction or interferes with the brain release of acetylcholine and affects the behaviour of these animals (Prado et al. 2006).

The most characterized protein of the cholinergic synapse, choline acetyltransferase, was purified from the Pacific electric ray *Torpedo californica* (Brandon and Wu 1978), rat (Ryan and McClure 1979), and human (Bruce and Hersh 1989; Oda et al. 1992). Human ChAT cDNA codes for a 748 amino acid polypeptide. This protein is expressed in two different forms: the soluble ChAT form and the membrane bound ChAT form, which is associated with plasma membrane and synaptic vesicles (Benishin et al. 1983). Moreover, ChAT activity is controlled by phosphorylation mediated by protein kinase C (Dobranky et al. 2000, 2001). In CNS, detection of ChAT using several polyclonal and monoclonal antibodies and *in situ* hybridization methods was performed by many laboratories, but generally got converging results. In rat brain, ChAT was visualized in the caudate putamen, nucleus accumbens, olfactory tubercle, islands of Calleja, medial septal nucleus, diagonal band of Broca, basal nucleus of Meynert, amygdala, pedunculopontine tegmental nucleus, all cranial nerve motor nuclei and also in areas, where no VAChT or CHT1 cell bodies were observed: the substantia nigra and the ventral tegmental area (Eckenstein et al. 1982; Armstrong et al. 1983; Martinez-Murilo et al. 1989; Oh et al 1991; Butcher et al. 1992). These studies added to VAChT- and CHT1-mapping, enormously contributed to a better understanding of the organization and distribution of cholinergic neurons in the central and peripheral nervous system, and also to understand the role of these neurons in health and pathologies, such as Alzheimer's disease and Huntington's chorea.

1.2 Aim of the Work

Until 2004, the solute carrier family 10 comprised only two proteins (NTCP and ASBT). Using bioinformatic tools, five new members of the SLC10 family were identified and termed as SLC10A3, SLC10A4, SLC10A5, SLC10A6 (SOAT), and SLC10A7 (Geyer et al. 2004; Hagenbuch et al. 2004; Fernandes et al. 2007, Godoy et al. 2007).

Rat Slc10a4 was cloned at the Institute of Pharmacology and Toxicology in 2004 and deposited under GenBank accession number AY825923. The aim of the present was to characterize the Slc10a4 protein at the molecular and functional level and provide detailed expression analyses in particular in the brain using a newly raised polyclonal rabbit antibody.

In addition the other aim was the cloning of human, mouse, and rat SLC10A5/Slc10a5 as well as their molecular and functional characterization.

2. Material

2.1 Primers and Assays

2.1.1 Primers for sequencing

Target	Denomination	T_m (°C)	Sequence (5'→3')
pBluePolyA	pBluePolyA-R	54.0	GAA AAA TGA CCC TTG AAA GAC
	Oatp2ratF1	57.3	TGA CCA TGA TTA CGC CAA GC
	FLAG-R	54.5	CTT ATC GTC GTC ATC CTT G
pGEM-T	pGEMT-R	55.9	TAC TCA AGC TAT GCA TCC AAC
	Oatp2ratR1	57.3	ATA CGA CTC ACT ATA GGG CG
pcDNA9	CMV-F		CGC AAA TGG GCG GTA GGC GTG
	BGH-R		TAG AAG GCA CAG TCG AGG

2.1.2 Primers for expression profiles (RT-PCR)

Target (Species)	Denomination	T_m (°C)	Sequence (5'→3')
GAPDH	G3PDH-F2	60.3	CAT CAA GAA GGT GGT GAA GCA G
(rat,	G3PDH-F1*	61.4	ACG GGA AGC TCA CTG GCA TG
human,	G3PDH-R3	61.0	CGC CTG CTT CAC CAC CTT C
mouse)	G3PDH-R4*	61.4	CCA CCA CCC TGT TGC TGT AG
SLC10A4	P4-Fn	62.0	CTC TCC AAT CTT ATG TCC CTG
(human)	P4-Rn	62.0	CCT ATG AAT TGC GGT GGA AAG
Slc10a4 *(rat)*	rUP2-GSP-F*	69.5	CTG GTG TTG ATG CCC CTC TGC CTC TG
	rUP2-GSP-R*	69.5	ACG GTG CCA TAG GAG GTG TCT GCC AG
Slc10a4	mP4-F	57.3	CAT GAC CAT TTC CTC CAC AC
(*mouse*)	mP4-R	57.3	TCG CTT GTG CAG TAT CTC AC
SLC10A5	UP7-F	60.3	GGC TAT CTC TTT GCT CTG CTT C
(human)	UP7-R	60.3	GCT AAA TTG GCC TTG GAC TGT G
Slc10a5 *(rat)*	rP5-F*	68.0	AGT GCT GCA GGT GGT GAA TGT G
	rP5-R*	68.0	TAG GTT AGC CAT TCT CAG AAA CAC
Slc10a5 *(mouse)*	mP5-F	57.3	GCT CGT GAA GTT AGA GGA TC
	mP5-R	57.3	AAA GTG ACA TCC CCT TCC AG

* These primers were also used to synthesize cDNA probes for northern blot

2.1.3 TaqMan gene expression assays for quantitative real time PCR (qPCR)

Assay	Species	Gene Symbol	Ref.Seq.	Exon Boundary	Assay Location	Amplicon Lenght
Hs00293728_m1	human	SLC10A4	NM_152679.2	1-2	719	58
Rn02350050_m1	rat	Slc10a4	NM_001008555.1	1-2	587	132
Mm00557788_m1	mouse	Slc10a4	NM_173403.2	1-2	751	67
Hs01049585_s1	human	SLC10A5	NM_001010893.2	1-1	228	121
Rn02585862_s1	rat	Slc10a5	NM_001025280.1	1-1	1266	71
Mm02345249_s1	mouse	Slc10a5	NM_001010834.2	1-1	1277	145
Hs99999903_m1	human	ACTB	NM_001101.2	1-1	36	171
Rn00667869_m1	rat	actb	NM_031144.2	4-5	882	91
Mm00607939_s1	mouse	actb	NM_007393.1	6-6	1230	115

2.1.4 Primers for cloning

Target (Species)	Denomination	T_m (°C)	Sequence (5'→3')
SLC10A5 *(human)*	P5_MGF_SacI	52.0	AGC TGA GCT CAT GAT TAG AAA ACT TTT TAT TG
	P5_MGR_SacI	52.0	TTG TGA GCT CAT TGT TAG ATT AGG AAA TTT C
	P5_MGR_SacII	52.0	GCT GCC GCG GAT TGT TAG ATT AGG AAA TTT C
Slc10a5 *(mouse)*	mP5_MGF_SacII	60.0	TCA CCC GCG GTT GTT TAA ACT TTC AAA ATG TCT G
	mP5_MGF_XbaI	62.0	GAT CTA GAC TGT ACA TTT TAA ACT AGA GGA G
Slc10a5 *(rat)*	rP5_T/A_F	64.0	ATG TCT GGA AAA CTT TTC ATA ATT C
	rP5_T/A_R	60.0	TTA AAC GAG AGG AGC CTT TTC

*The underlined nucleotides represent restriction sites of Sac*I*, Sac*II *and Xba*I*.*

2.1.5 Primers for sequence insertion of the FLAG-epitope

Target (Species)	Denomination	Sequence (5'→3')
Slc10a4 (*Rat)*	P4-FLAG-F	CAC CCA GAC TTC CCT CGA TTA CAA GGA TGA CGA CGA TAA GTG ATC TAG AGA CTG AAG GAG GGT TG
	P4-FLAG-R	CAA CCC TCC TTC AGT CTC TAG ATC ACT TAT CGT CGT CAT CCT TGT AAT CGA GGG AAG TCT GGG TG
SLC10A5 *(Human)*	P5-FLAG-F	GAA AAG AAA TTT CCT AAT CGA TTA CAA GGA TGA CGA CGA TAA GTA ACA ATC CGC GGT GG
	P5-FLAG-R	CCA CCG CGG ATT GTT ACT TAT CGT CGT CAT CCT TGT AAT CGA TTA GGA AAT TTC TTT TC
Slc10a5 *(Rat)*	rP5-FLAG-F	CAG AAA ATG AAA AGG CTC CTC TCG TTG ATT ACA AGG ATG ACG ACG ATA AGT AAA ATC AAG CGG TGG
	rP5-FLAG-R	CCA CCG CGG GAT TTT ACT TAT CGT CGT CAT CCT TGT AAT CAA CGA GAG GAG CCT TTT CAT TTT CTG
Slc10a5 *(Mouse)*	mP5-FLAG-F	GAA AAA ACT CCT CTA GTT GAT TAC AAG GAT GAC GAC GAT AAG TAA AAT GTA CAG TCT AGA GAC
	mP5-FLAG-R	GTC TCT AGA CTG TAC ATT TTA CTT ATC GTC GTC ATC CTT GTA ATC AAC TAG AGG AGT TTT TTC

The underlined nucleotides code for the FLAG-epitope

2.1.6 Primers for sequence insertion of the HA-epitope

Target (Species)	Denomination	Sequence (5'→3')
Slc10a4 *(Rat)*	P4-HA-F	CTC CGA GCA TCG GCT TCT ACC CCT ACG ACG TCC CCG ACT ACG CCA GTC CCG ACT TGA CCC CG
	P4-HA-R	CGG GGT CAA GTC GGG ACT GGC GTA GTC GGG GAC GTC GTA GGG GTA GAA GCC GAT GCT CGG AG

The underlined nucleotides code for the HA-epitope

2.1.7 Primers for subcloning into the pcDNA5/TO vector

Target (Species)	Denomination	Sequence (5'→3')
Slc10a4*(rat)*	P4_FLAG_MGF_*Kpn*I	AGC TGG GTA CCA TGG ACG GCC TGG AC
	P4_FLAG_MGR_*Xho*I	AGT CTC GAG ATC ACT TAT CGT CGT C
SLC10A5 *(human)*	P5_FLAG_MGF_*Kpn*I/2	CAA AAG CTG GTA CCC ATG ATT AGA AAA CTT TTT ATT G
	P5_FLAG_MGR_*Xho*I/2	CCA CCT CGA GTT GTT ACT TAT CGT CGT CAT CC
Slc10a5 *(mouse)*	mP5_FLAG_MGF_*Kpn*I	CCC GCG GTA CCT TAA ACT TTC AAA ATG
	mP5_FLAG_MGR_*Xho*I	AGA CTC GAG ATT TTA CTT ATC GTC GTC

*The underlined nucleotides represent restriction sites of Kpn*I *and Xho*I*, respectively.*

2.1.8 Primers for control of the FLAG- and HA-insertions

Species	Denomination	Sequence (5'→3')
All	K_FLAG_R	CTT ATC GTC GTC ATC CTT G
All	K_HA_R	CGT AGT CGG GGA CGT CGT AG

2.2 Agarose/Formaldehyde Gel Electrophoresis and Northern Blot

2.2.1 Solutions and buffers

DEPC treated water 0.1 %

1 ml Diethylpyrocarbonate (DEPC, 1 mg/ml).
Add 1 l of ddH_2O
Overnight at room temperature and autoclave at 121°C for 20 min.

5 x MOPS Buffer (2 l)

3-[N-morpholino]-2-hydroxypropanesulfonic acid (MOPS)	83.72 g
Sodium Acetat	8.23 g
Add DEPC water and add EDTA	20 ml

Adjust pH to 7.0 with 10 N NaOH, add DEPC water to a final volume of 2 l and autoclave at 121°C for 20 min.

2.2.2 Gel electrophoresis

RNA sample buffer

Deionized formamide	10 ml
37 % formaldehyde	3.5 ml
5 x MOPS buffer	2 ml

Aliquots frozen at –20°C are stable for 6 months

RNA loading buffer 2 x (PeqLab, Erlangen, Germany)

Formamide	95 %
Bromophenol blue	0.025 %
Xylene Cyanol FF	0.025 %
Ethidium bromide	0.025 %
SDS	0.025 %
EDTA	0.5 mM

1 x MOPS Buffer

in DEPC treated water as running buffer

1 % Agarose/ Formaldehyde gel

5 x MOPS buffer	56 ml
Agarose	2.79 g
DEPC Water	174 ml

Mix and cook, cool to 55°C and add

Formaldehyde	50 ml

RNA Ladder High Range (MBI Fermentas, St. Leon-Roth, Germany)

200 bp, 500 bp, 1000 bp, 1500 bp, 2000 bp, 3000 bp, 4000 bp, and 6000 bp

2.2.3 Blotting

20 x SSC (1 l)

NaCl	175.4 g
Sodium Citrate	88.2 g

Dissolve in 800 ml of DEPC water, adjust pH to 7.2 with 10 N NaOH and bring the volume to 1l, dispense into aliquots and autoclave at 121°C for 20 min

20 x SSPE (1 l)

NaCl	175.3 g
NaH_2PO_4 H_2O	27.6 g
EDTA	7.4 g

Dissolve in 800 ml of DEPC water, adjust pH to 7.4 with 10 N NaOH, bring the volume to 1 l and autoclave at 121°C for 20 min

Denhardt' s Reagent, 50x (500 ml)

Ficoll® (Type 400)	5 g
Polyvinylpyrrolidone	5 g
Bovine serum albumin BSA (Fraction V)	5 g

Dissolve in DEPC water and adjust the volume to 500 ml. Sterilize by filtration (0.45 mm) and store at – 20°C

Prehybridization/ Hybridization solution (50 ml)	Deionized Formamide 50 %	25 ml
	SSPE 20 x	6.25 ml
	Denhardt´s Reagent 50 x	1 ml
	SDS 0.1 %	50 mg
	ddH_2O	17.75 ml
Stringency Wash Solution I (SWS I) (600 ml)	SSC 20 x	60 ml
	SDS	600 mg
Stringency Wash Solution II (SWS II) (600 ml)	SSC 20 x	3 ml
	SDS	600 mg
Stripping solution (50 ml)	Deionized Formamide 50 %	25 ml
	SSC 20 x	250 µl
	SDS	50 mg
	at 68°C for 1-2 h	

2.2.4 Other materials

Gel blotting paper Schleicher und Schuell	MAGV, Rabenau-Londorf, Germany
Hybond-N Nylon Membrane	Amersham Biosciences, Freiburg, Germany
Nick Translation Kit®	Amersham Biosciences, Freiburg, Germany
Kodak BioMax MR Film	Sigma-Aldrich, Taufkirchen, Germany

2.3 Cloning, Expression Profiles, cRNA-Synthesis and Insertion of the FLAG and HA epitopes

2.3.1 Bacterial strains

XL1-Blue supercompetent cells (Stratagene, Heidelberg, Germany)
*rec*A1 *end*A1 *gyr*A96 *thi-1 hsd*R17 *sup*E44 *rel*A1 *lac* [F' *pro*AB *lac*I^qZ M15 Tn*10* (Tet^r)]

TOP10 chemically competent cells (Invitrogen, Karlsruhe, Germany)
F^- *mcr*A (*mrr-hsd*RMS-*mcr*BC) ϕ80*lac*Z M15 *lac*X74 *deo*R *rec*A1 *ara*D139 (*ara-leu*)7697 *gal*K *rps*L (Str^R) *end*A1 *nup*G

Electrocompetent *E. coli* cells
F^- *mcr*A (*mrr-hsd*RMS-*mcr*BC) ϕ80*lac*Z M15 *lac*X74 *deo*R *rec*A1 *ara*D139 (*ara-leu*)7697 *gal*K *rps*L (Str^R) *end*A1 *nup*G

2.3.2 Vectors

pGEM-T (Promega, Mannheim, Germany)

3.0 kb, *lac*-Operon, Amp^r, T7-Promotor, SP6-Promotor, MCS (*Apa*I, *Aat*II, *Aph*I, *Nco*I, *Sac*II, *Spe*I, *Not*I, *Pst*I, *Sal*I, *Nde*I, *Sac*I, *Bst*XI, *Nsi*I).

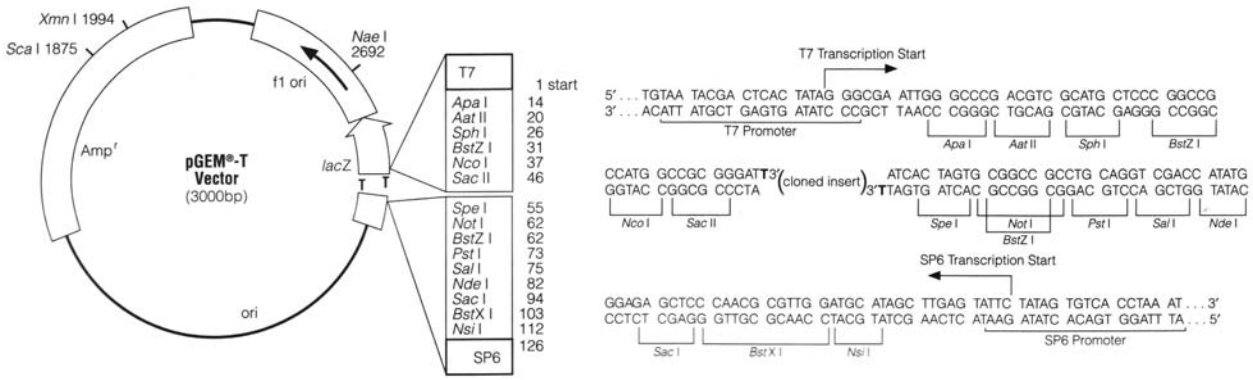

pBluescript SK(+/-) (Stratagene, Heidelberg, Germany)

2.96 kb, LacZ, Amp^r, T3-Promotor, T7-Promotor, f1 origin, MCS (*Sac*I, *Bst*XI, *Sac*II, *Not*I, *Eag*I, *Xba*I, *Spe*I, *Bam*HI, *Sma*I, *Pst*I, *Eco*RI, *Xho*I, *Apa*I, *Dra*I, *Kpn*I).

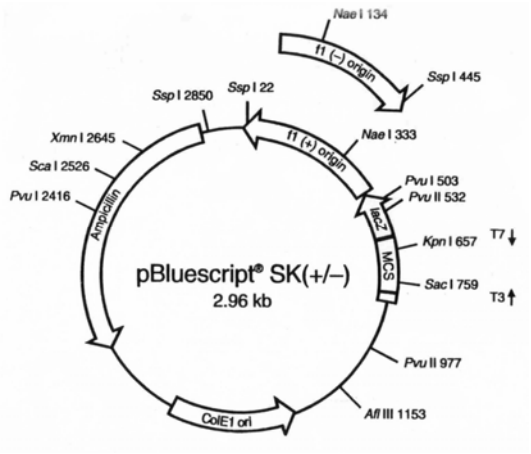

pBlue-PolyA-*Xba*I (based on pBluescript, Stratagene, Heidelberg, Germany)

3.1 kb, LacZ, Amp^r, T3-Promotor, f1 origin, PolyA, MCS (*Sac*I, *Bst*XI, *Sac*II, *Not*I, *Eag*I, *Xba*I).

*Bst*XI *Eag*I
β-Galactosidase → T3 promotor +1 → *Sac*I *Sac*II *Not*I *Xba*I
CAGCTATGACCATGATTACGCCAAGCTCGAAATTAACCCTCACTAAAGGGAACAAAAGCTGGAGCTCCACCGCGGTGGCGGCCGCTCTAGA
GTCGATACTGGTACTAATGCGGTTCGAGCTTTAATTGGGAGTGATTTCCCTTGTTTTCGACCTCGAGGTGGCGCCACCGCCGGCGAGATCA

*Xba*I PolyA *Xho*I *Apa*I *Kpn*I
TCTAGAGACTGAAGGAGGGTTGAACTCTGTATTGTCTTTCAAGGGTCATTTTTCCTAAAAAAAAAAAAAAAAAAAAAAAAAAAAAACTCGAGGGGGGGCCCGGTACCC
AGATCTCTGACTTCCTCCCAACTTGAGACATAACAGAAAGTTCCCAGTAAAAAGGATTTTTTTTTTTTTTTTTTTTTTTTTTTTTGAGGTCCCCCCCGGGCCATGGG

pcDNA5/FRT (Invitrogen, Karlsruhe, Germany)

5.07 kb, CMV-Promotor, BGH Poly A, FRT Site, Hyg^r, Amp^r, pUC origin, *bla*-Promotor, MCS (*Nhe*I, *Pme*I, *Afl*II, *Hin*dIII, *Asp*718I, *Kpn*I, *Bam*HI, *Bst*XI, *Not*I, *Xho*I, *Apa*I, *Pme*I).

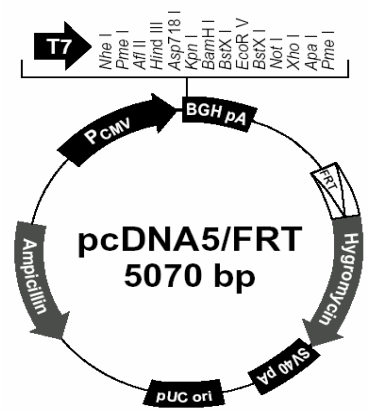

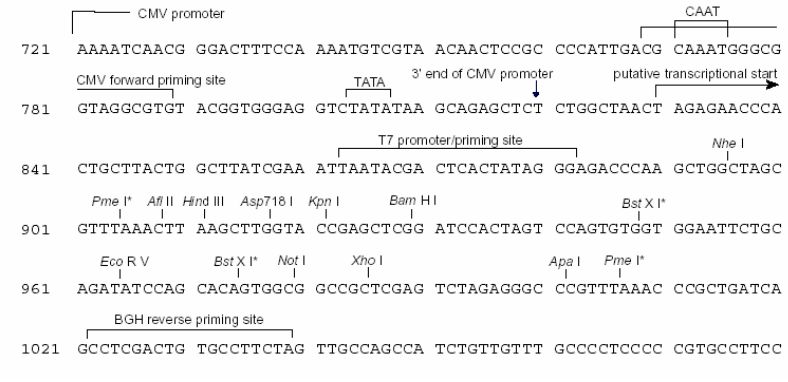

pcDNA4/TO (Invitrogen, Karlsruhe, Germany)

5.0 kb, CMV-Promotor, 2x Tetracyclin-Operon ($TetO_2$), *lox*H, Zeo^r, pUC origin, Amp^r, *lox*P, *Apa*I, *Pme*I

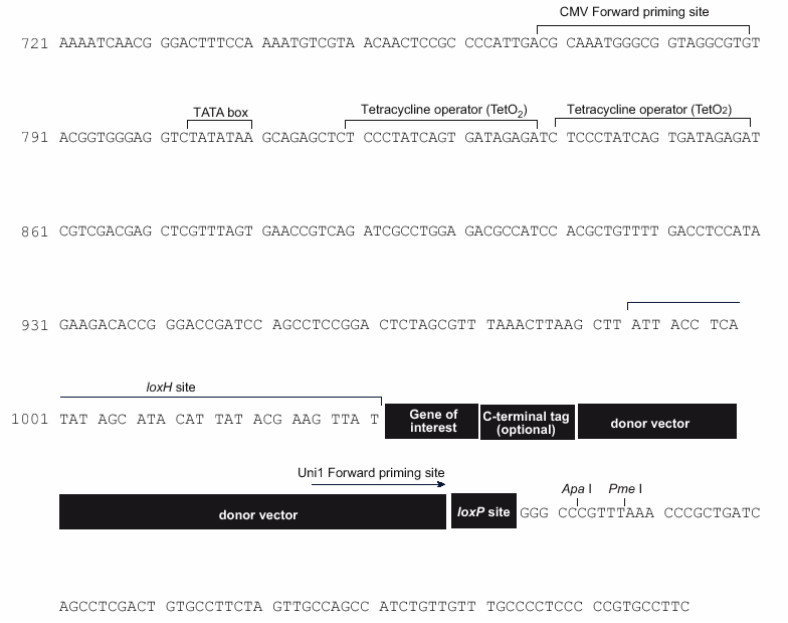

pcDNA5/TO (based on pcDNA5/FRT and pcDNA4/TO)

This plasmid is a combination of pcDNA5/FRT (Invitrogen) plus the TET operon of pcDNA4/FRT (Invitrogen).

5.07 kb, CMV-Promotor, 2x Tetracyclin-Operon ($TetO_2$), BGH Poly A, FRT Site, Hyg^r, Amp^r, pUC origin, *bla*-Promotor, MCS (*Nhe*I, *Pme*I, *Afl*II, *Hin*dIII, *Asp*718I, *Kpn*I, *Bam*HI, *Bst*XI, *Not*I, *Xho*I, *Apa*I, *Pme*I).

pcDNA5/FRT/V5-HIS TOPO (Invitrogen, Karlsruhe, Germany)

5.01 kb, CMV promotor, T7 promoter, MCS (*Nhe*I, *Asp*718I, *Kpn*I, *Bam*HI, *Age*I, *Pme*I), V5 epitope, 6xHis, BGH Poly A, FRT site, Hyg^r, SV40 Poly A, pUC origin, *bla*-promotor, Amp^r.

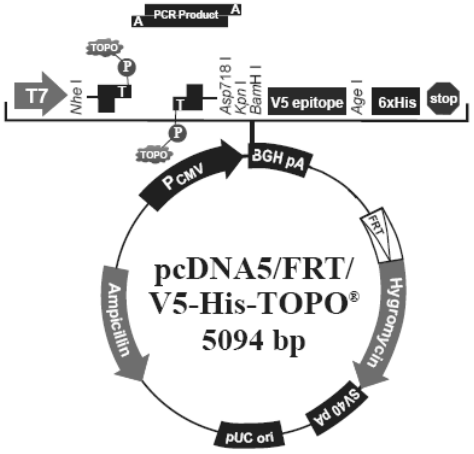

2.3.3 Media

Luria-Bertani (LB) Broth	NaCl	10 g/l
	Tryptone	10 g/l
	Yeast-Extract	5 g/l
	Adjust pH to 7.0 with 5N NaOH, autoclave (121°C, 1 bar, 20 min). Cool down to 55°C, and add ampicillin 100 µg/ml	
LB-Agar (500 ml)	as LB-broth	
	Add agar-agar	20 g/l
	autoclave (121°C, 1 bar, 20 min) Cool down to 55°C, and add the following supplements:	
	IPTG [25 mg/ml H_2O]	1 ml
	X-Gal [20 mg/ml DMF]	1 ml
	Ampicillin [100 µg/ml]	500 µl
NZY$^+$ Broth	NZ amine (casein hydrolysate)	10 g/l
	Yeast- Extract	5 g/l
	NaCl	5 g/l
	Adjust pH to 7.0 with 5N NaOH, autoclave (121°C, 1 bar, 20 min) Cool down to 55°C and add the following supplements:	
	1 M $MgCl_2$	12.5 ml
	1 M $MgSO_4$	12.5 ml
	20 % glucose	20 ml

SOC Medium (Invitrogen)	Trypton	2 %
	Yeast-Extract	0.5 %
	NaCl	10 mM
	KCl	2.5 mM
	$MgCl_2$	10 mM
	$MgSO_4$	10 mM
	Glucose	20 mM

2.3.4 Agarose gel electrophoresis

6 x Loading buffer	Bromophenol blue	0.2 %
	Xylene Cyanol FF	0.2 %
	Glycerol	60 %
	EDTA	60 mM
10 x TAE buffer	Tris	484 g
	Acetic acid	114.2 ml
	0.25 M EDTA, pH 8.0	400 ml
1 x TAE buffer	in ddH_2O as running buffer	
Agarose gel	1 % Agarose in 1 x TAE-Buffer	

Molecular weight markers

DNA Molecular Weight Marker XIV (100 bp ladder) (Roche Diagnostics, Mannheim, Germany)
100 bp, 200 bp, 300 bp, 400 bp, 500 bp, 1000 bp, 1500 bp, and 2642 bp

GeneRuler™ DNA Ladder Mix (MBI Fermentas, St. Leon-Roth, Germany)
100 bp, 200 bp, 300 bp, 400 bp, 500 bp, 600 bp, 700 bp, 800 bp, 900 bp, 1031 bp, 1200 bp, 1500 bp, 2000 bp, 2500 bp, 3000 bp, 3500 bp, 4000 bp, 5000 bp, 6000 bp, 8000 bp, and 10000 bp

2.3.5 Enzymes

Restriction Enzymes

Enzyme	Recognition Site	Buffer	Require BSA	Manufacturer
*Sac*I	5'...GAGCTC...3' 3'...CTCGAG...5'	NEBuffer 1	Yes	NEB*
*Sac*II	5'...CCGCGG...3' 3'...GGCGCC...5'	NEBuffer 4	No	NEB*
*Xba*I	5'...TCTAGA...3' 3'...AGATCT...5'	NEBuffer 2	Yes	NEB*
*Xho*I	5'...CTCGAG...3' 3'...GAGCTC...5'	NEBuffer 2	Yes	NEB*
*Kpn*I	5'...GGTACC...3' 3'...CCATGG...5'	NEBuffer 1	No	NEB*
*Dpn*I	5'...GATC...3' 3'...CTAG...5'	Buffer # 7	No	Stratagene**

** New England Biolabs, Frankfurt am Main, Germany*
*** Stratagene, La Jolla, CA, USA*

DNA Polymerases

Expand™ High Fidelity PCR System	Roche Diagnostics, Mannheim, Germany
YieldAce™ DNA Polymerase	Stratagene, La Jolla, CA, USA
Thermoprime Plus™ DNA Polymerase	ABGene, Hamburg, Germany
Pfu Turbo® DNA Polymerase	Stratagene, La Jolla CA, USA

Reverse Transcriptase

Advantage™ RT-for-PCR Kit MMLV *(Murine Moloney Leukaemia Virus)*	BD Clontech, Heidelberg, Germany

DNA Ligases

T4 DNA Ligase	BD Clontech, Heidelberg, Germany
Rapid DNA Ligation Kit	Roche Diagnostics, Mannheim, Germany
T4 DNA Ligase	Promega, Madison, WI, USA

Other Enzymes

DNA-Polymerase I Large Fragment (Klenow Fragment)	NEB, Frankfurt, Germany
T3 RNA-Polymerase	Promega, Madison, WI, USA
RQ1 RNase-free DNase	Promega, Madison, WI, USA

2.3.6 Commercialized kits and material

High Pure® PCR Product Purification Kit	Roche Diagnostics, Mannheim, Germany
PeqGOLD RNA Pure ™	PegLab, Erlangen, Germany
Oligotex™ mRNA Kit	Qiagen GmbH, Hilden, Germany
Advantage® RT-for-PCR Kit	BD Clontech, Heidelberg, Germany
QIAEX II® Gel Extraction Kit	Qiagen GmbH, Hilden, Germany
QIAGEN® Plasmid Midi Kit	Qiagen GmbH, Hilden, Germany
QIAprep® Plasmid Mini Kit	Qiagen GmbH, Hilden, Germany
Rapid DNA Ligation Kit®	Roche Diagnostics, Mannheim, Germany
pGEM®-T Vector System I	Promega, Mannheim, Germany
Riboprobe® in vitro Transcription System T3	Promega, Mannheim, Germany
QuikChange® Site-Directed Mutagenesis Kit	Stratagene, La Jolla, CA, USA
Sephadex G-50® Quick Spin Columns for RNA purification	Roche Diagnostics, Mannheim, Germany
$m^7G(5')ppp(5')G$ (Capping Analog)	Promega, Mannheim, Germany
TaqMan Universal PCR Master Mix	Applied Biosystems, Darmstadt, Germany

2.3.7 cDNA-Panels and RNAs

Human Adult Normal Tissue cDNA Panel - Neural System panels 2, 3 and 4	BioCat, Heidelberg, Germany
Human Brain Accumbens RNA total	Clontech, Heidelberg, Germany
Human Brain Putamen RNA total	Clontech, Heidelberg, Germany
Human Brain Substantia Nigra RNA total	Clontech, Heidelberg, Germany
Human Multiple Tissue cDNA (MTC™) Panel I	Clontech, Heidelberg, Germany
Human Multiple Tissue cDNA (MTC™) Panel II	Clontech, Heidelberg, Germany
Mouse Multiple Tissue cDNA (MTC™) Panel I	Clontech, Heidelberg, Germany
Mouse Multiple Tissue cDNA (MTC™) Panel III	Clontech, Heidelberg, Germany
Rat Multiple Tissue cDNA (MTC™) Panel I	Clontech, Heidelberg, Germany

2.4 Expression in *Xenopus laevis* oocytes

2.4.1 Animals

To heterologous expression of the proteins, adult female African clawed frogs (*Xenopus laevis*) were purchased from H. Kähler (Hamburg, Germany) and kept under standard conditions as described (Colman, 1984).

2.4.2 Solutions and buffers for the *X.laevis* oocytes

Modified Barth's solution	NaCl	88 mM
	HEPES	15 mM
	$NaHCO_2$	2.4 mM
	KCl	1.0 mM
	$Ca(NO_3)$ x 4 H_2O	0.3 mM
	$CaCl_2$ x 6 H_2O	0.41 mM
	$MgSO_4$ x 7 H_2O	0.82 mM
	Adjust pH to 7.6 with NaOH	
	Add 0.1% gentamicin	
OR-2 Buffer	NaCl	82.5 mM
	HEPES	5.0 mM
	KCl	2.5 mM
	$MgCl_2$ x 6 H_2O	1.0 mM
	Na_2HPO_4 x 2 H_2O	1.0 mM
	Adjust pH to 7.8 with KOH	
Sodium solution	NaCl	100 mM
	HEPES	10 mM
	KCl	2 mM
	$CaCl_2$ x 6 H_2O	1 mM
	$MgCl_2$ x 6 H_2O	1 mM
	Adjust pH to 7.5 with 1M Tris	

2.4.3 Radiochemicals

Radiochemical	Specific activity	Concentration	fmol / dpm
[^{3}H]Chenodeoxycholate	0.1 mCi/ml, 0.051 Ci/mmol	1949.3 µM	8.86062
[^{3}H]Cholate	0.1 mCi/ml, 0.055 Ci/mmol	1818.2 µM	8.2645
[^{3}H]DHEAS	1.0 mCi/ml, 74.0 Ci/mmol	13.5 µM	0.0061426
[^{3}H]Estrone-3-sulfate	1.0 mCi/ml, 57.3 Ci/mmol	17.5 µM	0.0079328
[^{3}H]Pregnenolone sulfate	1.0 mCi/ml, 20 Ci/mmol	50 µM	0.022727
[^{3}H]Taurocholate	1.0 mCi/ml, 3.5 Ci/mmol	285.7 µM	0.12987

Radiochemicals were purchased from PerkinElmer Life Sciences Inc., Boston, MA, USA.and AmericanRadiolabeled Chemicals, St. Louis, USA

2.4.4 Material

Aminobenzoic acid ethyl ester (MS-222, Tricaine)	Sigma, Taufkirchen, Germany
Collagenase D	Roche Diagnostics, Mannheim, Germany

Gentamicin	Sigma, Taufkirchen, Germany
Surgical instruments	diverse
Skalpel	Swann-Morton, Sheffield, England
Vicryl 4.0	Ethicon GmbH, Nordersted, Germany

2.5 Immunofluorescence in *Xenopus laevis* oocytes

2.5.1 Solutions and buffers

K-aspartate solution	K-aspartate	200 mM (34.24 g/l)
	KCl	20 mM (1.49 g/l)
	$MgCl_2$	1 mM (0.20 g/l)
	EGTA	10 mM (3.80 g/l)
	HEPES	10 mM (2.38 g/l)
	Adjust pH to 7.4 with KOH	
Dent´s Fixans (100 ml)	Methanol	80 ml
	DMSO	20 ml

Methanol 90 %, 70 %, 50 % und 30 % in PBS

PBS	NaCl	137.00 mM (8.0 g/l)
(Phosphate buffered saline)	KCl	2.68 mM (0.2 g/l)
	KH_2PO_4	1.47 mM (0.2 g/l)
	Na_2HPO_4	7.30 mM (1.3 g/l)
	Adjust pH to 7.4	
PBSAG	BSA	2 %
(PBS + BSA + Goat serum)	Goat serum	4 %
	In PBS	
3.7 % Formaldehyde/PBS	Formaldehyde 37 %	10 ml
(100ml)	PBS	90 ml

Ethanol 30 %, 50 %, 70 % and 100 % in PBS

Infiltration solution A (100 ml)	GMA monomer* (Technovit 7100®)	50 ml
	Ethanol	50 ml
Infiltration solution B (IS B)	GMA monomer* (Technovit 7100®)	10 %
	HardenerI*	1 g/100 ml
	Keep at 4°C	
Infiltration solution B	Hardener II*	1 ml
+ Hardener II	in 15 ml IS B	

** Technovit 7100® Glycol Methacrylate Embedding Kit, from Heraeus Kulzer, Wehrheimof, Germany, consists: GMA monomer, hardener I and hardener II.*

2.5.2 Antibodies

Anti-FLAG® M2 monoclonal mouse antibody	Sigma, Schnelldorf, Germany
Alexa Fluor® 488 Goat anti-mouse IgG (H+L)	MoBiTec, Göttingen, Germany

2.6 Cell Culture

2.6.1 Eukaryotic cell line HEK293 (Invitrogen, Karlsruhe, Germany)

This cell line was established from primary embryonic human kidney transformed with human adenovirus type 5 DNA.

Medium for HEK293 Cells (100 ml)	D-MEM	44 ml
	HAM 12	44 ml
	Glutamine (4 mM)	2 ml
	FCS (10 %)	10 ml

2.6.2 Eukaryotic cell line PC 12 (American Type Tissue Cell Collection, Rockville, MD, USA)

The PC 12 cells are a neuroendocrine cell line derived from *Rattus norvegicus* pheochromocytoma.

Medium for PC 12 Cells (100 ml)	D-MEM	81 ml
	Glutamine (4 mM)	2 ml
	Penicilin/streptomycin (5000 IU/ml)	2 ml
	FCS (5 %)	5 ml
	NHS (10 %)	10 ml

2.6.3 Material for cell culture

24 well plates	Sarstedt, Nümbrecht, Germany
25 cm^2 and 75 cm^2 culture flasks	Sigma-Aldrich, Taufkirchen, Germany

2.6.4 Cell culture medium and supplements

D-MEM (Dulbecco's Modified Eagle Medium)	Invitrogen, Karlsruhe, Germany
FCS (Fetal calf serum)	Sigma-Aldrich, Taufkirchen, Germany
F-12 Nutrient Mixture (HAM) + L-Glutamine	Invitrogen,Karlsruhe, Germany
L-Glutamine (200 mM)	Invitrogen,Karlsruhe, Germany
Penicillin/Streptomycin	Invitrogen, Karlsruhe, Germany
Trypanblau	Fluka, Buchs, Schweiz
Trypsin	Gibco, Karlsruhe, Germany
Poly-D-Lysin	Sigma-Aldrich, Taufkirchen, Germany

2.6.5 Transient transfection using HEK293-Cells

Lipofectamine 2000	Invitrogen, Karlsruhe, Germany
Tetracycline	Sigma-Aldrich, Taufkirchen, Germany

2.7 Immunocytochemistry

2.7.1 Primary and secondary antibodies

Antibody	Description	Manufacturer
anti-FLAG M2	Monoclonal mouse antibody against the FLAG epitope DYKDDDDK	Sigma-Aldrich, Taufkirchen, Germany
anti-FLAG	Polyclonal rabbit antibody against the FLAG epitope DYKDDDDK	Sigma-Aldrich, Taufkirchen, Germany
anti-HA M2	Monoclonal mouse antibody against the HA (hemagglutinin) epitope PYDVPDYA of the influenza virus	Roche, Mannheim, Germany
Alexa Fluor 488	Polyclonal goat antibody against mouse IgG (H+L)	MoBiTec, Goettingen, Germany
Cy3 anti IgG	Polyclonal goat antibody against rabbit IgG (H+L)	Dianova, Hamburg, Germany

2.7.2 Reagents

BSA	Sigma-Aldrich, Taufkirchen, Germany
DAPI	Roche, Mannheim, Germany
Glycine	Serva, Heidelberg, Germany
Normal goat serum	Dako Cytomation, Hamburg, Germany
Mowiol	Calbiochem, Darmstadt, Germany
Triton X-100	Sigma-Aldrich, Taufkirchen, Germany

2.7.3 Buffer and solutions

Paraformaldehyde (PFA) 2 % (50 ml)

PFA	1 g
H_2O (50-60°C)	45 ml
10 x PBS (50-60°C)	5 ml

Stir and heat solution (not over 60°C) until it becomes clear and adjust pH to 6.8-7.2

Buffer A (1 x PBS + 20 mM Glycine) (110 ml)

1 x PBS	110 ml
Glycine	165.22 mg

Buffer A + 0.2 % Triton X-100 (20 ml)

Buffer A	20 ml
Triton X-100	40 µl

Buffer B (Buffer A + 1 % BSA) (70 ml)

Buffer A	70 ml
BSA	700 mg

Blocking solution (Buffer B + 4 % goat serum)

Buffer B	70 ml
Goat serum	2.8 ml

DAPI/Methanol 1: 5000

DAPI dissolved in ddH_2O to a final concentration of 1 mg/ml	50 µl
Methanol	250 ml

Mowiol

Mowiol	2.4 g
Glycerol	6.0 g
Stir, add H_2O	6 ml
leave for 2h at RT, add 0.2 M Tris (pH 8.5)	12 ml

and incubate at 53°C until the mowiol has dissolved. Clarify by centrifugation at 4000-5000 rpm for 20 min and aliquot. Stable at – 20°C for 12 months.

Add prior to use:

DABCO (Diazabicyclooctane)	0.1 %

2.8 Western Blot

2.8.1 HEK293 cells

2.8.2 Solutions and buffers

PBS (see above)

RIPA buffer

NaCl	150 mM
Nonidet P-40	1 %
Sodium deoxycholic acid	0.5 % (w/v)
SDS	1 % (w/v)
Protease Inhibitor Cocktail (Sigma)	

BCA Protein Assay Kit (Novagen, Darmstadt, Germany)

Laemmli sample buffer (Sigma, Taufkirchen, Germany)

Blocking solution

ECL-blocking agent (Amersham Biosciences)
5 % (w/v) in TBS-T

TBS-T

NaCl	137 mM
Tris	10 mM
Tween-20	0.05 %

ECL detection kit (Amerscham Biosciences)

2.8.3 Membranes

Nitrocellulose membrane (Schleicher&Schuell, Dassel, Germany)

ReadyBlot Adult Rat Brain Protein Explorer (alpha diagnostics, San Antonio, Texas, USA)

2.8.4 Other materials and reagents

12 % SDS polyacrylamide gel

2.9 *In situ* Hybridization

2.9.1 Animals

Animal care, breeding, and experimental procedures were conducted according to the guidelines approved by the Hessian Ethical Committee. Wistar rats (200-300g) bred at the Institute of Veterinary Pharmacology of the Justus-Liebig University were used for this study. The rats housed individually in polycarbonate type IV cages with *ad libitum* access to standard laboratory chow and water. Room temperature was controlled at 24±1ºC and relative humidity at 60%. Lights were on from 7:00 AM to 7:00 PM.

2.9.2 Solutions and buffers

DEPC treated water (see above)

1 M $MgCl_2$ solution

20x SSC solution (see above)

PBSM buffer 1x (200ml)

PBS tablet (Sigma, Taufkirchen, Germany) 1
1 M $MgCl_2$ solution 1ml
Solubilize into DEPC water and store at 4-8°C.
One tablet dissolved in 200 ml of deionized water yields 0.01 M phosphate buffer, 0.0027 M potassium chloride and 0.137 M sodium chloride, pH 7.4, at 25°C.

10x TNMT buffer

Tris-HCl	121.1 g
NaCl	58.4 g
$MgCl_2$	4.17g

Solubilize into ddH_2O, adjust pH to 7.5 and the volume to 1 l. Add 1 ml DEPC, leave overnight at 37°C, autoclave and add 5 ml Triton-X 100.

5x NTB buffer

Tris-HCl	60.5 g
NaCl	29.2 g

Solubilize into ddH_2O, adjust pH to 9.6 and the volume to 1 l. Add 1 ml DEPC, leave overnight at 37°C and autoclave. Prior to use add 25 ml 1 M $MgCl_2$ solution for 500 ml 1x NTB buffer

Proteinase K stock solution

Proteinase K	10 mg
PBSM buffer (1x)	1 ml

20 µl aliquots frozen at –20°C

Glycine solution 0.2 %	Glycine	200 mg
	PBSM buffer	100 ml
Acetic acid 20 %	Solubilize into DEPC treated water	
Paraformaldehyde 4 % (50ml)	PFA	2 g
	H_2O (50-60°C)	45 ml
	10 x PBS (50-60°C)	5 ml
	Stir and heat solution (not over 60°C) until it becomes clear and adjust pH to 6.8-7.2	
Prehybridization solution	Glycerol	20 %
	Solubilize into DEPC treated water	
Probe solution	DEPC treated water	4 µl
	Salmon sperm DNA [1 mg/ml]	4 µl
	Yeast t-RNA [1 mg/ml]	8 µl
	DIG-cRNA probe (1:100)	4 µl
Dextrane sulphate	Dextrane sulfate	5 g
	DEPC treated water	5 ml
	Leave two days at 4-8°C, add 10 ml DEPC water, aliquot and store at – 20°C	
Hybridization solution	DEPC treated water	56 µl
	20x SSC	40 µl
	50 % Dextrane sulphate	80 µl
	Denhardt´s reagent	4 µl
	Deionized formamide (50%)	200 µl
	Probe solution	20 µl
Denhardt's Reagent	BSA	200 mg
	Ficoll	200 mg
	Polyvinylpyrrolidone	200 mg
	Dissolve in DEPC water and adjust the volume to 10 ml. Aliquot and store at – 20°C	
RNaseA / RNaseT1	RNaseA / RNaseT1 stock solution	150 µl
	4x SSC	1.35 ml
RNaseA / RNaseT1 stock solution		
	2x SSC	1 ml
	RNaseA [25 mg/ml]	12 µl
	RNaseT1 [10^5 U/ml]	0.1 µl
Blocking solution	BSA	6 g
	TNMT 1x	200 ml
Incubation solution	TNMT 1x	666 µl
	BSA 3%	333 µl
	Anti-DIG antibody, AP conjugated	2 µl

Levamisol stock solution	Levamisol	2.4 g
	NTB buffer (1x)	10 ml

2.9.3 Probe preparation

Vector: pGEM-T (promega)

Restriction Enzymes

Enzyme	Recognition Site	Buffer	Require BSA	Provided by
*Sac*I	5'...GAGCTC...3' 3'...CTCGAG...5'	NEBuffer 1	yes	NEB*
*Sac*II	5'...CCGCGG...3' 3'...GGCGCC...5'	NEBuffer 4	no	NEB*

** New England Biolabs, Frankfurt am Main, Germany*

DIG RNA labeling Mix	Roche, Mannheim, Germany
100x DTT	Roche, Mannheim, Germany
Transcription buffer	Roche, Mannheim, Germany
RNA Polymerases: T7 and SP6	Roche, Mannheim, Germany

2.9.4 Other materials and reagents

NBT-BCIP	Roche, Mannheim, Germany
Glycergel	Dako Cytomation, Hamburg, Germany

2.10 Immunohistochemistry

2.10.1 Animals

Animal care, breeding, and experimental procedures were conducted according to the guidelines approved by the Hessian Ethical Committee. Ten adult male Wistar rats (180-250g) bred at the Institute of Veterinary Physiology of the Justus-Liebig University Giessen were used for this study. The rats housed individually in polycarbonate type IV cages with *ad libitum* access to standard laboratory chow and water. Room temperature was controlled at 24±1ºC and relative humidity at 60%. Lights were on from 7:00 AM to 7:00 PM.

2.10.2 Solutions and buffers

0.1 M Phosphate buffer (2 l)

Stock solution A (1 l)	
Na_2HPO_4	0.2 M
Stock solution B (1 l)	
NaH_2PO_4	0.2 M

	0.1M Phosphate buffer (2 l)	
	NaH_2PO_4 0.2 M	720 ml
	Na_2HPO_4 0.2 M	280 ml
	add ddH_2O to a final volume of 2l	
	pH 7.2 - 7.4 (check it with pH paper)	
Blocking solution (10 ml)	Normal horse serum (NHS)	1 ml
	Triton X-100	30 µl
	Solubilize into phosphate buffer	
Incubation buffer (10 ml)	Normal horse serum (NHS)	0.2 ml
	Triton X-100	10 µl
	Solubilize into phosphate buffer	
Paraformaldehyde (PFA)	PFA	4%
	Solubilize into phosphate buffer at 50-60°C until it becomes clear, filtrate, adjust pH to 7.4 and cool to 4°C	
NaCl 0.9%	NaCl	0.9%
	Solubilize into ddH_2O	
Sucrose solution (100 ml)	sucrose	20 ml
	Solubilize into 0.1 M phosphate buffer and store at 4°C	

2.10.3 Antibodies and antibodies combination

Primary Antibody	Manufacturer	Secondary Antibody	Manufacturer
Rabbit anti-Slc10a4	Eurogentec, Seraing Belgium	Goat anti-rabbit biotinylated	Chemicon, Temecula, USA
Rabbit anti-Slc10a4	Eurogentec, Seraing Belgium	Cy3 donkey anti-rabbit	Dianova, Hamburg, Germany
Mouse anti-CHT1	Chemicon, Temecula,USA	Alexa Fluor 488 goat anti-mouse	Sigma-Aldrich, Taufkirchen, Germany
Goat anti-VAChT	Chemicon, Temecula, USA	Alexa Fluor 488 donkey anti-goat	Sigma-Aldrich, Taufkirchen, Germany
Mouse anti-TH	Chemicon, Temecula, USA	Alexa Fluor 488 goat anti-mouse	Sigma-Aldrich, Taufkirchen, Germany

2.10.4 Other materials and reagents

Synthetic SLC10A4 antigen	Eurogentec, Seraing, Belgium
Vectastain Elite ABC Kit	Linaris Biologische Produkte, Wertheim, Germany
Avidin/Biotin blocking kit	Linaris Biologische Produkte, Wertheim, Germany
Diaminobenzidine hydrochloride (DAB)	Sigma-Aldrich, Taufkirchen, Germany
Hydrogen peroxide	Sigma-Aldrich, Taufkirchen, Germany

DAPI	Roche, Mannheim, Germany
Cresyl violet acetate (0.1%)	Sigma-Aldrich, Taufkirchen, Germany
Histoclear	Shandon, Frankfurt, Germany
Xylol	Merck, Darmstadt, Germany
Entellan	Merck, Darmstadt, Germany
Coverslips 24 x 60 mm	Menzel GmbH, Bielefeld, Germany
Object slides 76 x 26 mm	Menzel GmbH, Bielefeld, Germany

2.11 Reagents

β-Mercaptoethanol, C_2H_6OS	Merck, Darmstadt, Germany
Acetic acid, CH_3COOH	Roth, Karlsruhe, Germany
Agar-Agar	Roth, Karlsruhe, Germany
Agarose	Roth, Karlsruhe, Germany
Aminobenzoic acid ethyl ester (MS-222)	Sigma-Aldrich, Taufkirchen, Germany
Ampiciline	Sigma-Aldrich, Taufkirchen, Germany
Calcium nitrat, tetrahydrate, $Ca(NO_3) \times 4\ H_2O$	Merck, Darmstadt, Germany
Calcium chloride, dihydrate, $CaCl_2 \times 2\ H_2O$	Roth, Karlsruhe, Germany
Casein enzymatic hydrolysate, N-Z-amine A	Sigma, Steinheim, Germany
Chloroform, $CHCl_3$	Roth, Karlsruhe, Germany
DHEAS	Sigma, Steinheim, Germany
N,N-Dimethylformamide, $HCON(CH_3)_2$	Sigma, Steinheim, Germany
Digoxin	Roth, Karlsruhe, Germany
Sodium dodecyl sulfat (SDS), $CH_3(CH_2)_{11}OSO_3Na$	Serva, Heidelberg, Germany
EDTA (ethylene diamine tetracetic acid)	Sigma-Aldrich, Taufkirchen, Germany
Estrone-3-sulfate	Sigma-Aldrich, Taufkirchen, Germany
Estradiol-17β-glucuronide	Sigma-Aldrich, Taufkirchen, Germany
Ethanol (> 99.8 %)	Roth, Karlsruhe, Germany
Ethidium bromide	Roth, Karlsruhe, Germany
Formaldehyde, CH_2O	Sigma-Aldrich, Taufkirchen, Germany
Formamide, CH_3NO	Sigma-Aldrich, Taufkirchen, Germany
Glucose	Merck, Darmstadt, Germany
Glycerine, $CH_3H_8O_3$	Merck, Darmstadt, Germany
IPTG (Isopropyl-β-D-Thiogalactoside)	BioTech, St. Leon-Roth,Germany
Isopropyl alcohol, $CH_3CHOHCH_3$	Roth, Karlsruhe, Germany
Lithium chloride, LiCl	Sigma-Aldrich, Taufkirchen, Germany
Magnesium sulfate, heptahydrate, $MgSO_4 \times 7\ H_2O$	Merck, Darmstadt, Germany
Magnesium chloride, hexahydrate, $MgCl_2 \times 6\ H_2O$	Merck, Darmstadt, Germany
Mineral oil	MBI Fermentas, St. Leon-Roth,Germany
Liquid nitrogen, N_2	Messer, Griesheim, Germany
Ouabain	Sigma-Aldrich, Taufkirchen, Germany
Potassium chloride, KCl	Merck, Darmstadt, Germany
SOC Medium	GibcoBrl, Paisley, Schottland
Sodium acetate, trihydrate, $NaC_2H_3O_2 \times 3H_2O$	Merck, Darmstadt, Germany
Sodium chloride, NaCl	Roth, Karlsruhe, Germany
Sodium hydrogen carbonate, $NaHCO_3$	Roth, Karlsruhe, Germany
Scintillation fluid (Rotiszint 22 eco)	Roth, Karlsruhe, Germany
Taurocholate	Sigma-Aldrich, Taufkirchen, Germany
TEMED (N,N,N',N',-Tetramethyl ethylene diamine)	Bio-Rad, München, Germany
Trisodium citrate dihydrate, $Na_3C_6H_5O_7 \times 2H_2O$	Roth, Karlsruhe, Germany
Tryptone Peptone	Difco, Detroit, USA
5-bromo-4-chloro-3-indolyl- beta-D-galacto pyranoside (X-Gal)	BioTech, St. Leon-Rot, Germany
Yeast Extract	Difco, Detroit, USA

2.12 Equipments

Accupette (1-100 ml)	NeoLab, Heidelberg, Germany
Aqua bidest System Milli-Q Biocel	Millipore, Schwalbach, Germany
Analysis balance:	
- AE 260 Delta Range	Mettler-Toledo, Gießen, Germany
- Precisa 3000C-6000D	DAK-Oerlikon, Zurich, Switzerland
Applied Biosystems 7300 Real Time PCR System	Darmstadt, Germany
Autoclave Sanoclav	Wolf, Geislingen, Germany
Centrifuges:	
- Megafuge 1.0	Heraeus, Mainz, Germany
- Sorvall refrigerated RC5C Rotor HB4	Du Pont, Bad Homburg, Germany
- centrifuge 5415D	Eppendorf, Wesseling-Berzdorf Germany
- Vacuum centrifuge SpeedVac SC 110	Savant, Farmingdale, USA
Cryostat HM 500 O	Microm, Walldorf, Germany
Electrophoresis power supply (max. 200 mA, 1 kV, 150 W)	Workshop MZI, Gießen, Germany
Electrophoresis tank	Workshop MZI, Gießen, Germany
- 14.5 x 6.5 cm	
- 35.5 x 11.0 cm	
Fluorescence microscope Olympus BX50	Olympus Optical, Hamburg, Germany
- Olympus Camedia C-3030 camera	
- Olympus Camedia Master 2.0 software package	
Fluorescence microscope DM6000B	Leica Mikrosysteme, Bensheim,
- S/W camera DFC350FX	Germany
Freezing microtome, 1205	Jung, Heidelberg, Germany
G24 Environmental Incubator shaker	New Brunswick Scientific, Edison, USA
Gel tray	Workshop MZI, Gießen, Germany
- 7.5 x 5 cm	
- 12 x 18 cm	
Incubator	Heraeus, Mainz, Germany
Image Master VDS	Amersham, Freiburg, Germany
Laminar flow clean bench, DLF-REL 6	Heraeus, Mainz, Germany
Liquid scintillation counter Wallac 1409	Pharmacia, Freiburg, Germany
Microinjector Nanoliter 2000	World Precision Inst., Sarasota, USA
pH Meter HI 221	Hanna, Kehl am Rhein, Germany
Perkin-Elmer GeneAmp Cycler 2400	Perkin-Elmer, Rodgau, Germany
Pipettes (1000, 200, 100, 20, 10, and 0.5-2µl)	Eppendorf, Wesseling-Berzdorf Germany
Photometer BioPhotometer	Eppendorf, Wesseling-Berzdorf
- Cuvette (Eppendorf UVete)	Germany
Scale (0.01-500 g)	Mettler-Toledo, Gießen, Germany
SpeedVac SPD111V	Savant, Holbrook, NY, USA
UV-Transilluminator	Bachofer, Reutlingen, Germany
Video Printer Papier	MS Laborgeräte, Wiesloch, Germany
Vortex VF 2	Janke and Kunkel, Staufen, Germany
Water bath	Memmert, Schwabach, Germany

2.13 Bioinformatic

BLAST, NCBI *www.ncbi.nlm.nih.gov/BLAST/*	Compare nucleotide or protein sequences to sequence databases
Boxshade 3.21 *www.ch.embnet.org/software/BOX_form.html*	Graphic presentation of alignments
Chromas 2.23 *technelysium.com.au*	Evaluation of sequencing
EMBL-EBI, European Bioinformatics Institute *www.ebi.ac.uk/Information/sitemap.html*	Nucleotide Database EU
Ensembl, EBI *www.ensembl.org/*	Access to eukaryotic genomes
HMMTOP 2.0 *enzim.hu/hmmtop/*	Transmembrane topology prediction program
HUGO Gene Nomenclature Committee *www.gene.ucl.ac.uk/nomenclature/*	Human genome nomenclature committee
NCBI *www.ncbi.nlm.nih.gov*	National Center for Biotechnology Information, USA
NetNGlyc 1.0 Server *http://www.cbs.dtu.dk/services/NetNGlyc/*	Prediction of N-glycosylation sites
NetPhos 2.0 Server *http://www.cbs.dtu.dk/services/NetPhos/*	Prediction of serine, threonine, and tyrosine phosphorylation sites
Oligo 4.0, Wojciech Rychlik, Oslo, Norwegen	Primer selection
PSORT II Prediction *http://psort.ims.u-tokyo.ac.jp/form2.html*	Prediction of protein sorting signals
TC (Transporter Classification System) *www-biology.ucsd.edu/~msaier/transport/*	Classification of transporter genes
TMAP *www.mbb.ki.se/tmap/*	Transmembrane topology prediction program
TMHMM Server v. 2.0 *www.cbs.dtu.dk/services/TMHMM-2.0/*	Transmembrane topology prediction program
TMPred *www.ch.embnet.org/software/TMPRED_form.html*	Transmembrane topology prediction program
TopPred 2 *www.sbc.su.se/ erikw/toppred2/*	Transmembrane topology prediction program
TreeView 1.6.6 *http://taxonomy.zoology.gla.ac.uk/rod/treeview*	Graphic presentation of phylogenetic trees

3. Methods

In this work, several methods of molecular and cellular biology were applied to clone and to characterize new members of the SLC10 family, in particular rat Slc10a4, human SLC10A5, mouse Slc10a5, and rat Slc10a5. Figure 3 summarizes the main methods used and shows an overview from gene expression to cloning and expression of the proteins in two different expression systems (*X. laevis* oocytes and HEK293 cells), localization of Slc10a5 mRNA by *in situ* hybridization, and Slc10a4 protein by immunohistochemistry.

3.1 General Methods in Molecular Biology

3.1.1 PCR product purification

For efficient purification of PCR products, the High Pure PCR Product Purification Kit (Roche, Mannheim, Germany) was used. After contact with guanidine thiocyanate, the amplified DNA binds to glass fibers pre-packed in the filter tubes. Subsequently, the bound DNA is submitted to some wash-and-spin steps to remove primers, nucleotides, polymerase, salt, and contaminants, and then eluted using low salt conditions. The eluate obtained was used for posterior cloning and sequencing.

3.1.2 Concentration and purity determination of nucleic acid preparations

To quantify DNA and RNA concentrations, the absorbance of the samples was measured at 260 nm in a spectrophotometer. The 260/280 ratio was used to monitor protein contaminations; this ratio should be ≥ 1.8 for pure DNA and ≥ 2.0 for pure RNA.
The nucleic acid concentration was calculated as follows:

$$[\mu g/\mu l] = \frac{A_{260} \times E \times Vs}{Vna}$$

A_{260}: Sample absorbance at 260nm

E: Extinction coefficient

- Double-stranded DNA: 50 µg/ml per 1 A_{260} unit
- Single-stranded DNA : 33 µg/ml per 1 A_{260} unit
- RNA:40 µg/ml per 1 A_{260} unit

Vs: Sample volume

Vna: Volume of applied nucleic acids

3.1.3 Agarose-gel electrophoresis

In order to promote separation of nucleic acids to control the presence and size of the amplified DNA after PCR, or to control the insertion of DNA into a vector after cloning experiments, 1 %,

1.5 % and 2 % agarose gels were used. Each 10 µl DNA was mixed with 1 µl of 6 x Loading Dye solution and loaded into the gels; the Molecular Weight Marker XIV (Roche, Mannheim, Germany) and the Gene Ruler DNA Ladder Mix (MBI, Fermentas, St. Leon-Roth, Germany) were used as markers; and the TAE was required as running buffer. The separation of the DNA bands was performed at 70 mA for 40 min (7.5 x 5 cm gel) and 120 mA for 90 min (15 x 10.5 cm gel), and gels were stained with ethidium bromide and than visualized under an UV-transilluminator.

3.1.4 Restriction enzyme digestion

To digest 1µg plasmid DNA, 5-10 U of a restriction enzyme was used. To this reaction, 4 µl selected buffer, provided by the manufacturer, and water were added to a final volume of 40 µl. For optimal activity, some restriction enzymes require BSA. The reaction was carried out at 37°C for 1 h, and controlled by electrophoresis.

3.1.5 Plasmid purification

Recombinant *E. coli* were grown in selective LB medium containing ampicillin overnight at 37°C with shaking (approx. 225 rpm). Then, this culture was transferred to 2 ml (for mini preparations) or 50 ml tubes (for midi preparations) and centrifugated. The bacterial pellet was resuspended in 500 µl (mini) or 5 ml (midi) water and the plasmid purification was performed according to the manufacturer´s protocols (*QIAprep Miniprep Kit* or *Qiagen Plasmid Midi Kits*, Qiagen, Hilden, Germany).

3.1.6 Preparation of electrocompetent *E.coli* cells

To prepare electrocompetent cells, 50 µl Top10 competent cells (Invitrogen, Karlsruhe, Germany) were inoculated in 50 ml LB-broth without antibiotic, and the mixture was incubated over night at 37°C with shaking. Then, the cell suspension was diluted 1/100 into 250 ml LB-broth without antibiotic and incubated at 37°C with shaking until an OD_{578} of 0.5 to 0.8. Cells were chilled on ice for 10 to 15 min, transferred to pre-chilled 250 ml centrifuge bottles, and centrifugated at 4°C/16300 x g for 10 min. For all subsequent steps, the cells were maintained at 4°C. Pellets were resuspended in 0.5 volume 1 mM HEPES-buffer (125 ml HEPES buffer), cell suspension was centrifugated at 4°C/16300 x g for 10 min, and pellets resuspended in 0.25 volume 1 mM HEPES-buffer (62.5 ml HEPES buffer). Then, the cell suspension was centrifugated as above, the pellets resuspended in 50 ml glycerol (10%), and again centrifugated as described. Finally, pellets were resuspended in 2°ml glycerol (10%), aliquoted to 100°µl into 1.5 ml microcentrifuge tubes and stored at -80°C.

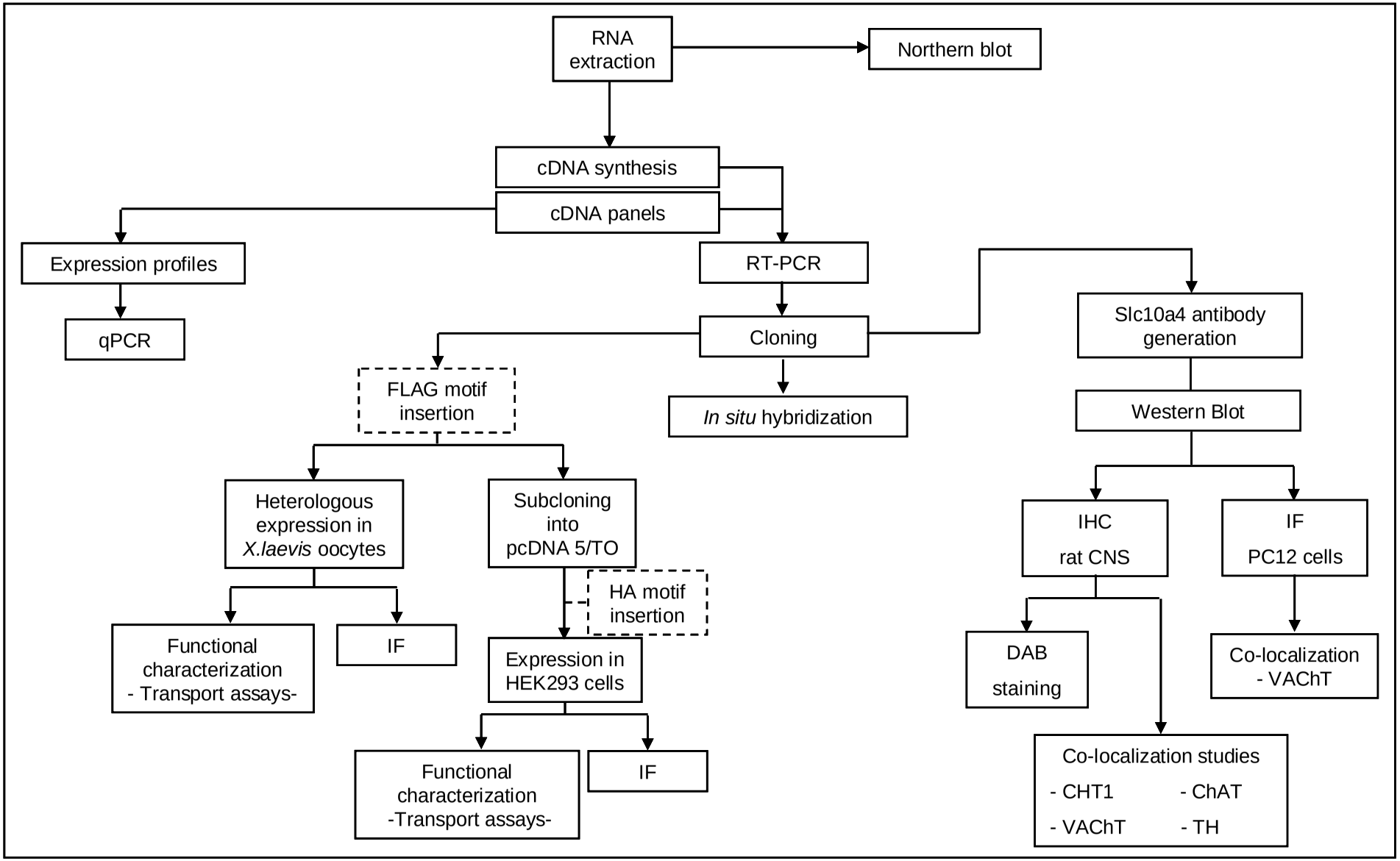

Figure 3: **Overview from gene expression to cloning, expression of proteins, and localization of mRNA or proteins.** DAB: diaminobenzidine, IF: immunofluorescence, IHC: immunohistochemistry.

3.2 RNA Extraction

3.2.1 Isolation of total RNA

Total RNA was isolated from adult Wistar rat and mouse (stem C57BL/6J) tissues. After euthanasia by carbon dioxide asphyxiation, mouse liver and rat intestine were removed, promptly frozen in liquid nitrogen and stored at - 80°C. For total RNA extraction, the tissue samples were pulverized in liquid nitrogen, homogenized using rotor/stator homogenizator and 1 ml/ 50 mg tissue of peqGOLD RNAPure* was added fallowed by incubation for 5 min at room temperature. Then, 0.2 ml chloroform per 1 ml peqGOLD was added, shaked, incubated at 4°C for 5 minutes, and centrifugated for 15 min at 12000 x°g/ 4°C to promote the solution separation into three phases, in which the upper aqueous phase contains the RNA. DNA and proteins remain in the lower organic phase and the interphase, respectively. The RNA phase was transferred to a new tube and an equal volume of isopropanol was added. Then, the samples were mixed, incubated for 15 min at 4°C and centrifugated for 15 min at 12000 x°g/ 4°C. After centrifugation, the supernatant was removed, and the RNA precipitate was washed twice with 75 % ethanol and the pellets were air-dried. Finally, pellets were resuspended in RNase-free water on ice for 30 minutes.
The purity and concentration of the RNA were measured at 260 nm in a spectrophotometer as described above.
To determine the quality of RNA, a denaturing 1 % agarose/formaldehyde gel electrophoresis was performed. Prior to electrophoresis, complete working area as well as the tank, gel tray and comb were washed with alcohol 70% and DEPC treated water. The gel was prepared by melting of 0.5 g agarose in 43 ml TAE buffer, cooling to 50°C and adding 7 ml of 37 % formaldehyde. After the polymerization, gel was run at 20 mA for 10 minutes. Prior to loading, 5 µg RNA was mixed with 1 µl of 2 x sample buffer, heated to 65°C for 10 min and cooled on ice. Then, 2 µl RNA Loading Dye was added and the samples were applied on the gel. The electrophoresis ran with buffer recirculation at 60 mA and 100V for approximately 90 min. To visualize the RNA, ethidium bromide was added to the gel. Visualization was performed under UV light.

**peqGOLD RNAPure is a one-phase solution containing phenol and guanidine isothiocyanate, which is a chaotropic agent that promotes the sample lysis and RNase inactivation. Used in combination with chloroform and alcohol, this solution provides high-quality intact RNA.*

3.2.2 Purification of Poly(A)$^+$ RNA from total RNA

Mammalian cells contain 10 - 30 pg total RNA, but only 1-5 % represent protein coding messenger RNA (mRNA). The presence of a poly-A tail (20-250 adenosine nucleotides), at the end of the mRNA molecule, distinguishes mRNA from the other tRNAs or rRNAs molecules. Therefore, this

poly-A tail provides a tool for isolation of eukaryotic mRNAs as provided by the Oligotex kit* principle (Qiagen, Hilden, Germany).

To obtain the Poly(A)$^+$ RNA, 0.25 – 1 mg total RNA was used. Briefly, Oligotex suspension was heated to 37°C, mixed by vortexing, and placed at room temperature. The OEB buffer (elution buffer) was heated to 70°C. Appropriate volume of Oligotex suspension (15 – 55 µl) and 500 µl OBB buffer (binding buffer) was added to the samples, mixed by pipetting, incubated for 3 min at 70°C in a water bath, and then placed at room temperature for 10 minutes to allow hybridization between the poly-A tail of the mRNAs and the oligo dTs of the Oligotex suspension. The samples were centrifugated for 2 min at 13000 x g, the supernatant was removed by pipetting, the mRNA pellet was resuspended in 400 µl OW2 buffer (wash buffer), transferred to a spin column (placed in a 1.5 ml microcentrifuge tube), and centrifugated again for 1 min at 13000 x g. The columns were put on new 1.5 ml microcentrifuge tubes, the mRNA complexes washed again with 400 µl OW2 buffer, centrifugated for 1 min, and the flow-through discarded. Finally, the spin columns were transferred to new 1.5 ml microcentrifuge tubes and the Poly(A)$^+$ RNAs were eluated with 20-100 µl OEB buffer. The purity and concentration of the Poly(A)$^+$ RNA were measured at 260 nm in a spectrophotometer as described above.

**Oligotex kit provides oligotex suspension, OBB buffer, OEB buffer, and OW2 buffer.*

3.3 Northern Blot

To determine the size of the Slc10a4 and Slc10a5 transcripts and to identify alternatively spliced transcripts, northern blots were performed using different rat tissues. Poly(A)$^+$ RNA samples were blotted onto nylon membranes, hybridized with radiolabeled probes, and visualized by autoradiography.

3.3.1 Preparation of radiolabeled cDNA probes

Rat cDNA probes were generated by PCR using 50 pg of pBluescript (Stratagene, Heidelberg, Germany) containing Slc10a4, Slc10a5 or GAPDH sequences in the MCS and primers were described under 2.2.1. The thermocycling conditions were: 1 cycle of 94°C x 2min; 10 cycles of 94°C x 15s, 58.7°C x 30s minus 0.5°C each cycle, and 72°C x 30s; 25 cycles of 94°C x 15s, 53.7°C x 30s, and 72°C x 30s plus 5s each cycle; and final extension of 72°C x 10 min. PCR products were purified with the High Pure PCR Product Purification Kit (Roche, Mannheim, Germany) and then the nick translation kit (Amersham Biosciences, Freiburg, Germany) was used to incorporate α[^{32}P]-dCTP into the amplified fragments.

3.3.2 Blotting and hybridization

After purification of Poly(A)$^+$ RNA, 3 µg from different rat tissues (brain, heart, liver, lung, skeletal muscle and spleen) were denatured in RNA sample buffer for 5 min at 65ºC and subjected to electrophoresis in a 1.0% agarose-formaldehyde gel. Then, RNAs were transferred to a nylon membrane (Hybond-N: Amersham Biosciences, Freiburg, Germany) overnight by capillary transfer and UV-crosslinked. The membranes had been prehybridized for 30 minutes at 42ºC in a solution containing 50% deionized formamide, 5X SSPE buffer, 2X Denhardt´s Reagent, and 0.1% SDS, and hybridized at 42ºC overnight in the same buffer containing the radiolabeled [^{32}P]-Slc10a4, [^{32}P]-Slc10a5, or [^{32}P]-GAPDH probes. After hybridization, membranes were washed twice with stringency wash solution I at room temperature for 5 min, twice with stringency wash solution II at 65ºC for 15 min, and once with 2X SSC at room temperature for 10 min to remove excess of SDS. Finally, hybridized membranes were exposed to autoradiography film for 2 - 4 days at – 70°C.

3.4 cDNA Synthesis

To analyse gene expression and for cloning of the Slc10a4 and SLC10A5/Slc10a5 ORF sequences, Poly(A)$^+$ RNA was reverse transcribed into cDNA using the Advantage RT-for-PCR Kit (Clontech). This kit provides MMLV reverse transcriptase, and an oligo $(dT)_{18}$ primer, which converts the entire population of mRNA into a pool of cDNA molecules.

Briefly, 1 µg of total or Poly(A)$^+$ RNA was diluted into DEPC-treated water to a total volume of 12.5 µl and 1 µl oligo $(dT)_{18}$ primer was added. The samples were heated at 70°C for 2 min and then 4 µl 5X reaction buffer, 1 µl dNTP mix, 0.5 µl Recombinant RNase inhibitor, and 1 µl MMLV reverse transcriptase were added into each reaction tube. The samples were incubated at 42°C for 1 h to start the cDNA synthesis, heated at 94°C for 5 min to stop the reaction and to destroy DNase activity, and then diluted to a final volume of 100 µl using DEPC-treated water. The cDNAs were aliquoted into 10 µl portions and stored at -70°C until required.

3.5 PCR – Polymerase Chain Reaction

PCR-methodes were used to analyse the SLC10A4/Slc10a4 and SLC10A5/Slc10a5 gene expressions in human, mouse, and rat tissues, to clone the respective nucleotide sequences, and to insert the FLAG epitope or HA epitope.

3.5.1 RT-PCR

In order to identify new members of the SLC10 family, the cDNA sequences of NTCP/Ntcp and ASBT/Asbt were used as queries for a MegaBlast analysis. The MegaBlast analysis revealed

several hitherto uncharacterized cDNA sequences including GenBank accession number XM 579196 which was predicted by automated computational analysis from the rat genome, because of some homology to Ntcp. This sequence was used for an RT-PCR-based approach to obtain the full putative open reading frame (ORF) of Slc10a4 (Geyer, 2004).

The ORFs of other sequences further referred to as SLC10A5 for the human protein and the homologous sequences from rat and mouse that are further referred to as Slc10a5, were obtained using the same strategy. Oligonucleotide primers were designed for PCR amplification based on cDNA sequences of GenBank accession nos. XM_376781 and XM_143078 (primers described into material part, 2.1.4 Primers for cloning). RT-PCR was performed from 1 µg human and mouse liver Poly(A)$^+$RNA (Clontech) using the Expand High Fidelity PCR system (Roche, Mannheim, Germany) according to the following thermocycling conditions: 1 cycle of 94°C x 2 min; 10 cycles of 94°C x 15 s, 60°C x 30 s minus 0.5°C each cycle, and 72°C x 1 min; 30 cycles of 94°C x 15 s, 55°C x 30 s, and 72°C x 1 min plus 5 s each cycle; and a final extension of 72°C x 10 min. We obtained SLC10A5/Slc10a5 amplicons of ~1300 bp which were gel purified and cloned downstream from the T3 promoter into pBluescript (Stratagene, Heidelberg, Germany).

In order to obtain the Slc10a5 orthologue from rat, too, the same approach was used as described above using RT-PCR amplification of 1 µg rat small intestine Poly(A)$^+$RNA with the following primers: 5'-atg tct gga aaa ctt ttc ata att c-3' forward and 5'- tta aac gag agg agc ctt ttc-3' reverse.

3.5.2 Real time quantitative PCR

Quantitative expression analyses were performed using cDNA panels of 12 human tissues, 9 rat tissues, and 18 mouse tissues (Clontech, Heidelberg, Germany) and ABI PRISM 7300 technology (Applied Biosystems, Darmstadt, Germany). The PCR amplification was performed with TaqMan gene expression assays described under material (2.1.3 TaqMan gene expression assays for quantitative real time PCR). For endogenous control, expression of β- actin was analyzed in each tissue using expression assays for human, rat, and mouse tissues. For each tissue, quadruplicate determinations were performed in a 96-wells optical plate using 5 µl cDNA, 1.25 µl TaqMan gene expression assay, 12.5 µl of TaqMan Universal PCR Master Mix, and 6.25 µl of water in each 25 µl reaction. Plates were heated for 10 min at 95°C, and then 45 cycles of 15 s at 95°C and 60 s at 60°C were applied. Relative SLC10A4/Slc10a4 and SLC10A5/Slc10a5 expressions (ΔC_T) were calculated by subtracting the signal threshold cycle (C_T) of the endogenous control β-actin from the C_T value of SLC10A4/Slc10a4 and SLC10A5/Slc10a5, respectively. Then $\Delta\Delta C_T$ values were calculated by subtracting the ΔC_T value of the organ with the lowest expression of each panel from the ΔC_T value of each individual tissue and transformed by the equation $2^{-\Delta\Delta CT}$.

3.5.3 Site-directed mutagenesis by PCR to insert FLAG and HA epitopes

In order to evaluate whether the Slc10a4 and SLC10A5/Slc10a5 proteins were expressed at the plasma membrane of *Xenopus laevis* oocytes, the Slc10a4 cDNA and SLC10A5/Slc10a5 cDNAs were extended at the 3' end by the sequence 5'-gat tac aag gat gac gac gat aag-3' coding for the FLAG epitope (DYKDDDDK). Sequence insertion was performed by QuickChange site-directed mutagenesis kit (Stratagene, Heidelberg, Germany) using 125 ng oligonucleotide primers (see 2.1.5 Primers for sequence insertion of the FLAG epitope), 50 ng plasmid DNA, 5 µl reaction buffer (10x), 1 µl dNTP mix, double distilled water (to a final volume of 50 µl), and 1 µl PfuTurbo DNA polymerase. The cycling parameters for the reactions were: 1 cycle of 95°C x 30 s; 18 cycles of 95°C x 30 s, 55°C x 1 min, and 68°C x 4.5 min. After PCR, the samples were digested with 1 µl *Dpn*I to degradate the methylated parental DNA template, and transformed into XL1-Blue supercompetent cells. The cells were thawed on ice, 50 µl aliquots were transferred to prechilled 14 ml Falcon tubes, and 1 µl *Dpn*I-treated DNA was added. The reactions were gently mixed and incubated on ice for 30 min. Subsequently, the samples were placed in a water bath at 42°C for 45 s, incubated on ice for 2 min, and 0.5 ml of NZY^+ broth was added. Finally, the reactions were incubated at 37°C/225 rpm for 1 h, and plated on LB-agar plates supplemented with ampicilin. Plasmids were isolated (see 3.1.5) and sequence verification was carried out by SeqLab Laboratories.

Using the same method as described for FLAG-tag insertion, the HA epitope (YPYDVPDYA) was inserted between amino acid residues 57 and 58 of the Slc10a4-FLAG protein and the construct was used to clarify the membrane topology of Slc10a4 when expressed in the HEK293 cells (see 2.1.6 Primers for sequence insertion of the HA-epitope).

To verify the insertion of the FLAG-epitope or HA-epitope coding sequences, a RT-PCR was performed using the primers described under 2.1.8. Samples were controlled by agarose-gel electrophoresis.

3.6 Cloning

After RT-PCR, the SLC10A5/Slc10a5 amplicons of ~1300 bp were purified using the High Pure PCR Product Purification Kit (Roche, Mannheim, Germany) and digested with the restriction enzymes previously selected during the primers' design (see 2.1.4, 2.2.5, and 3.1.4). Subsequently, the amplicons were retrieved from the previous agarose-gel electrophoresis, purified with the Qiaex II Gel Extraction Kit (Qiagen, Hilden, Germany), and controlled by electrophoresis. To insert the amplified DNAs into the bacteria plasmids (pBlue-PolyA-*Xba*I), ligation was carried out to join the complementary sticky ends into the vector. The reaction was performed according to the Rapid DNA Ligation Kit (Roche, Mannheim, Germany). Protocol as follows:

Desired Insert	2 µl
Plasmid DNA	6 µl
DNA (2) Buffer (2x)	2 µl
DNA Ligase Buffer (2x)	10 µl
T4 DNA Ligase	1 µl

After addition of the ligase, the mixture was incubated at room temperature for 1 h and subsequently, at 14°C overnight.

To transform electrocompetent *Escherichia coli* (*E.coli*), the plasmids were previously purified by High Pure PCR Product Purification Kit (Roche, Mannheim, Germany) to remove salt and impurities from the ligation reaction. Briefly, 10 µl each plasmid DNA was added to 100 µl *E.coli*, incubated on ice, the mixtures were transferred to cooled electroporation cuvettes, placed in the electroporator, and submitted to electroporation, where cells allow to uptake foreign plasmids by increase of permeability of the plasma membrane and electrical conductivity caused by an applied electrical field. The settings for electroporation were: voltage, 2.5 kV; capacitance, 25 µF; resistance, 200 Ω; and time constant ≥ 4 ms. Then, 1 ml SOC medium was added to the cell suspension, the cells were incubated at 37 C for 1 h, centrifugated for max. 20 s, and the pellets were resuspended in 250 µl SOC medium. The cells were plated and grown at 37°C for 12-16 hours.To select the positive clones, LB-agar plates were prepared with X-Gal (5-bromo-4-chloro-3-indolyl-β-D-galactopyranoside) and IPTG (isopropyl-β-D-thiogalactopyranoside) to enable the blue/white screening of positive clones. The pBlue-PolyA-*Xba*I plasmid contains, at the multiple cloning sites, the LacZ gene, which codes for the enzyme β-galactosidase. This enzyme converts the colorless substrate X-Gal into a bright blue product (5-bromo-4-chloro-indigo). IPTG was added to the medium in order to activate the *lac* operon and subsequently induce β-galactosidase production. Nonrecombinant plasmids produce normal enzyme activity, however when the ligation with insert DNA occurs, the LacZ gene is disrupted and the β-galactosidase production is discontinued. Therefore, white bacterial colonies (positive colonies) are observed. If the vector religates without the insertion of desired DNA blue colonies are visualized (negative colonies).
Several positive colonies were picked using sterile plastic pipette tips and grown over night at 37°C/225 rpm for 12-16 h in 5 ml LB-broth supplemented with ampicilin. Plasmid preparations were performed as described under 3.1.5. Three clones of each species were sequenced on both strands by SeqLab (Göttingen, Germany) or GENterprise (Mainz, Germany), and the sequences were deposited into the GenBank database with accession nos. AY825924 for human SLC10A5 and AY825925 for mouse Slc10a5.
In order to obtain the Slc10a5 orthologue from rat, too, the same approach as described above was used. After RT-PCR amplification of 1 µg rat small intestine Poly(A)$^+$RNA with the primers 5'-atg tct gga aaa ctt ttc ata att c-3’ forward and 5’- tta aac gag agg agc ctt ttc-3’ reverse, the rat

Slc10a5 PCR amplicon of ~1300 bp was gel purified and ligated into pGEM-T (Promega, Mannheim, Germany). Three clones were sequenced on both strands and the sequence was deposited into the GenBank database with accession no. DQ074435. For *in situ* hybridization experiments, this Slc10a5-pGEM-T construct was used. For expression experiments in *Xenopus laevis* oocytes, the full length rat Slc10a5 cDNA sequence was subcloned into pBluescript as described above.

3.7 Heterologous Expression in *Xenopus laevis* Oocytes for Transport

The Slc10a4- and SLC10A5/Slc10a5-pBlue-PolyA constructs with or without the FLAG-epitope were expressed in *X.laevis* oocytes in order to verify whether these exogenous proteins were inserted in the plasma membrane and show transport function.
The pBlue-PolyA vector contains a T3 RNA polymerase promoter site that was used for the *in vitro* transcription, as well as a polyA sequence at the 3' end of the multiple cloning site that rendered stabile transcribed cRNAs for expression in oocytes.

3.7.1 Linearization of plasmid DNA

To linearize the plasmid samples, the DNA templates were digested with the restriction enzyme *Xho*I, which cut the pBlue-PolyA plasmid after its polyA tail. The reaction was performed as follows:

Plasmid DNA	5 µg
NEBuffer 2	10 µl
BSA	1 µl
Enzyme *Xho*I	3 µl
H_20 added to a final volume of 100 µl and reaction was incubated over night at 37°C.	

Then, the digested DNAs were cleaned from the restriction enzyme and respective buffer by phenol/chloroform extraction and precipitated with ethanol. Pellets were resuspended in 5.5 µl TE-buffer at room temperature for 30 min, 0.5 µl was analyzed by agarose-gel electrophoresis and 5 µl used to cRNA synthesis.

3.7.2 cRNA synthesis

For cRNA synthesis, the Riboprobe *in vitro* Transcription System (Promega, Mannheim, Germany) was used. The following components were added to the reaction to generate a 5'-capped cRNA from the T3 promoter:

Transcription Optimized 5x Buffer	10 µl
DTT,100mM	5 µl
RNasin	5 µl
rATP, rCTP, rUTP each	2.5 µl
rGTP	0.5 µl
Cap Analog, 5mM	5 µl
Linearized template DNA [1 µg/µl]	5 µl
T3 RNA Polymerase	2 µl
Nuclease-Free Water to a final volume of 50 µl	

The reaction was incubated at 37°C for 1 h, and 1 µl DNase I was added to remove the template DNA. After incubation at 37°C for 15 min, the reaction was stopped with 75 µl nuclease-free water and 25 µl TE-buffer. Samples were cleaned twice by phenol/chloroform extraction, and the aqueous phases were purified using G-50 sephadex columns. Subsequently, cRNAs were precipitated with 13 µl of 3M sodium acetate and 390 µl of 100% chilled ethanol, and incubated at -80°C for 2 h. Samples were centrifugated at room temperature / 13200 rpm for 30 min, and supernatants were removed. The pellets were dried by Speed-Vac centrifugation for 3 min and resuspended in 10 µl RNase-free water for 30 min on ice. Concentration and purity of cRNAs were determinated by photometer using 1 µl each sample, and another 1 µl was used to check the quality of cRNAs by an agarose-gel electrophoresis. Finally, the samples were diluted to a concentration of 0.1 µg/ µl and stored at -80°C.

3.7.3 Frog surgery and preparation of oocytes

Oocytes were extracted from adult female *Xenopus laevis* frogs. The animals were anesthetized by immersing in 1 % aminobenzoic acid ethyl ester (MS-222) in water. The frogs were placed side up on ice to maintain anesthesia during the surgical procedure. Using scalpel, 1 cm incision in the lower abdominal wall (near one leg) was made and the ovarian lobes were exposed. Oocytes were carefully removed and placed in sterilized OR2 buffer. Then, the abdominal wall and the skin were sutured separately with 4.0 Vicryl and skin clips and the frogs returned to anesthetic-free water for recovery.

Isolated oocytes were incubated in 2 mg/ml collagenase D/OR2 buffer at 18°C for 45 min with gentle agitation to permit defolliculation. Then, oocytes were washed five times with OR2 buffer

and five times with modified Barth's solution. Oocytes were transferred to a Petri dish and selected for quality.

3.7.4 Microinjection

After oocytes selection, the microinjection was done using a nanoliter 2000 oocyte microinjector. Approximately 46 nl (4.6 ng) of each cRNA was injected in the “vegetal” white pole of defolliculated oocytes. NTCP cRNA expression was used as positive control, and water injection as negative control. Injected oocytes were kept at 18°C in sterile modified Barth's solution supplemented with gentamicin with daily solution changes.

3.8 Functional Characterization

After 3 days of culture, intact oocytes were selected for transport experiments. They were washed in an ice-cold medium (see sodium solution, item 2.3.2), transferred to 2 ml microcentrifuge tubes containing 50 µl sodium solution, and set on ice until transport measurements.
The ethanol diluted radiolabeled substrates were vaporizated by nitrogen gas, and 50 µl sodium solution containing the desired concentration of non-labeled substrates was added. Then, uptake of radiolabeled substrates ([1,2,6,7-^{3}H(N)]dehydroepiandrosterone sulfate, [6,7-^{3}H(N)]estrone-3-sulfate, [^{3}H]taurocholate, and [^{14}C]Cholate) was measured at 25°C for 60 minutes in 100 µl solution. The reaction was stopped with 1.5 ml ice-cold sodium solution and the oocytes were washed three times with the same buffer. Subsequently, each individual oocyte was dissolved in 500 µl of 10% SDS and 4 ml scintillation fluid. They were mixed on a vorterx, and the radioactivity was counted in a liquid scintillation counter.

3.9 Immunofluorescence Detection of the Slc10a4-FLAG and SLC10A5/ Slc10a5- FLAG Proteins in *Xenopus laevis* Oocytes

Three days after cRNA injection, the vitelline membrane was removed, and the oocytes were fixed in a solution of 80% methanol / 20% dimethylsulfoxide (v / v). Oocytes were washed in decreasing concentrations of methanol (90%, 70%, 50%, and 30%) in phosphate buffered saline (PBS; containing 137 mM NaCl, 2.7 mM KCl, 1.5 mM KH_2PO_4, and 7.3 mM Na_2HPO_4, at pH 7.4). They were then incubated with the mAb M2-anti-FLAG (Sigma-Aldrich, Taufkirchen, Germany) overnight at 4°C in blocking solution (1% BSA and 4% goat serum in PBS) at a 1:1000 dilution. Oocytes were washed 11 times with PBS and were incubated with the Alexa-Fluor-488-labeled goat anti-mouse IgG secondary antibody (Molecular Probes) at a 1:500 dilution in blocking solution for 2 h at room temperature. After a second washing (6 x with PBS), the oocytes were fixed with 3.7%

formaldehyde in PBS and washed with increasing concentrations of ethanol (30%, 50%, 70%, and 100%) in PBS. The oocytes were embedded in Technovit 7100 (Heraeus Kulzer), and 5 µm sections were cut. Fluorescence imaging of the Slc10a4-FLAG, and SLC10A5/Slc10a5-FLAG proteins was performed with a Leica DM6000B fluorescence microscope (Leica, Bensheim, Germany) at 488 nm excitation wavelength.

3.10 Subcloning into pcDNA 5/TO

The rat Slc10a4-FLAG, human SLC10A5-FLAG, and mouse/rat Slc10a5-FLAG cDNA sequences were excised from the pBluescript plasmid or pGEM-T plasmid (only rat Slc10a5-FLAG) and subcloned into the mammalian expression vector pcDNA5/TO (Invitrogen, Karlsruhe, Germany) downstream of the CMV/*tetO*$_2$ promoter for expression in human embryonic kidney 293 cells (HEK293). The primers designed for this experiment are described under item 2.1.7 (Primers for subcloning in the vector pcDNA5/TO).

3.11 Transient Transfection into HEK293 Cells

MSR-GripTite HEK293 cells (Invitrogen, Karlsruhe, Germany) were seeded in 24-well plates at a density of 4 x 10^5 cells per well on poly-D-lysine coated glass coverslips and grown to ~80-90% confluency in antibiotic-free D-MEM/F12 medium (Gibco, Karlsruhe, Germany) supplemented with 10% fetal calf serum (Sigma-Aldrich, Taufkirche, Germany) and 2 mM L-glutamine. Cells were transfected using 1 µg of desired plasmid DNA to 2 µl lipofectamine 2000 (ratio 1:2). For each transfection sample, plasmid DNAs and lipofectamine were diluted separately to a final volume of 50 ml medium. After five minutes incubation at room temperature, the diluted lipofectamine was added to the diluted DNA, and the mixture was incubated for 30 minutes. Then, 100 µl of liposome complexes were added to each well. The cells were incubated at 37°C in a CO_2 incubator and the medium was replaced after 6 hours.

3.12 Immunofluorescence Detection of the HA-Slc10a4-FLAG Protein in HEK293 Cells

Cells were transfected with 1 µg of HA-Slc10a4-FLAG vector DNA by lipofectamine 2000 reagent, as described above. The parental pcDNA5/TO vector lacking any insert was used as the control. After 6 h, the medium was changed to standard medium (D-MEM/F12 supplemented with 10% fetal calf serum, 2 mM L-glutamine, 100 U/ml penicillin, and 100 µg/ml streptomycin), and expression of the HA-Slc10a4-FLAG protein was induced by tetracycline treatment (1 µg/ml). One day after transfection, the cells were washed with PBS, fixed with 4 % paraformaldehyde in PBS for 15 min at 4°C, again washed with PBS, and incubated with 20 mM glycine in PBS for 5 min.

Subsequently, a part of the transfected HEK293 cells was permeabilized for 5 min in PBT buffer (0.2% Triton X-100 and 20 mM glycine in PBS) and nonspecific binding sites were blocked with 1% BSA (Roche, Mannheim, Germany) plus 4% goat serum (Dako, Hamburg, Germany) in PBS for 30 min at room temperature. Non-permeabilized cells were not treated with PBT. Then, cells were incubated with the primary antibodies, rabbit anti-FLAG (0.025 µg/ml, Sigma-Aldrich, Taufkirche, Germany), and mouse anti-HA (1:200 dilution, Roche, Mannheim, Germany) in blocking solution overnight at 4°C. The next day, the cells were washed three times with PBS and incubated with the fluorophor-labeled secondary antibodies: goat Cy3-conjugated anti-rabbit IgG (1:800 dilution, Jackson ImmunoResearch, Northfield, UK) and goat Alexa-Fluor-488-conjugated anti-mouse IgG (1:200 dilution, Molecular Probes, Karlsruhe, Germany) in blocking solution for 60 min at room temperature. After a final washing step with PBS, the cells were covered with a DAPI / methanol solution containing 1 µg/ml DAPI (Roche, Mannheim, Germany) and incubated for 5 min at room temperature. The cells were rinsed with methanol, air dried, and mounted onto slides with Mowiol mounting medium (Calbiochem, Darmstadt, Germany). Immunofluorescence was viewed on a Leica DM6000B fluorescence microscope, and cell images were analyzed with the Leica FW4000 Fluorescence Workstation software (Leica, Bensheim, Germany).

3.13 *In situ* Hybridization of Slc10a5 in Rat Liver and Kidney Sections

In order to visualize the Slc10a5 gene expression in rat liver and kidney, *in situ* hybridization was performed. This method was introduced by Gall and Pardue, 1969; John et al., 1969, and Buongiorno-Nardelli and Amaldi, 1970. It consists of the use of labeled oligonucleotide probes to detect and localize specific DNA or RNA sequences in a tissue or on a chromosome.

3.13.1 Production of digoxigenin-labeled cRNA probes

DIG-labeled rat Slc10a5 cRNA-probes were synthesized from the rat Slc10a5-pGEM-T plasmid. Plasmid DNA was digested with *Sac*II and *Sac*I (New England Biolabs, Frankfurt am Main, Germany) for the production of the Slc10a5-sense-cRNA and Slc10a5-antisense-cRNA, respectively. Subsequently, *in vitro* transcription was performed using the 10 x RNA-DIG Labeling-Mix (Boehringer, Mannheim, Germany) by T7-RNA polymerase and SP6-RNA polymerase (Promega, Mannheim, Germany). The reaction was performed as follows:

DEPC treated water	8 µl
5x transcription buffer	4 µl
10x DIG RNA labelling mix	2 µl
100x DTT	2 µl
Plasmid (after single digestion)	2 µl
RNA polymerase SP6 / T7	7 µl

The reaction was incubated at 37°C for 1 h in a water bath, then 0.5 µl 0.5 M EDTA, 1.2 µl 8 M LiCl, and 70.7 µl 96% ethanol (-20°C) were added and the samples were stored at -80°C for 1 h. Subsequently, samples were centrifugated at 13000 rpm /4°C for 15 min, the supernatant was discarded, 200 µl 75% ethanol (-20°C) was added, the samples were centrifugated again as above, and the pellets were dried at 37°C. Then, samples were resuspended with 50 µl of dH_20. For alkaline hydrolysis, 30 µl of 2 M sodium carbonate (Na_2CO_3) and 20 µl of 2 M sodium bicarbonate ($NaHCO_3$) were added and the probes were incubated at 60ºC for 1 h. The reaction was stopped by adding 3 µl of 3 M sodium acetate, pH 6.0, and 5 µl 10% glacial acetic acid and the cRNA probes were precipitate again by ethanol as described above. Finally, the samples were resuspended with 50 µl dH_20 at 70°C and stored at -20°C.

3.13.2 *In situ* hybridization

Slc10a5 *in situ* hybridization was performed in rat liver and kidney samples with normal histologies. All solutions were prepared using distilled deionized water that was treated with 0.1% diethylpyrocarbonate (DEPC). To prevent RNase contamination, both gloves and sterile glasswares were used during the handling of the samples.

The slices and the xylene cuvette were incubated at 60°C overnight. At the next day, the tissue sections were deparaffinized and rehydrated with alcohol series: with xylene, sections were initially washed at 60°C and twice washed at room temperature for five minutes. Then, they were twice washed with 100% ethanol, once with 96% ethanol, and once with 70% ethanol at room temperature for five minutes. Subsequently, using a sterile cuvette, tissue sections were washed with DEPC treated water. They were incubated at room temperature for 20 minutes in 0.2 N HCl, in 2xSSC buffer at 70°C for 15 min and shortly in PBSM-buffer.

To promote an access of the labelled probes into the cells, the tissues were permeabilized with RNase-free proteinase K ([20 µg/µl] for kidney sections and [2 µg/µl] for liver sections) at 37°C for 25 min. The reaction was stopped with 0.2% glycine incubation for 5 minutes and the endogenous phosphatase was blocked by washing slices with 20% acetic acid and with PBSM buffer.

In order to better fix the mRNAs onto slides, post fixation was carried out. Slides were incubated for 10 minutes in 4% paraformaldehyde. For pre-hybridization, the slices were washed shortly in PBSM buffer, and incubated in 20% glycerol for 1 h. To start the hybridization, the DIG-labeled probes and hybridization buffer were prepared as follows:

DIG-labelled probes	
DEPC treated water	4 µl
Salmon-sperm DNA [1 mg/ml]	4 µl
Yeast-t-RNA [1 mg/ml]	8 µl
DIG-cRNA probe	4 µl

Hybridization buffer	
DEPC treated water	25 µl
20xSSC buffer	40 µl
50% Dextrane sulphate	80 µl
Denhardt's reagent	8 µl
Formamide	200 µl

The labeled probes and hybridization buffer were mixed and put on slices. The slices were placed on the heating surface for 10 min at 70°C for denaturation. Then, they were put on ice and the hybridization occurred at 42°C overnight in a humid chamber (DEPC treated water).
To eliminate non-specific binding, the slices were submitted to a posthybridization step. They were washed three times with 4x SSC buffer at room temperature for 10 min, four times with 4 x SSC buffer at 47°C for 5 min, once with 2 x SSC buffer at 65°C for 15 min, once with 0.2 x SSC buffer at 47°C for 5 min once with 0.1 x SSC buffer at room temperature for 5 min, and once with 2 x SSC buffer at room temperature 5 min.
For immunohistochemistry, the slices were washed with TNMT buffer at room temperature, pre-incubated with 3% BSA/TNMT buffer, and incubated with anti-DIG-antibody (dilution 1:500 in TNMT buffer) at 4°C overnight in a humid chamber. At the next day, slices were washed two times with TNMT buffer for 10 minutes, and staining was visualized by developing sections with nitroblue-tetrazolium/5-bromo-4-chloro-3-indolyl-phosphate in a humidified chamber protected from light. Finally, the sections were mounted in Glycergel (Dako, Hamburg, Germany).

3.14 Slc10a4 Antibody Generation

The polyclonal rabbit anti-Slc10a4 antiserum used in this study was raised against amino acid residues 422-437 of the deduced Slc10a4 protein sequence (VGTDDLVLMETTQTSL, GenBank accession no. **AAV80706**). The synthetic peptide was coupled *via* the carboxy-terminal glutamic acid residue to keyhole limpet hemocyanin and used to immunize two rabbits (Eurogentec, Seraing, Belgium). Antigenicity of the rabbit serum was confirmed by ELISA analysis using the synthetic peptide as antigen and the polyclonal antiserum was affinity-purified (Eurogentec). An overview of the Slc10a4-peptide and Slc10a4-antisera syntheses are shown in the figure 4.

3.15 Western Blot Analysis

HEK293 cells were grown in six-well plates to 90% confluence and transiently transfected with 4 µg of the Slc10a4-FLAG-pcDNA5 construct or pcDNA5 empty vector as described above. After

6 h, 1 µg/ml tetracycline was added to the medium for protein induction. Two days later, the cells were washed with PBS and lysed in ice-cold RIPA buffer containing 150 mM NaCl, 50mM Tris·HCl (pH 8.0), 1% Nonidet P-40, 0.5% (w / v) sodium deoxycholic acid, 0.1% (w / v) SDS, and protease inhibitor cocktail (Sigma-Aldrich). Cell lysates were cleared by centrifugation, and the protein content was determined using the BCA Protein Assay Kit (Novagen, Darmstadt, Germany). Samples of 15 µg protein were boiled for 10 min in Laemmli sample buffer (Sigma-Aldrich), separated on 12% SDS polyacrylamide gel, and transferred to nitrocellulose membrane (Schleicher&Schuell, Dassel, Germany). ReadyBlot Adult Rat Brain Protein Explorer prefabricated blots (Alpha Diagnostics, San Antonio, USA) were used for Slc10a4 expression analysis in different regions of rat CNS. All the blotted membranes were blocked with blocking solution containing 5% (w / v) ECL-blocking agent (Amersham Biosciences, Freiburg, Germany) in TBS-T (137 mM NaCl, 10 mM Tris, pH 8.0, 0.05% Tween-20). The membranes were then incubated overnight at 4°C with the mouse anti-FLAG antibody (dilution 1:3000; Sigma-Aldrich), rabbit anti-Slc10a4 antiserum (dilution 1:10000), or rabbit anti-ß-actin antiserum (dilution 1:500; Sigma-Aldrich), diluted in TBS-T. The specificity of the affinity-purified anti-Slc10a4 antiserum was verified by preincubation with a 100-fold molar excess of the $Slc10a4_{422-437}$ synthetic peptide, diluted in TBS-T for 60 min at 4°C. After washing, the membranes were probed with the appropriate horseradish-peroxidase-labeled secondary antibodies for 60 min at room temperature. Signals were developed using the ECL detection kit and visualized by exposure to Hyperfilm ECL (Amersham Biosciences).

3.16 Immunohistochemical Analysis of Slc10a4 in Rat CNS

3.16.1 DAB staining

For Slc10a4 immunohistochemistry, male Wistar rats were deeply anesthetized by an intraperitoneal injection of 180 mg/kg sodium-pentobarbital (Nacoren; Merial, Hallbergmoos, Germany). The animals were then perfused transcardially with 500 ml of 0.9% NaCl at a pressure of 120 mmHg (Transcard-pump; Max-Planck Institute, Bad Nauheim, Germany), followed by 200-300 ml of 4% paraformaldehyde in 0.1 M Sørensen phosphate buffer (PB), pH 7.4, at 4°C. The brain and spinal cord were quickly dissected and postfixed in the same fixative at 4°C for 2 h, cryoprotected overnight with 20% sucrose solution and frozen in powdered dry ice. In order to locate Slc10a4 expression throughout the CNS in a first experimental approach, serial coronal sections (40 µm) were obtained on a freezing microtome (model 1205; Jung, Heidelberg, Germany). The “free-floating” sections were washed in PB (30 min) and pre-incubated with PB containing 10% normal horse serum (PAA Laboratories, Linz, Austria) and 0.3% Triton X-100, for 60 min at room temperature. Tissue sections were subsequently incubated for 48 h at 4°C with the rabbit anti-Slc10a4 antiserum (1:1000 dilution in 2% normal horse serum and 0.1% Triton-X 100 in

PB = immunobuffer), rinsed three times (5 min each) with PB, and then transferred to immunobuffer containing biotinylated goat anti-rabbit IgG antiserum at 1:200 dilution (Chemicon, Hampshire, UK) for 60 min at room temperature. Finally, the sections were incubated for 60 min with the avidin / biotin / horseradish peroxidase complex (Vectastain Elite ABC Kit, Linaris Biologische Produkte, Wertheim, Germany), which was visualized by diaminobenzidine hydrochloride (0.5 mg/ml) reaction (Sigma-Aldrich) in the presence of 0.01 % hydrogen peroxide. Some sections were counterstained with cresyl violet, and coverslips were applied with Entellan (Merck, Darmstadt, Germany) for light microscopic analysis (BX50, Olympus Optical, Hamburg, Germany). To verify specificity of the Slc10a4 antiserum, control experiments were performed with pre-absorption of the antiserum with 100-fold molar excess of the synthetic Slc10a4 antigen (30 min) prior to the immunohistochemical protocol.

1. Peptide design

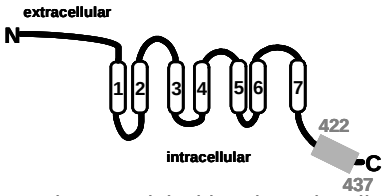

Topology model with epitope localization

2. Peptide synthesis

H_2N - VGTDDLVLMETTQTSL - COOH

Immuno-grade peptides (> 70 % purity).

After synthesis, the sequence integrity was verified by Mass Spectrometry.

3. Peptide/carrier conjugation

Slc10a4 **KLH**

The Slc10a4 peptide was coupled to the carrier protein keyhole limpet hemocyanin (KLH), which increases antigenic response to weak antigens.

KLH is a protein isolated from the marine mollusc keyhole limpet and promotes stronger immune response than BSA or OVA.

4. Rabbit immunization

Day	0	14	28	38	56	66	90	99	113
Boost No.	1	2	3		4		5		
Bleeding	PIB			SB		GP1		GP2	S

5. ELISA analysis

Protocol:

a. Coating: Antigen: Slc10a4 100 ng in PBS
Carrier: KLH 100 ng in PBS
Incubation: 25°C for 16 h

b. Saturation: Protein: BSA 1 mg/ml
Incubation: 25°C for 2 h

c. Bleeding: GP1 and GP2
Initial dilution: (line A) 1:100
Incubation: 25°C for 2 h

d. 2.Antibody: anti-rabbit-IgG-HRP conjugate (Sigma)
Dilution: 1:1000
Incubation: 25°C for 2 h

e. Substrate: Ortho-phenylenediamine (OPD)
0.4 mg/ml
Incubation: 25°C for 2 h
Stop: H_2SO_4 4 M

f. Analysis: Wavenlength: 492 nm

		Against Peptide								Against Carrier			
		1337				1338				1337		1338	
		GP 1		GP 2		GP 1		GP 2		GP 1	GP 2	GP 1	GP 2
Dilution		1	2	3	4	5	6	7	8	9	10	11	12
100	A	3,262	3,226	3,616	3,609	3,562	3,562	3,632	3,639	3,662	3,636	3,658	3,641
300	B	2,658	2,695	3,584	3,595	3,562	3,625	3,642	3,631	3,695	3,676	3,642	3,683
900	C	1,325	1,325	3,221	3,189	3,023	3,125	3,535	3,553	3,625	3,640	3,658	3,674
2700	D	0,752	0,759	1,712	1,738	2,036	2,225	3,120	3,034	3,656	3,625	3,689	3,693
8100	E	0,352	0,365	0,773	0,748	1,069	1,169	2,008	1,820	3,326	3,364	3,225	3,215
24300	F	0,192	0,182	0,333	0,328	0,541	0,549	0,942	0,843	2,023	2,060	2,015	2,025
72900	G	0,098	0,099	0,244	0,254	0,239	0,267	0,449	0,412	0,036	0,048	0,048	0,042	- contr.
218700	H	0,086	0,086	0,133	0,131	0,125	0,152	0,234	0,224	1,695	1,596	1,841	1,693	+ contr.

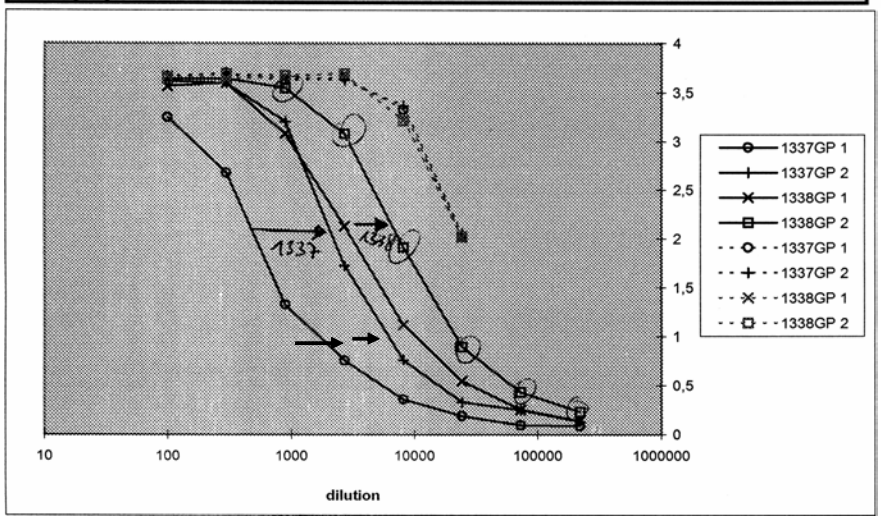

Rabbit antibody levels against peptide (straight line) and carrier (discontinuous); GP1: Large taking of blood 1, GP2: Large taking of blood 2; 1337 – rabbit 1, 1338 – rabbit 2.

⬇

6. Affinity purification of the Slc10a4 antiserum

Affinity Chromatography:
Sample name: Slc10a4-1338
Injection volume: 80 µl
Run time: 20 min

⬇

7. Slc10a4 Antiserum purification analysis by ELISA

		Against Peptide									Against Carrier			
		serum (S)			col. flow-through (FT)			purif. antibodies (PA)			S	FT	peak	
Dilution		1	2	3	4	5	6	7	8	9	10	11	12	
100	A	3,666	3,663	3,6589	1,689	1,649	1,6451	3,675	3,663	3,674	3,683	3,639	3,492	
300	B	3,648	3,648	3,6344	0,852	0,889	0,953	3,67	3,691	3,663	3,69	3,611	2,01	
900	C	3,532	3,523	3,5003	0,347	0,356	0,3512	3,593	3,574	3,555	3,709	3,664	0,693	
2700	D	2,509	2,482	2,2828	0,152	0,155	0,1459	2,939	2,982	2,757	3,688	3,587	0,316	
8100	E	1,015	1,097	0,9723	0,05	0,061	0,0474	1,635	1,408	1,364	3,642	3,359	0,237	
24300	F	0,405	0,447	0,4323	0,058	0,06	0,0468	0,652	0,631	0,511	2,733	2,556	0,141	
72900	G	0,235	0,233	0,2063	0,048	0,056	0,0587	0,286	0,299	0,245	0,046	0,046	0,047	- contr.
218700	H	0,13	0,141	0,1409	0,047	0,047	0,062	0,159	0,17	0,164	1,654	1,666	1,652	+ contr.

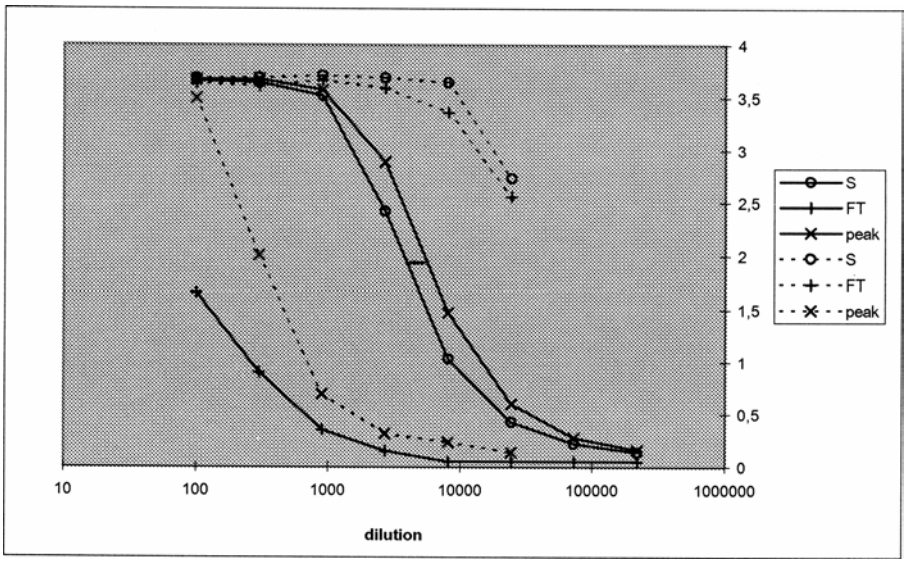

Rabbit antibody levels against peptide (straight line) and carrier (discontinuous); S: Final bleed serum, FT: Flow-through; PA: Purified antibodies. *ELISA protocol: see item 5, Bleeding: final bleed serum.*

Figure 4. The Slc10a4 peptide and antiserum made by Eurogentec, from design to purification. After Slc10a4 peptide design and synthesis, the Slc10a4 antigene was conjugated to the carrier protein KLH and used to immunize two rabbits. ELISA test was used for determining the serum antibody concentration of both rabbits and the antiserum was purified by chromatography using the sample containing the best antibody levels. After purification, the purity of the Slc10a4-antiserum was analyzed by ELISA. PIB: Pre-immune bleeding, SB: small bleeding (2 ml), GP: Large taking of blood (20 ml), S: final bleed serum (60 ml).

3.16.2 Co-localization studies with ChAT, CHT1, VAChT, and TH

Double immunofluorescence experiments were performed to elucidate the putative co-localization of Slc10a4 with ChAT, VAChT, or CHT1. Co-localization study with the catecholaminerge marker Tyrosine hydroxylase was performed in order to clarify the origin of Slc10a4 in the substantia nigra and ventral tegmental area. Serial coronal tissue sections of the whole brain and the spinal cord (16 µm) were obtained with a Microm HM-500-O cryostat (Walldorf, Germany) at -20°C and mounted on poly-L-lysine coated slides. The pre-incubation was carried out as described above, and the slide-attached tissue sections were uniformly overlayed with immunobuffer containing the rabbit anti-Slc10a4 antiserum (dilution 1:1000) in combination with either goat anti-VAChT antiserum (1:1000 dilution; Chemicon, Hampshire, UK), mouse anti-CHT1 antibody (1:500 dilution; Chemicon), mouse anti-ChAT antibody (1:250 dilution; Chemicon), or mouse anti-TH antibody (1:600, Chemicon) in a humidified chamber at 4°C for 48 h. The slides where rinsed in PB (3 x 5 min) and incubated for 2 h at room temperature with the secondary antibodies, Cy3-conjugated donkey anti-rabbit IgG (1:800 dilution; Dianova, Hamburg, Germany) and either Alexa-Fluor-488-conjugated donkey anti-goat IgG (1:500; Sigma-Aldrich, Taufkirche, Germany) or Alexa-Fluor-488-conjugated goat anti-mouse IgG (1:500; Sigma-Aldrich). After washing steps with PB, the tissues were coverslipped with Citifluor. The primary anti-Slc10a4 antiserum employed was tested for specificity by pre-incubation with the Slc10a4 antigen (see above). Omission of the antigen-specific primary antisera was used as a further immunohistochemical control experiment for each antiserum/antibody. Tissue sections were analyzed with an Olympus BX50 microscope equipped with appropriate filter sets, a spot-insight B/W digital camera (Visitron Systems; Puchheim, Germany), and the image editing software MetaMorph 5.05 (Universal Imaging Corporation, West Chester, PA).

3.17 Immunocytochemical Studies in PC12 Cell Line

In order to identify a cell line that express Slc10a4 endogenously to study it functions and possible interactions with other proteins, immunocytochemical studies were performed with PC12 cells, which is a neuroendocrine cell line derived from rat pheochromocytoma. Previously it was shown that PC12 cells express the vesicular acetylcholine transporter into synaptic-like microvesicles (SLMVs) (Liu,Y and R.H. Edwards, 1997). Cells were cultivated in D-MEM medium containing 10 % NHS, 5 % FCS, 2 % penicillin/streptomycin, and 2 % glutamine. Cells were seeded in 24-well plates at a density of 2 x 10^5 cells per well on poly-D-lysine coated glass coverslips and grown to 80-90% confluency. Then, the cells were washed with PBS, fixed with 2 % PFA in PBS for 15 min at 4°C, again washed with PBS, and incubated with 20 mM glycine in PBS for 5 min. Cells were permeabilized for 5 min in PBT buffer (0.2% Triton X-100 and 20 mM glycine in PBS) and

incubated in blocking solution containing 1% BSA (Roche, Mannheim, Germany) plus 4% goat serum (Dako, Hamburg, Germany) in PBS for 30 min at RT. Cells were incubated with the primary antibodies, rabbit Slc10a4 antiserum (1:1000 dilution), and goat anti-VAChT antiserum (1:1000 dilution, Chemicon) in blocking solution overnight at 4°C. Then, the cells were washed three times with PBS and incubated with the secondary antibodies: Cy3-conjugated donkey anti-rabbit IgG (1:800; Dianova, Hamburg, Germany) and Alexa-Fluor-488-conjugated donkey anti-goat IgG (1:500; Sigma-Aldrich) in blocking solution for 60 min at room temperature. After a final washing step with PBS, the cells were covered with a DAPI / methanol solution containing 1 µg/ml DAPI (Roche) and incubated for five min at room temperature. The cells were rinsed with methanol, air dried, mounted, and visualized as described above.

3.18 Transport Experiments into HEK 293 Cells

Transient transfection of HEK293 cells with the Slc10a4-pcDNA5, NTCP-pcDNA5, and CHT1-pcDNA5 constructs was performed as described above. Before starting the transport experiments, transfected cells were washed three times with PBS and preincubated with transport buffer (142.9 mM NaCl, 4.7 mM KCl, 1.2 mM $MgSO_4$, 1.2 mM KH_2PO_4, 1.8 mM $CaCl_2$, and 20 mM HEPES, pH 7.4). Uptake experiments were initiated by replacing the preincubation buffer with 300 µl transport buffer containing the radiolabeled test compound and were performed at 37°C. For inhibition studies, cells were preincubated with transport buffer containing 1 µM hemicholinium-3 as inhibitor for 10 min and then hemicholinium-3 was maintained during the transport experiment at equal concentration. Uptake studies were terminated by removing the transport buffer and washing five-times with ice-cold PBS. Cell monolayers were lysed in 1N NaOH with 0.1% SDS, and the cell-associated radioactivity was determined in a Wallac 1409 liquid scintillation counter (PerkinElmer, Offenbach, Germany). The protein content was determined according to Lowry et al. (1951) using aliquots of the lysed cells with BSA as the standard.

4. Results

To provide the data of this work, the results are summarized in two sections:

Sect. 4.1. The orphan carrier Slc10a4 and it expression in the central nervous system

Sect. 4.2. The novel putative bile acid transporter SLC10A5/Slc10a5

4.1 The Orphan Carrier Slc10a4 and its Expression in the CNS

4.1.1 Cloning of rat Slc10a4, sequence alignment, and structure divergence

After identification of the predicted sequence by automated computational analysis from the rat genome (GenBank accession no. XM 579196), a 1314-bp transcript was obtained from the adrenal gland using a RT-PCR based approach for cloning (Geyer, 2004). This sequence was deposited into the GenBank database with accession no. AY825923 (release date Dec 6th 2004). The cloned transcript codes for a 437 amino acid protein with a calculated molecular mass of 46.6 kDa; it is referred to as rat Slc10a4 protein. Amino acid sequence alignment revealed several highly conserved domains also found in other rat Slc10 carrier proteins Ntcp, Asbt, and Soat. However, the 'ALGMMPL' signature motif of all NTCP/Ntcp, ASBT/Asbt, and SOAT/Soat proteins (Geyer et al., 2006) is not present in the rat Slc10a4 protein sequence. Furthermore, the length of the N-terminal domain of the Slc10a4 protein clearly exceeds those of Ntcp, Asbt, and Soat by ~ 60 amino acids (Fig. 5). Slc10a4 amino acid sequence identities/similarities are almost identical to Ntcp, Asbt, and Soat, approximately 30 %/ 54%. From its structure homology with the other Slc carries it was concluded that Slc10a4 exhibits seven transmembrane domains with N- and C-terminal in a *trans* position regarding the orientation of the protein ends in the extracellular side of the membrane and cytosol, respectively. This was later verified by different transmembrane prediction computer programs (see chapter 4.1.3). For determination of putative N-glycosilation sites and serine, threonine, and tyrosine phosphorylation sites, two bioinformatic tolls were used: the NetNGlyc 1.0 Server and the NetPhos 2.0 Server. The SLC10A4/Slc10a4 proteins shown contain four conserved sites for N-linked glycosylation, where two predicted sites are located on the N-terminal hydrophilic loop (N6 and N20) and the other two sites on the second extracellular loop (N181 and N195), and three consensus sites for phosphorylation (S405, T417, and Y419) (see chapter 9.2). Studies are in progress to examine these evidences.

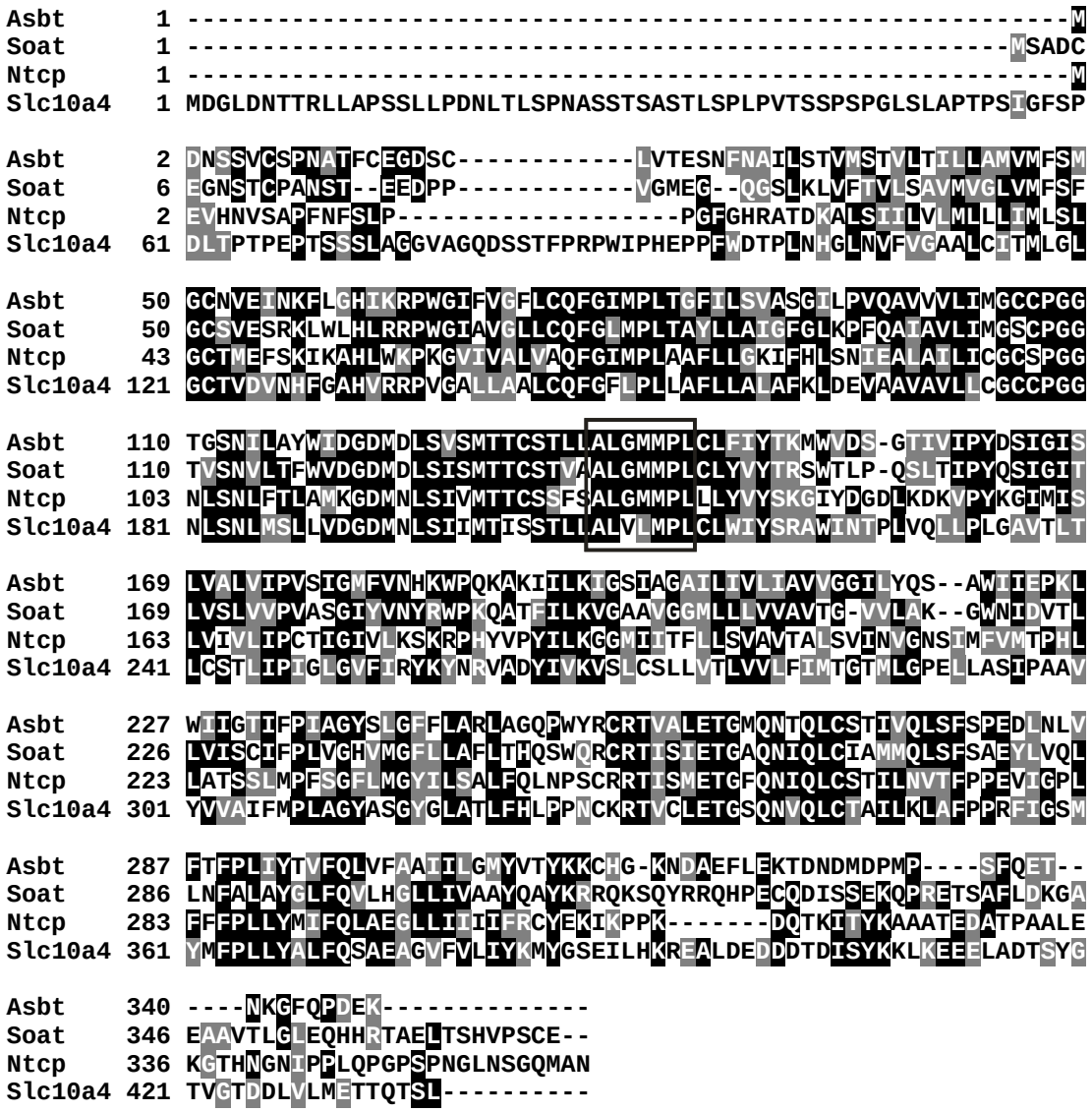

Figure 5. Amino acid sequence alignment of the rat Slc10 carriers Asbt (Slc10a2), Soat (Slc10a6), Ntcp (Slc10a1), and Slc10a4. The alignment was conducted using the *ClustalW* algorithm and was visualized by BOXSHADE 3.21. The amino acid sequence identities are displayed with black shading; amino acid similarities are highlighted in grey. Gaps (-) are introduced to optimize alignment. The signature motif of all NTCP/Ntcp, ASBT/Asbt, and SOAT/Soat proteins is highlighted.

4.1.2 Expression analysis of SLC10A4/Slc10a4 mRNAs in humans, rat, and mouse

Expression analysis of human SLC10A4 mRNA and of rat and mouse Slc10a4 mRNAs was performed with quantitative real-time PCR and northern blot (only for rat). Using qPCR, rat Slc10a4 expression was highest in the brain and was moderate in the adrenal gland, from which Slc10a4 had been cloned originally (Fig. 6A). Mouse Slc10a4 mRNA expression was also highest in the brain and significantly above background levels in the eye, prostate, and whole embryo tissue preparations (Fig. 6B). With regard to human tissues, SLC10A4 mRNA was highly expressed in brain and small intestine, and moderately expressed in colon, heart, prostate and testis (Fig. 6C).

Detailed expression analysis in the human CNS using cDNA probes from 14 different human brain regions revealed high SLC10A4 expression in both the putamen and substantia nigra, and moderate expression in the accumbens nucleus, the corpus callosum, and the spinal cord. In contrast, other limbic structures such as the hippocampus or the amygdala showed very low expression levels of human SLC10A4 mRNA (Fig. 6D). Results from northern blot experiments confirmed the high level of Slc10a4 in the rat brain and allowed to calculate the length of the rat Slc10a4 transcript to approximately 1.5 kb. No alternatively spliced transcription variants were detected for rat Slc10a4 (Fig. 7).

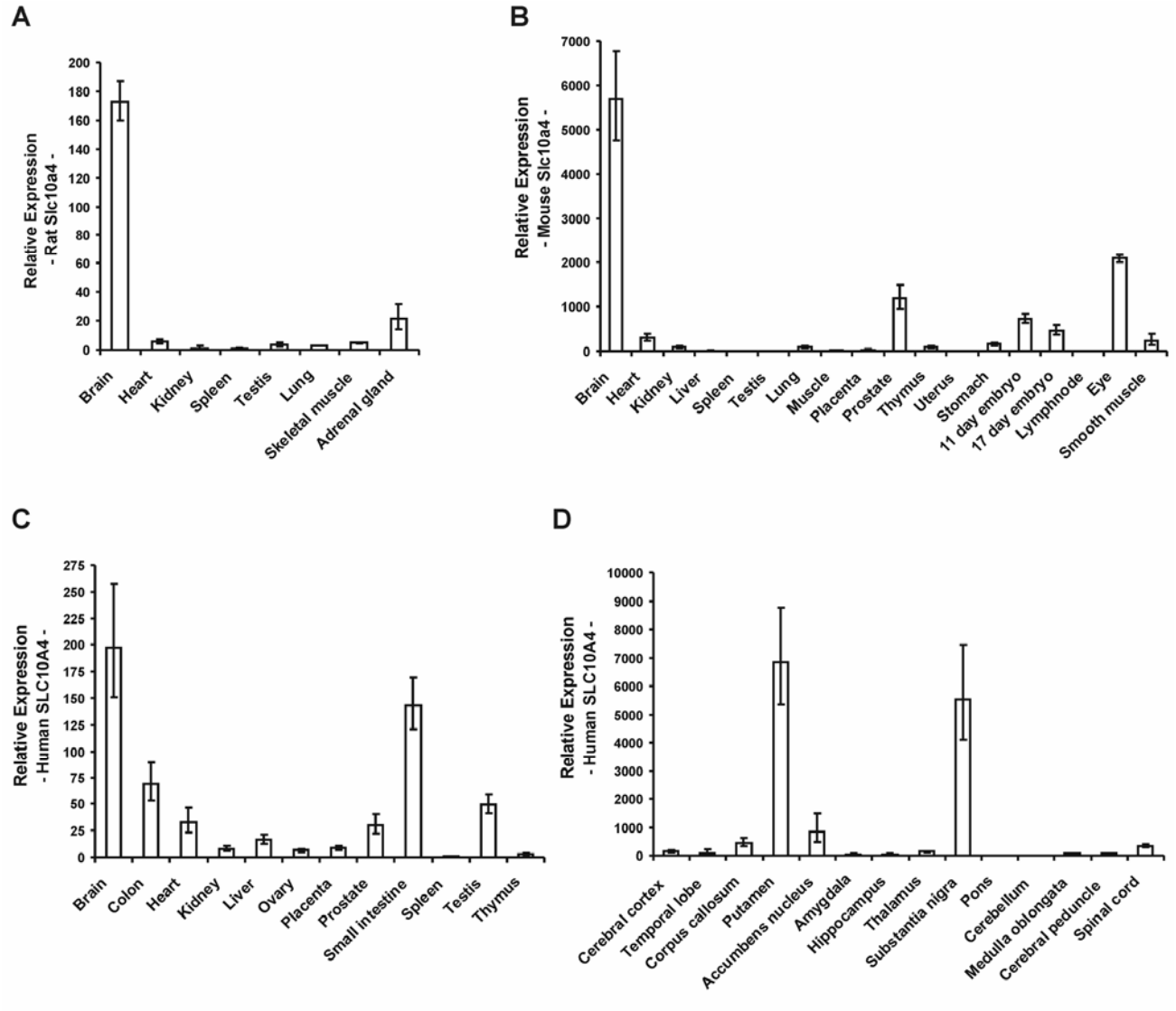

Figure 6. Expression patterns of rat and mouse Slc10a4 mRNAs (A+B) and human SLC10A4 mRNA (C+D) analyzed by real-time quantitative PCR analysis. Template cDNAs were derived from multiple tissue cDNA panels. Relative expression was calculated by $2^{-\Delta\Delta CT}$ transformation and represents x-fold higher SLC10A4/Slc10a4 expression in the respective tissue as compared to the organ of lowest expression among each panel. Data represent means ± SD of quadruplicate measurements.

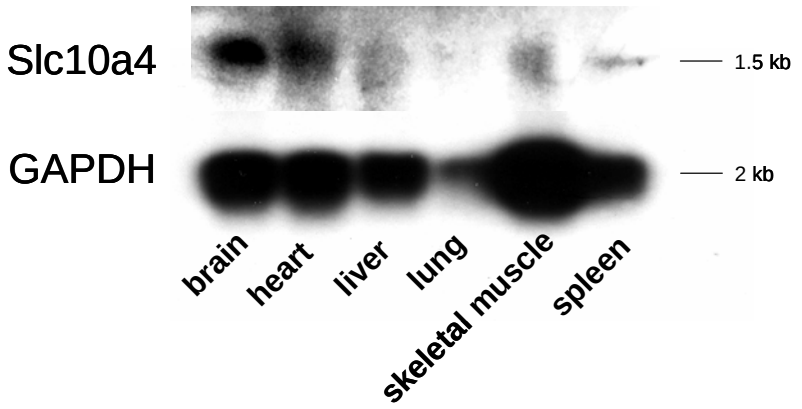

Figure 7. Northern Blot analysis of rat Slc10a4. Poly $(A)^+$ RNAs (3 µg) were separated by 1.6% agarose gelelectrophoresis and blotted onto a nylon membrane. A [^{32}P] Slc10a4 cDNA probe was hybridized to a nylon membrane and exposure was performed for 6 days at -70°C. GAPDH Poly $(A)^+$ RNA was used as control.

4.1.3 Transport studies and membrane expression of the rat Slc10a4 protein

Because of the close phylogenetic relationship between Slc10a4 and the liver bile acid carrier NTCP, transport experiments were performed in Slc10a4 transfected HEK293 cells using the radiolabeled NTCP substrates, taurocholate and estrone-3-sulfate. The neurosteroids dehydroepiandrosterone sulfate (DHEAS) and pregnenolone sulfate (PREGS) were also included in the transport measurements. In contrast to human NTCP, no specific Slc10a4-mediated transport activity was found for these compounds (Table 3). Identical results were obtained in NTCP-expressing and Slc10a4-expressing *Xenopus laevis* oocytes (Table 4). A FLAG-tagged Slc10a4 protein was generated and expressed in *Xenopus laevis* oocytes, in order to exclude the possibility that the absence of Slc10a4-specific transport activity might have been due to a defect in its functional expression at the plasma membrane. Membrane localization of the fusion protein was analyzed with a FLAG-specific monoclonal antibody by immunofluorescence microscopy and revealed that Slc10a4 expression in the oocytes was clearly directed to the plasma membrane (Fig. 8A). Membrane topology of the Slc10a4 protein was analyzed by six different topology prediction programs. Controversial protein structures with either seven or eight transmembrane domains (TMD) were obtained: the TMpred and MEMSAT programs placed the N-terminus and C-terminus at the extracellular compartment and predicted eight transmembrane domains (TMDs); the HMMTOP and TMHMM programs also predicted eight TMDs but with an intracellular localization of both terminals. In contrast, PRED-TMR2 and TMAP predicted seven transmembrane domains with an extracellular localization of the N-terminus and an intracellular C-terminus (Fig. 8B). In order to experimentally clarify the membrane topology of Slc10a4, a second Slc10a4-tagged protein, HA-Slc10a4-FLAG, was generated containing the hemagglutinin (HA) motif at its N-terminal end in addition to the C-terminal FLAG-motif. This fusion protein was expressed in HEK293 cells, and the accessibility of the HA-directed and FLAG-directed antibodies to their respective epitopes was analyzed by immunofluorescence under membrane permeabilizing and non-permeabilizing conditions. While the antibodies reached both epitopes in the permeabilized cells, the HA epitope but not the FLAG epitope was detectable under non-permeabilized conditions (Fig. 8C). This data clearly supports a 7-TMD model for rat Slc10a4 with a N_{exo}/C_{cyt} *trans*-

orientation of the N- and C-terminal domains, which represents an extracellular location of the N-terminus and an intracellular location of the C-terminus. Closer analysis of this immunofluorescence data showed that although Slc10a4 is detected at the plasma membrane of HEK293 cells, it is also present in intracellular compartments of yet unknown origin (Fig. 8C).

Table 3. Transport studies with rat Slc10a4 and human NTCP in HEK293 cells.

HEK293 cells were seeded in 12-well plates and grown to confluency under standard conditions. Tetracycline (1 µg/ml medium) was added to induce Slc10a4 and NTCP expression. HEK293 cells transfected with the empty vector were used as the control. Cells were incubated with the indicated radiolabeled compound for 10 min and cell-associated radioactivity was measured and calculated as the ratio value when compared to transport under control conditions. The values represent means ± SD of triplicate determinations of representative experiments.

	NTCP		**Slc10a4**	
test compound	Uptake (pmol/mg protein/10 min)	*ratio*	Uptake (pmol/mg protein/10 min)	*ratio*
Taurocholate *[1 µM]*	239.61 ± 26.47	**40.3***	7.03 ± 0.68	**1.2**
Estrone-3-sulfate *[1 µM]*	47.95 ± 6.61	**6.1***	9.6 ± 2.72	**1.2**
DHEAS *[1 µM]*	62.63 ± 13.93	**4.5***	21.15 ± 3.24	**1.5**
PREGS *[1 µM]*	663.78 ± 81.49	**2.94***	216.51 ± 18.6	**0.95**

* Significantly higher uptake into NTCP-transfected HEK293 cells compared with vector transfected HEK293 cells ($p < 0.01$).

Table 4. Transport studies with rat Slc10a4 and human NTCP in *Xenopus laevis* oocytes.

	NTCP		**Slc10a4**	
test compound	Uptake (fmol/oocyte/60 min)	*ratio*	Uptake (fmol/oocyte/60 min)	*ratio*
Taurocholate *[6.4 µM]*	11470 ± 7526	**468***	43.9 ± 13.4	**1.8**
Cholat *[5 µM]*	13132 ± 6612	**81***	210 ± 25.4	**1.2**
Chenodeoxycholate*[5 µM]*	17491± 5604	**2.9***	6648± 2120	**1.1**
DHEAS *[2 µM]*	3061± 1454	**4.5***	226.6 ± 78.4	**0.96**
PREGS *[100 nM]*	277 ± 140.5	**15***	31.4 ± 8.9	**1.7**
	SOAT		**Slc10a4**	
test compound	Uptake (fmol/oocyte/60 min)	*ratio*	Uptake (fmol/oocyte/60 min)	*ratio*
Estrone-3-sulfate *[100 nM]*	30.67 ± 11.4	**5.7***	5.51 ± 2.26	**1.0**

Note: Values represent means ± SD of 10 separate oocyte measurements. Ratio represents uptake into carrier-cRNA injected oocytes divided by uptake into water-injected oocytes.

* Significantly higher uptake into carrier-cRNA injected oocytes compared with water-injected oocytes ($p < 0.001$).

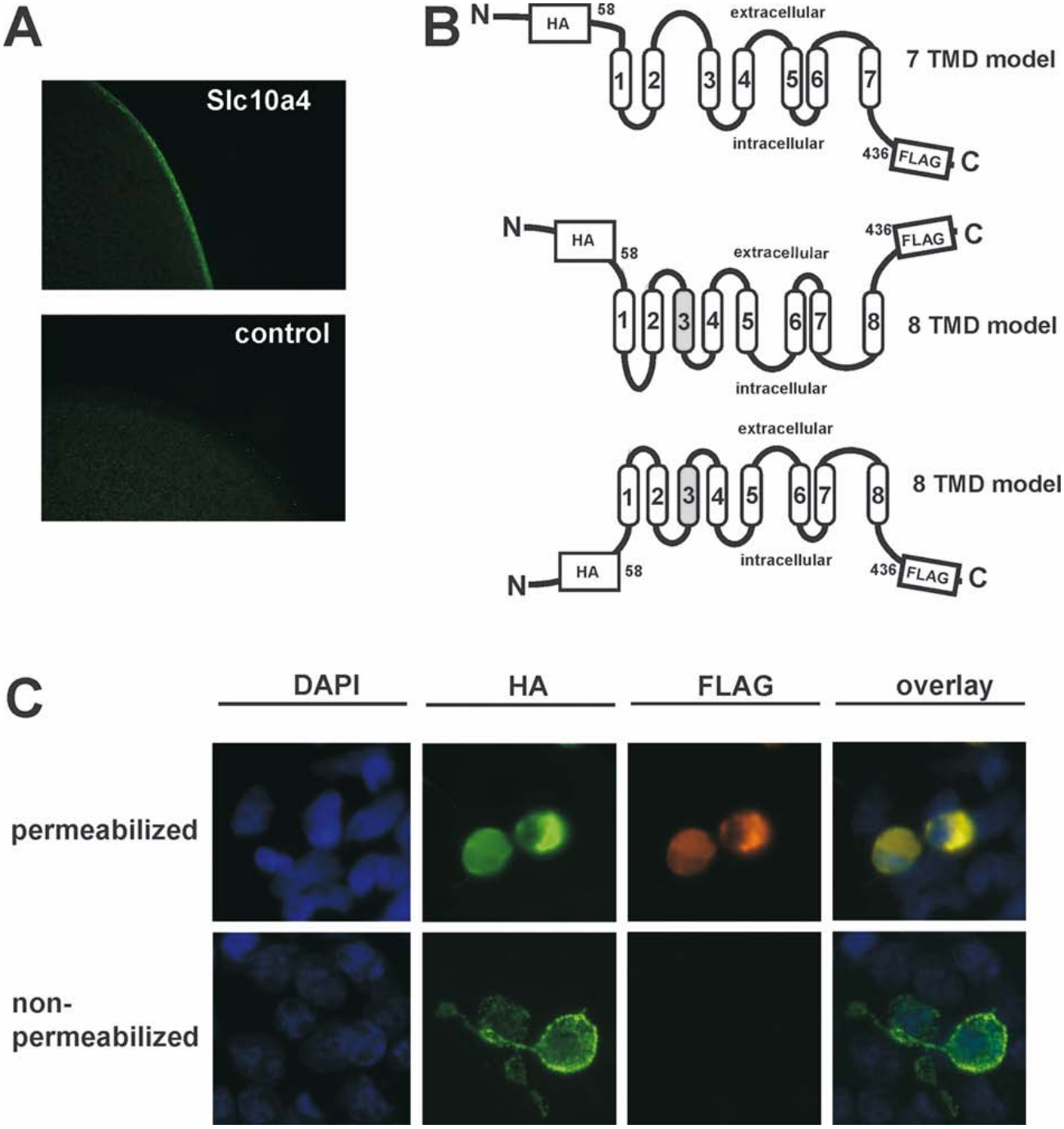

Figure 8. Membrane expression and topology of the rat Slc10a4 protein. (A) Detection of the Slc10a4-FLAG fusion protein in the plasma membrane of *Xenopus laevis* oocytes. Oocytes were injected with 4.6 ng (in 46 nl) of Slc10a4-FLAG-cRNA or 46 nl water (control). After three days in culture oocytes were fixed and processed for immunofluorescence microscopy. (B) Proposed membrane topologies of the rat Slc10a4 protein, based on the analysis of six different topology prediction programs for eukaryotic proteins (see text for further explanations). Cylinders indicate predicted transmembrane domains (TMD), and loops are depicted as lines. Strategically inserted FLAG and HA epitopes are illustrated as boxes. Amino acid positions immediately preceding these tags are indicated. Experimental data clearly support the 7-TMD model for the rat Slc10a4 protein. (C) Detection of the HA-Slc10a4-FLAG double-tagged protein by immunofluorescence microscopy. HEK293 cells were transfected with the HA-Slc10a4-FLAG construct and were analyzed under permeabilized and non-permeabilized conditions. Expression of the tagged proteins was detected by fluorescence labeling using a mouse anti-HA monoclonal primary antibody followed by Alexa-Fluor-488-conjugated anti-mouse IgG secondary antibody (green fluorescence) and rabbit anti-FLAG polyclonal primary antiserum followed by Cy3-conjugated anti-rabbit secondary antibody (orange fluorescence). Nuclei were stained with DAPI.

4.1.4 Antibody preparation and western blot analysis

In order to analyze macroscopic brain-region specific localization and microscopic cellular localization of Slc10a4 expression in the rat CNS, immunohistochemistry was performed with a polyclonal rabbit antiserum directed against the C-terminal epitope VGTDDLVLMETTQTSL (amino acid residues 422-437) of the rat Slc10a4 protein. The specificity of this antiserum was verified by Western blot analysis of Slc10a4-FLAG transfected HEK293 cells. A specific band of ~48 kDa was detected in the Slc10a4-transfected cells but not in the mock-transfected cells, when applying the anti-Slc10a4 or the anti-FLAG antibodies (Fig. 9A). In order to reveal epitope specificity, pre-absorption of the Slc10a4 antiserum with a 100-fold molar excess of the synthetic $Slc10a4_{422-437}$ peptide was performed, and it was found that immunostaining was substantially suppressed (Fig. 9A). The Slc10a4 antiserum was also used for Western blot analysis of various regions of the rat CNS (Fig. 9B). A specific band was detected at ~47 kDa; this fits the predicted molecular weight of Slc10a4 of 46.6 kDa and most likely represents the native form of the protein. This band was also seen in the Slc10a4-FLAG transfected HEK293 cells, representing 47 kDa for the Slc10a4 protein and 1 kDa for the FLAG epitope. Additionally, a strong band was present at ~73 kDa in almost all brain regions, possibly representing a mature glycosylated form of the Slc10a4 protein or a protein aggregate of higher molecular order (Fig. 9B). Amongst the brain regions investigated, the caudate putamen exhibited the highest levels of immunoreactivity; in contrast, only a faint band was detected in the cerebellum. The frontal cortex, posterior cortex, hippocampus, olfactory bulb, thalamus, mesencephalon, entorhinal cortex, pons, medulla oblongata, and spinal cord showed intermediate levels of Slc10a4 immunoreactivity. Preincubation of the Slc10a4 antiserum with the synthetic $Slc10a4_{422-437}$ peptide led to pronounced reduction of immunoreactivity signals (Fig. 9C).

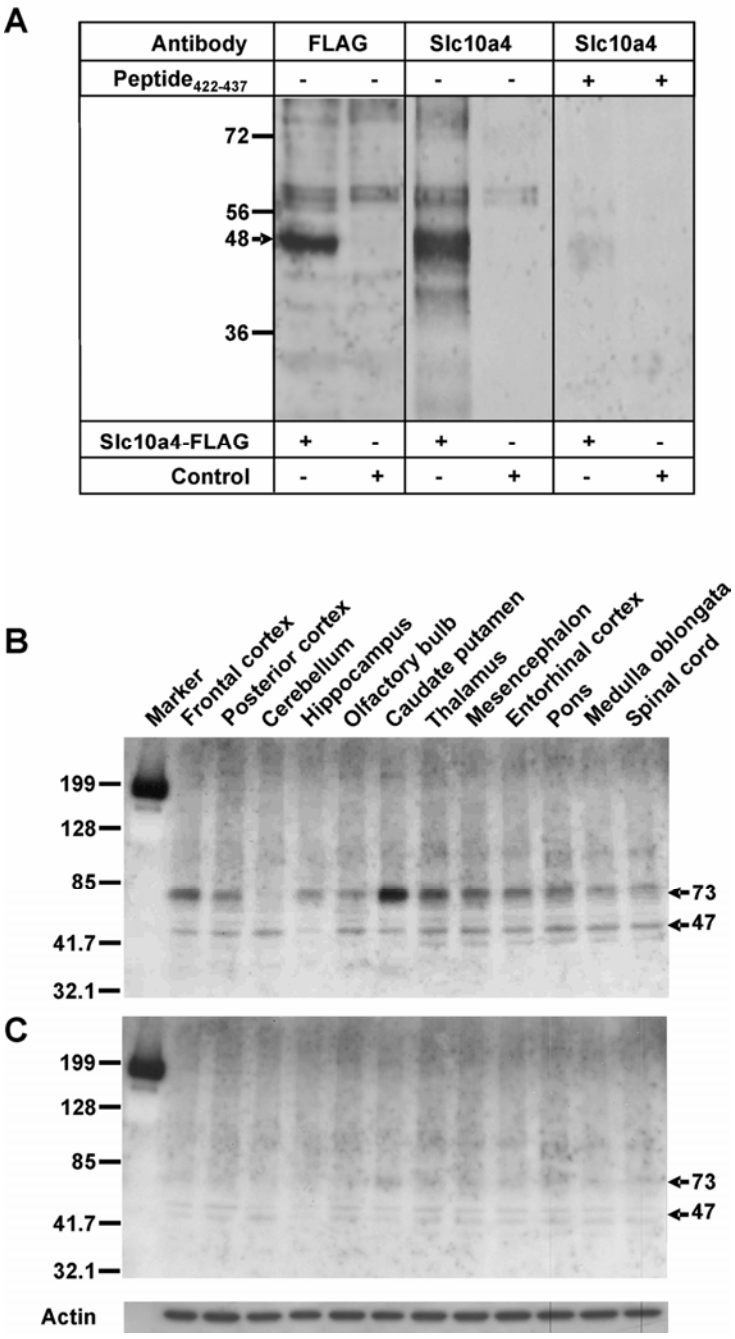

Figure 9. Western blot analyses of (A) cell lysates of transfected HEK293 cells and (B+C) different regions of the rat CNS. (A) HEK293 cells were transiently transfected with the Slc10a4-FLAG construct or empty vector (control) and cell lysates were separated on 12% SDS-polyacrylamide gel. Expression of the Slc10a4-FLAG fusion protein was detected by mouse anti-FLAG antibody (1:3000 dilution) and rabbit anti-Slc10a4 antiserum (1:5000 dilution), and both revealed bands at 48 kDa, which were completely suppressed after pre-incubation with the Slc10a4 antigen. (B+C) A pre-manufactured membrane with adsorbed protein extracts of various regions of the rat CNS was probed with the anti-Slc10a4 antiserum at 1:10000 dilution and showed specific bands at 47 kDa and 73 kDa (B), which were substantially suppressed after pre-incubation of the antiserum with the synthetic Slc10a4$_{422-437}$ peptide (C). Detection of actin was performed for loading control of the pre-fabricated blots.

4.1.5 Immunohistochemical analysis of Slc10a4 expression in the rat CNS

Using 40 µm floating sections of the rat brain and spinal cord, substantial Slc10a4-like immunoreactivity was detected in areas commonly described as cholinergic regions. Slc10a4-immunopositive perikarya and dentrites, as well as fibers, varicosities, and/or synaptic puncta were stained after DAB reaction at sites of Slc10a4 expression throughout the CNS (Table 5). Labeling for Slc10a4 was visualized along nerve fibers in the cerebral cortex, notably in the cingulate, prelimbic, infralimbic, and dorsal pendicular cortex. A high density of Slc10a4-immunopositive perikarya and puncta was identified in the islands of Calleja, the nucleus of the horizontal limb of the diagonal band of Broca (Fig. 10A), the olfactory tubercle (Fig. 10B), and the accumbens nucleus (Fig. 10C). The caudate putamen exhibited strong puncta-directed immunoreactivity; on the other hand, Slc10a4-like staining of cell bodies proved to be scarce in this area (Fig. 10D). Only a few Slc10a4 positive perikarya were detected in the basal nucleus of Meynert, whereas, the amygdala was densely innervated by Slc10a4-positive fibers, particularly the basolateral amygdaloid nucleus (Fig. 10E). In the hippocampus, the field CA3 presented a higher density of Slc10a4-positive puncta than CA1. A similar staining pattern of Slc10a4 was detected in the granular layer of the dentate gyrus. Slc10a4-positive fibers and nerve terminals were also widespread in the thalamus and epithalamus, especially in the reticular thalamic nucleus and medial habenular nucleus. In the latter region, we also found some small Slc10a4-immunoreactive cell bodies. Additionally, immunoreactive puncta and perikarya were visualized in many regions of the mesencephalon, such as the laterodorsal tegmental nucleus, pedunculopontine tegmental nucleus, periaqueductal gray, oculomotor nucleus, interpeduncular nucleus, ventral tegmental area, and substantia nigra (the latter region is shown in Fig. 10F). Positive immunoreactive cell bodies and puncta were also detected in the rhombencephalon, especially in the motor trigeminal nucleus, the facial nucleus (Fig. 10G), the dorsal motor nucleus of vagus (Fig. 10H), the hypoglossal nucleus (Fig. 10I), and the ambiguus nucleus (Fig. 10J). In these regions, neurons were found surrounded by Slc10a4-positive puncta, possibly representing synaptic C-boutons. This staining pattern was also found in layer IX of the spinal cord. Additionaly, positive staining of fibers was visualized in layer III of the dorsal horn (Fig. 10K).

Table 5. Regional distribution of Slc10a4, VAChT, and CHT immunoreactivities in the rat CNS.

Brain regions		*Immunoreactivities*					
		Density of perikarya			Density of puncta/fibers		
		Slc10a4	VAChT	CHT1	Slc10a4	VAChT	CHT1
Cortex							
Cingulate cortex	(Cg)	-	-	-	+	+	+
Prelimbic cortex	(PrL)	-	-	-	+	+	+
Infralimbic cortex	(IL)	-	-	-	+	+	+
Dorsal peduncular cortex	(DP)	-	-	-	+	+	+
Olfactory System							
Olfactory bulb	(OB)	-	-	-	+	+	++
Olfactory tubercle	(Tu)	++	++	++	+++	+++	+++
Septal/basal forebrain							
Islands of Calleja	(ICj)	++	++	++	+++	+++	+++
Horizontal limb of the diagonal band	(HDB)	+++	+++	+++	++	++	++
Vertical limb of the diagonal band	(VDB)	+	+++	+++	+	+++	+++
Medial septal nucleus	(MS)	+	+++	+++	+	+	+
Lateral septal nucleus	(LS)	-	-	-	+	++	++
Accumbens nucleus	(Acb)	++	++	++	++	++	++
Caudate putamen (striatum)	(CPu)	+	++	+++	++	+++	+++
Basal nucleus (Meynert)	(B)	+	+++	+++	+	+	+
Amygdala							
Lateral amygdaloid nucleus	(La)	-	-	-	+	+	+
Basolateral amygdaloid nucleus	(BL)	-	-	-	+++	++	++
Hippocampus							
Fimbria of the hippocampus	(fi)	-	-	-	++	++	++
Septofimbrial nucleus	(Sfi)	-	-	-	++	++	++
Field CA1 of the hippocampus	(CA1)	-	-	-	+	++	++
Field CA3 of the hippocampus	(CA3)	-	-	-	++	+++	++
Granular layer of the dentate gyrus	(GrDG)	-	-	-	++	++	++
Thalamus / Epithalamus							
Reticular thalamic nucleus	(Rt)	-	-	-	+++	++	++
Lateral habenular nucleus	(LHb)	-	-	-	+	+	+
Medial habenular nucleus	(MHb)	+	+++	++	++	+	+
Anterodorsal thalamic nucleus	(AD)	-	-	-	+	+	+
Anteromedial thalamic nucleus	(AM)	-	-	-	+	+	+
Anteroventral thalamic nucleus	(AV)	-	-	-	+	+++	++
Mediodorsal thalamic nucleus	(MD)	-	-	-	+	+	+
Paraventricular thalamic nucleus	(PV)	-	-	-	+	+	+
Reuniens thalamic nucleus	(Re)	-	-	-	+	+	+
Central medial thalamic nucleus	(CM)	-	-	-	+	++	+
Mesencephalon							
Superior colliculus	(SC)	-	-	-	++	+	+
Edinger-Westphal nucleus	(EW)	-	-	-	+	+	+
Laterodorsal tegmental nucleus	(LDTg)	++	+++	+++	+	+	+
Pedunculopontine tegmental nucleus	(PPTg)	++	+++	+++	+	+	+
Periaqueductal gray	(PAG)	++	-	-	++	+	+
Oculomotor nucleus	(3N)	++	+++	+++	++	+	++
Interpeduncular nucleus	(IP)	+	-	-	+	+++	+++
Ventral tegmental area	(VTA)	+	-	-	+++	+	+
Substantia nigra	(SN)	++	-	-	++	-	-
Parabigeminal nucleus	(PBG)	++	++	++	-	-	-
Rhombencephalon							
Pontine nuclei	(Pn)	-	-	-	+	++	+
Dorsal raphe nucleus	(DR)	-	-	-	+	+	+
Ventral tegmental nucleus	(VTg)	-	-	-	+	+	+
Raphe pallidus nucleus	(RPa)	-	-	-	+	+	+
Spinal trigeminal nucleus	(Sp5)	-	-	-	++	++	++
Motor trigeminal nucleus (5N) / peritrigeminal zone	(P5)	+++	+++	+++	+++*	+++*	++*
Paratrigeminal nucleus	(Pa5)	-	-	-	+	+	+
Vestibular nuclei	(Ve)	-	-	-	++	+	+
Facial nucleus	(7N)	+++	+++	+++	++*	++*	++*
Nucleus of the solitary tract	(Sol)	-	-	-	++	+	+
Dorsal motor nucleus of vagus	(10N)	++	+++	++	++	-	-
Hypoglossal nucleus	(12N)	+++	+++	+++	++*	++*	++*
Ambiguus nucleus	(Amb)	+++	+++	+++	+++*	++*	++*
Lateral reticular nucleus	(LRt)	-	-	-	+	+	+
Spinal cord							
Cervical and thoracic - layer IX		+++	+++	++	+++*	+++*	++*
Cervical and thoracic - layer III		-	-	-	++	+	+

The densities of Slc10a4, VAChT, and CHT1 immunopositive perikarya or puncta/fibers were rated as follows: "-", absent; "+", low; "++", moderate; "+++", high. In several cranial motor nuclei and the spinal cord, puncta represent synaptic C-boutons as indicated by asterisks (*). Brain regions and structures were attributed and named according to Paxinos and Watson (2004).

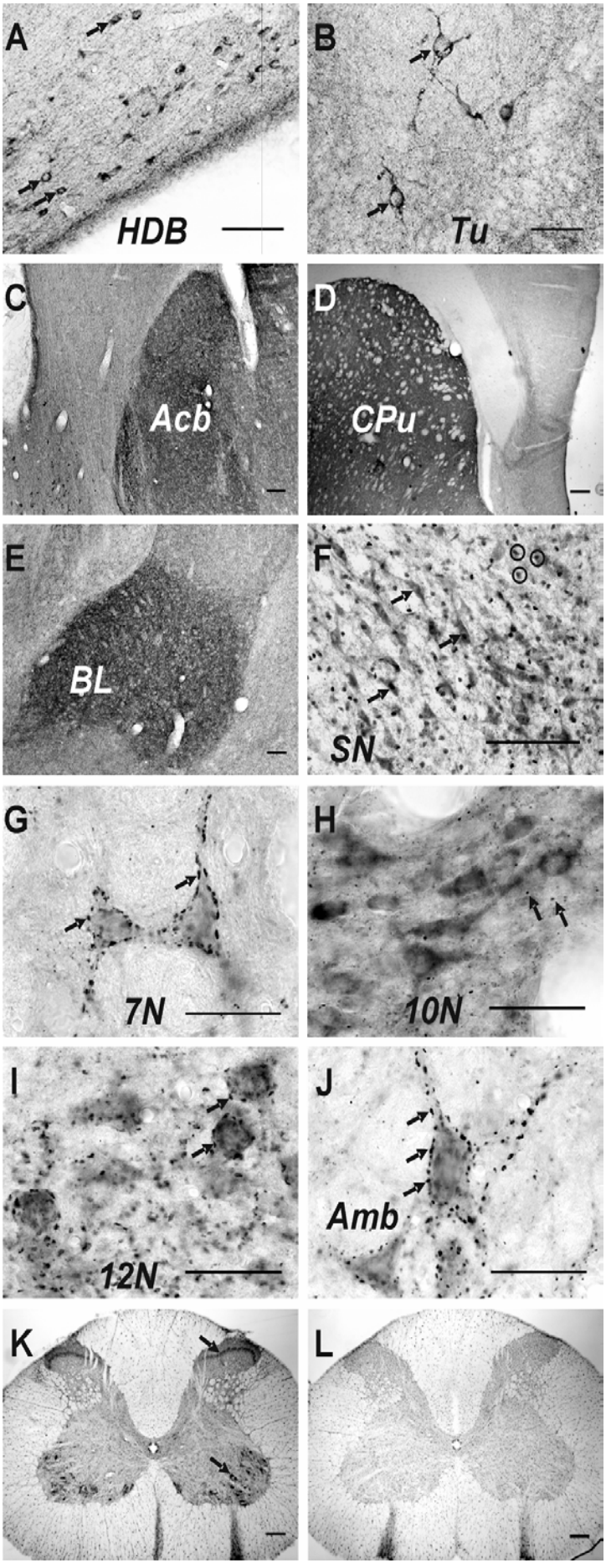

Figure 10. Light microscopic distribution of Slc10a4-like immunoreactivity in the rat CNS. Coronal sections (40 µm) of the rat CNS were incubated with the Slc10a4-antiserum and processed for indirect immunohistochemical staining according to the DAB technique. Labeled cell bodies (indicated by arrows) and puncta are present in (A) the nucleus of the horizontal limb of the diagonal band of Broca (HDB) and (B) the olfactory tubercle (Tu). In (C) the accumbens nucleus (Acb) and (D) the caudate putamen (CPu), dense immunolabeling for the Slc10a4 protein was seen. (E) Slc10a4-immunoreactive puncta and fibers are stained in the basolateral amygdaloid nucleus (BL). (F) Slc10a4-containing perikarya were found within the substantia nigra (SN); neurons are marked by arrows, and nuclei counterstained with cresyl violet are indicated by small circles. (G-J) Slc10a4-immunopositive cell bodies and puncta (indicated by arrows) were stained in the medullary motor nuclei such as the facial nucleus (7N), the dorsal motor nucleus of vagus (10N), the hypoglossal nucleus (12N), and the ambiguus nucleus (Amb). (K) In the spinal cord, Slc10a4-containing cell bodies and puncta are present in the ventral horn (layer IX, indicated by arrow), whereas only fibers are visualized in the dorsal horn (layer III, indicated by arrow). (L) A section from the spinal cord was incubated with the Slc10a4 antiserum pre-absorbed with the Slc10a4 immunizing peptide and showed pronounced reduction in immunoreactivity. Brain regions and structures were attributed and abbreviated according to Paxinos and Watson (2004). Scale bars: A, C, E, and F, 100 µm; B, G-J, 50 µm; D, and K-L, 200 µm.

4.1.6 Co-localization studies with VAChT, CHT1, and ChAT

Because the immunohistochemically identified Slc10a4 distribution pattern indicated its expression in cholinergic regions, nuclei or even neurons in the rat CNS, co-localization studies were performed for Slc10a4 immunoreactivity with that of three different marker proteins of cholinergic neurons, namely VAChT, CHT1, and ChAT. Significant immunoreactive co-labeling of neuronal perikarya and nerve terminals was found for Slc10a4 and VAChT (Fig. 11A-C) as well as for Slc10a4 and CHT1 (Fig. 11D-F) by fluorescence microscopy in all cholinergic nuclei and their projections, such as the islands of Calleja (Fig. 11A), the accumbens nucleus (Fig. 11B), the olfactory tubercle (Fig. 11D), and the horizontal limb of the diagonal band of Broca (Fig. 11E). Furthermore, clear synaptic co-expression of Slc10a4 and VAChT as well as of Slc10a4 and CHT1 was observed in motor neurons of the ventral horn of the spinal cord (Fig. 11C) and in the motor trigeminal nuclei (Fig. 11F), respectively. Visualization of Slc10a4-immunopositive neurons proved to be scarce, however, throughout the vertical limb of the diagonal band of Broca, the medial septal nucleus, the caudate putamen and the basal nucleus of Meynert, when compared to immunolabeling for CHT1 or VAChT (Table 5). In contrast, nerve fiber systems within the basolateral amygdaloid nucleus, the nucleus of the solitary tract, and the dorsal motor nucleus of the vagus revealed stronger specific immunoreactivity for Slc10a4 than for VAChT or CHT1 (Table 5). Numerous Slc10a4-immunoreactive cell bodies and puncta were also demonstrated in the ventral tegmental area and the substantia nigra, but these were not clearly labeled for the cholinergic marker proteins VAChT and CHT1. Therefore, additional co-labeling experiments were performed for Slc10a4 and the cholinergic marker protein ChAT in order to clarify the origin of Slc10a4 expression in these areas. A significant number of both Slc10a4 and ChAT immunopositive cell bodies at very high degree of co-localization was detected in the ventral tegmental area (Fig. 11G) and detailed analysis revealed apparent vesicular compartimentalization of both proteins (Fig. 11H). Also within cell bodies of the substantia nigra, Slc10a4-immunoreactivity proved to be co-localized with that of ChAT-immunoreactivity (Fig. 11I).

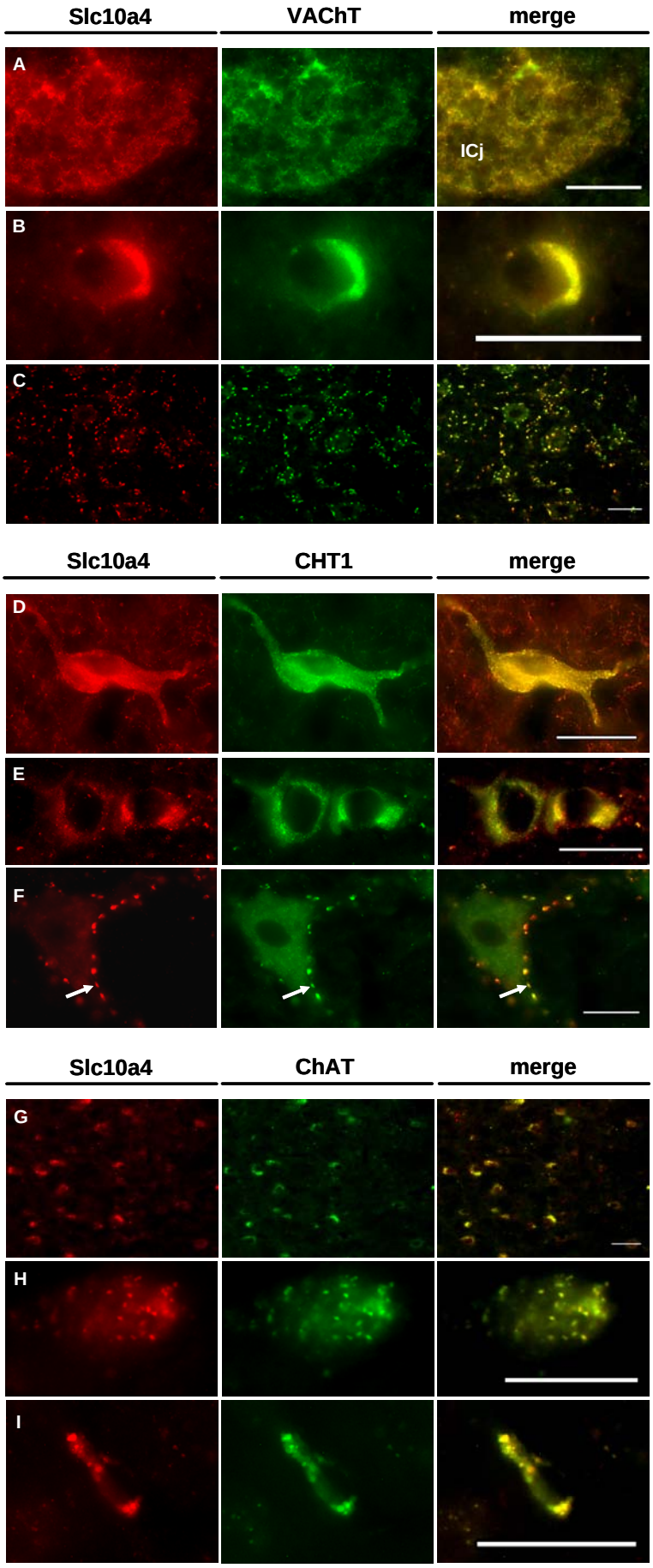

Figure 11. Co-localization of Slc10a4 expression with VAChT, CHT1, and ChAT. Coronal sections of the rat CNS were analyzed for Slc10a4 (A-I), VAChT (A-C), CHT1 (D-F), and ChAT (G-I) immunoreactivities. Merged images are shown illustrating co-localization between Slc10a4 and VAChT (A-C), Slc10a4 and CHT1 (D-F), and Slc10a4 and ChAT (G-I). (A) Dense staining of Slc10a4-immunopositive and VAChT-immunopositive fibers and puncta was observed in the island of Calleja. (B) Slc10a4 and VAChT co-expression was found in cell bodies of the accumbens nucleus. (C) In the ventral horn of the spinal cord, Slc10a4-immunoreactivity and VAChT-immunoreactivity are present in cell bodies of motor neurons as well as in the large presynaptic C-boutons that surround them. (D) Intense Slc10a4-like and CHT1-like immunoreactivities are detected in neuronal cell bodies of the olfactory tubercle. (E) Slc10a4-immunopositive and CHT1-immunopositive cell bodies are observed in the nucleus of the horizontal limb of the diagonal band. (F) Co-expression of Slc10a4 and CHT1 occurs in the motor trigeminal nuclei; nerve terminals are indicated by arrows. (G-H) Staining of Slc10a4-immunopositive and ChAT-immunopositive cell bodies was seen in the ventral tegmental area; immunoreactivity was concentrated in intracellular vesicular compartments. (I) Slc10a4 and ChAT co-expression in neuronal cell bodies was observed in the substantia nigra. Scale bars: A, C, and G, 50 µm; B, D-F, and H-I, 25 µm.

4.1.7 Co-localization studies with tyrosine hydroxylase

To investigate a possible Slc10a4 expression in dopaminergic neurons, co-localization experiments were performed using anti-Slc10a4 and anti-tyrosine hydroxylase antibodies. A staining of both proteins was visualized only in some neurons of the dopaminergic regions, substantia nigra and ventral tegmental area. In all other catecholaminergic regions, co-localization between Slc10a4 and TH was not observed. However, in some very near-by neighbouring regions, such as the motor trigeminal nucleus and sub-coeruleus, nucleus of the solitary tract and hypoglossal nucleus, or in the A1 region, the high density of TH-immunoreactive cell bodies independently co-ocurred with Slc10a4 positive cells (Fig. 12).

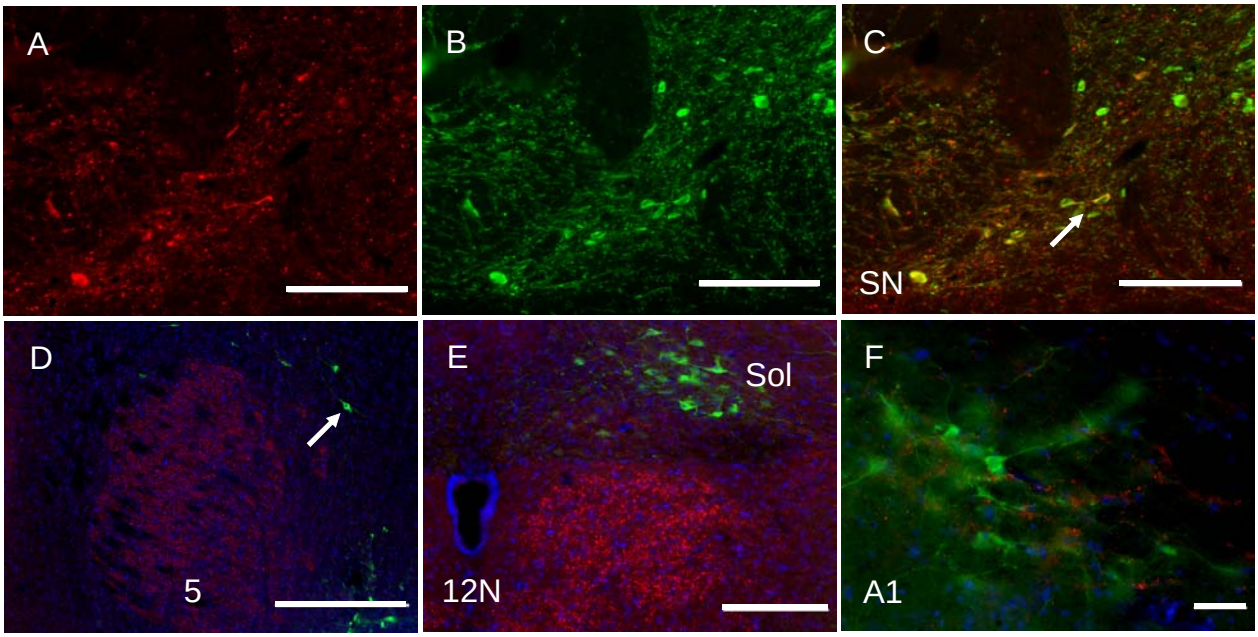

Figure 12. Detection of tyrosine hydroxylase (TH) and Slc10a4 proteins in coronal sections of the rat brain. Red staining represents Slc10a4-immunoreactivity (A, D-F), whereas green fluorescence shows TH (B, D-F). Nuclei are stained with DAPI (blue, D-F). A-C, Immunoreactivities of Slc10a4 and TH visualized in the substantia nigra (SN). C, The merged image shows co-localization of Slc10a4 and TH in some cell bodies (indicated by arrow). D, In the motor trigeminal nuclei (5) only Slc10a4-positive puncta and cell bodies are visualized, whereas catecholaminergic neurons of the subcoeruleus are only stained with TH (indicated by arrow). E, Nucleus of solitary tract (Sol) shows strong intensity of TH-positive cell bodies and some Slc10a4-puncta staining, but no coexpression of both proteins is observed in this region. The cranial motor nerve hypoglossus (12N) clearly exhibits only Slc10a4-staining. F, Both Slc10a4 and noradrenergic neurons were stained in the A1 region, but both proteins show no coappearance in the same neurons. Scale bars: *A-C*, 50 µm, *D-F*, 100 µm.

4.1.8 Slc10a4 expression in PC12 cells and co-localization study with VAChT

Using the anti-Slc10a4 and anti-VAChT antisera for immunocytochemical experiments, a clear Slc10a4 immunoreactivity as well as a co-expression with VAChT was observed in the neuroendocrine rat pheochromocytoma cell line PC12 (Fig 13). Localization of the Slc10a4 in these cells was very similar to the VAChT immunoreactivity, which was mainly localized to synaptic-like microvesicles.

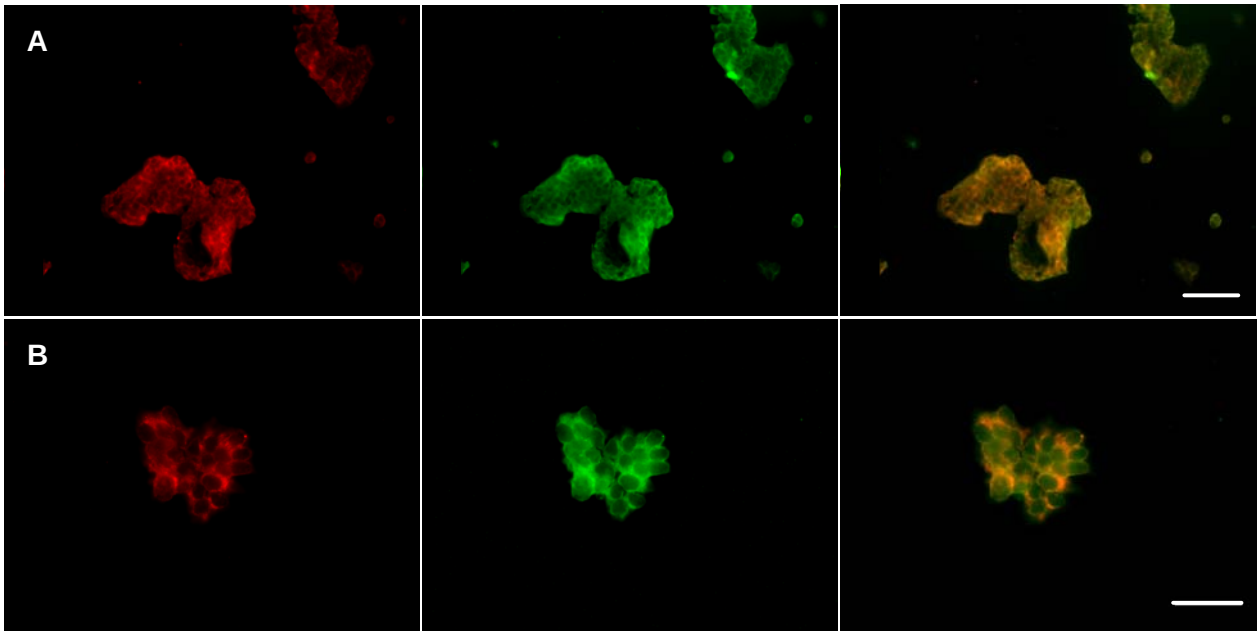

Figure 13. Co-expression of Slc10a4 and VAChT in PC12 cells. A and B show Slc10a4 (red staining) and VAChT (green staining) immunoreactivities in PC12 cells. The merged images illustrate co-localization of both proteins. Scale bars: *A*, 50 µm, *B*, 25 µm.

4.1.9 Transport studies with [^{3}H]choline chloride

As the proteins most related to Slc10a4 are membrane carriers, we speculated that besides the hemicholinium-3 sensitive choline transporter CHT1, Slc10a4 might also be involved in choline reuptake in the presynaptic membrane of cholinergic synapses. To test this hypothesis, we transiently transfected Slc10a4 and CHT1 into HEK293 cells and performed transport experiments with [^{3}H]choline chloride (1 µM) in the presence and absence of 1 µM hemicholinium-3 as inhibitor. In contrast to CHT1 though, which showed hemicholinium-3 sensitive choline chloride transport as described (Ribeiro et al., 2003), Slc10a4-specific transport activity for [^{3}H]choline chloride was not detected (Fig. 14).

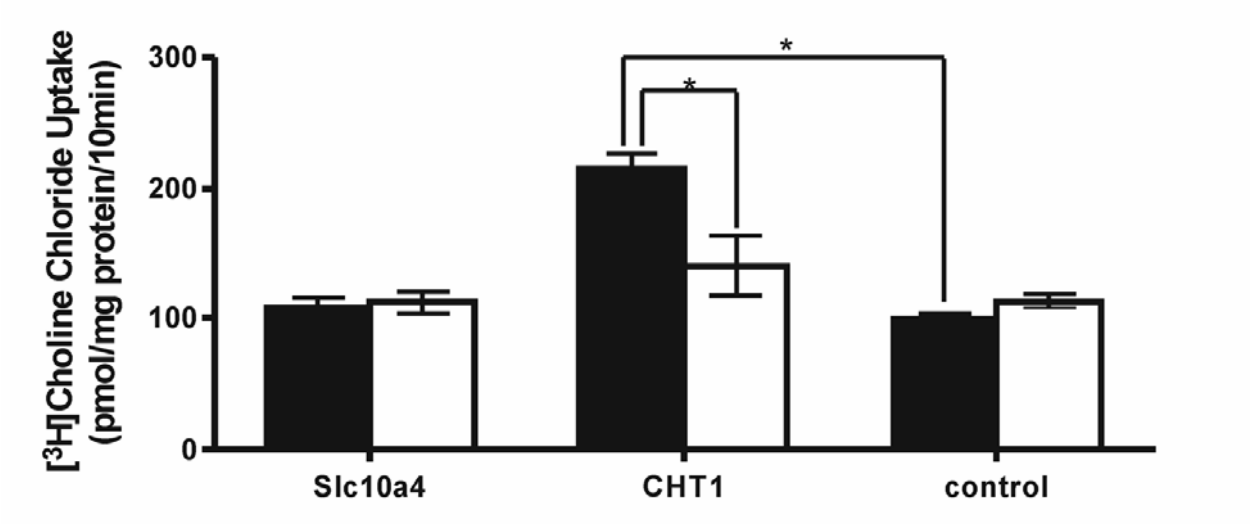

Figure 14. Transport experiments with choline in HEK293 cells transfected with rat Slc10a4 and rat CHT1. The uptake of [^{3}H]choline chloride (1 µM) was measured over a time period of 10 min in the presence (open bars) and absence (filled bars) of 1 µM hemicholinium-3 as inhibitor at 37°C. The cells were washed with ice-cold PBS, lysed, and subjected to scintillation counting. The values represent means ± SD of a representative experiment with quadruplicate determinations. * Statistically different uptake, $p < 0.01$.

4.2 The Novel Putative Bile Acid Transporter SLC10A5

4.2.1 Cloning of human, mouse, and rat SLC10A5 / Slc10a5

At the beginning of my work, we searched the available nucleotide and genomic databases for novel bile acid carriers using the amino acid and cDNA sequences of NTCP and ASBT as queries. Besides these two carriers, two hitherto uncharacterized sequences (GenBank accession nos. XM_376781 from human and XM_143078 from mouse) were identified. They were predicted by automated computational analysis from genomic sequences. Using an RT-PCR based approach for cloning of the predicted open reading frames, 1317 bp and 1305 bp transcripts from human and mouse livers were obtained. Using a similar approach, a 1305 bp transcript was also cloned from rat small intestine. These sequences were deposited into the GenBank database with accession nos. AY825924, AY825925, and DQ074435 and are henceforth referred to as human SLC10A5, mouse Slc10a5, and rat Slc10a5, respectively. The cloned human SLC10A5 cDNA sequence codes for a 438 amino acid membrane protein and the rat and mouse SLC10A5 proteins consist of 434 amino acids. The SLC10A5 proteins show the highest sequence identity/similarity (34%/61%) to the orphan carrier SLC10A3 and a lower sequence identity/similarity (at 22%/44%) to the bile acid carriers NTCP and ASBT. Fig. 15 shows an alignment of the deduced amino acid sequences of the human, rat, and mouse SLC10A5 proteins, which exhibit an overall sequence identity of

>70 %. SLC10A5-related sequences from cattle (Btau 3.1) and chimp (PanTro 2.1) were identified by Ensembl orthologue predictions (Ensembl release 43) and showed 76% and 98% sequence identities to the human SLC10A5 protein. Based on the analysis of three different topology prediction programs, SLC10A5 shows nine alpha-helical transmembrane domains with an extracellular orientation of the N-terminus and an intracellular location of the C-terminus. One conserved putative N-glycosylation site was detected in the SLC10A5 N-terminus (N^{99} in humans, and N^{96} in rat and mouse).

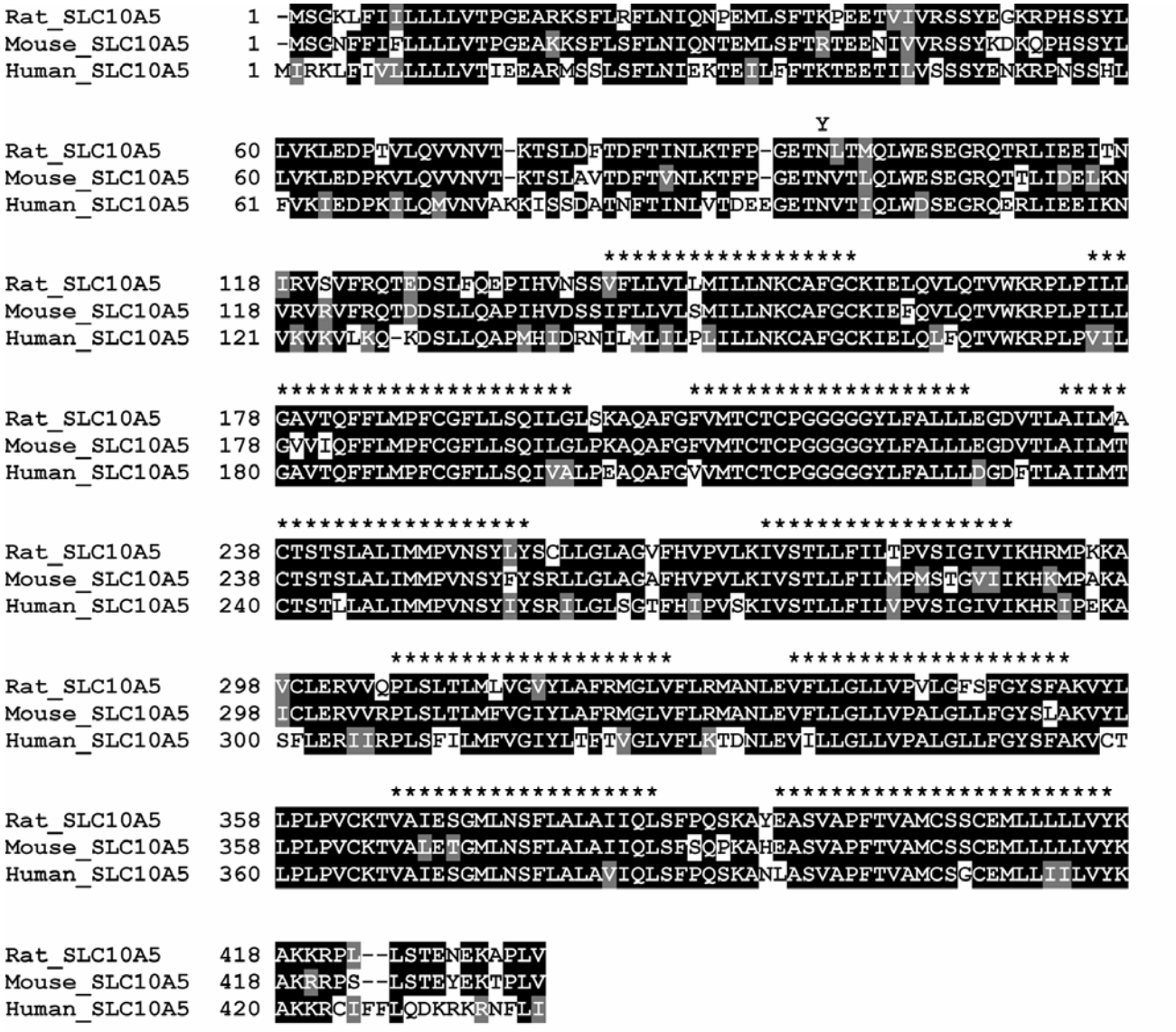

Figure 15. Amino acid sequence alignment of the human, rat, and mouse SLC10A5 proteins. Multiple sequence alignment was conducted using the *ClustalW* algorithm and was visualized by BOXSHADE 3.21. Amino acid sequence identity is displayed with black shading; amino acid similarities are highlighted in grey. Gaps (-) are introduced to optimize alignment. Putative transmembrane regions of SLC10A5 were predicted by HMMTOP, TMpred, and TopPred calculations and are indicated by asterisks (*). One conserved putative N-glycosylation site exists in the N-terminus of the SLC10A5 proteins (marked by Y).

4.2.2 Expression analysis of SLC10A5 / Slc10a5 in humans, rat, and mouse

SLC10A5/Slc10a5 mRNA expression was analyzed in different human, rat, and mouse tissues by real-time quantitative PCR using multiple tissue cDNA panels (Fig. 16) and northern blot (Fig. 17). In general, the detected mRNA levels were high in liver and kidney, but low in all other organs. This points to a tissue-specific expression pattern of SLC10A5/Slc10a5 that is identical across different species. The highest relative Slc10a5 expression in kidney and liver was detected in the mouse, where about 1000 and 800 times higher mRNA levels were detected than in the spleen, which was the tissue with the lowest Slc10a5 expression (Fig. 16C). Furthermore, it was found that SLC10A5 expression in humans is higher in liver than in kidney (Fig. 16A).

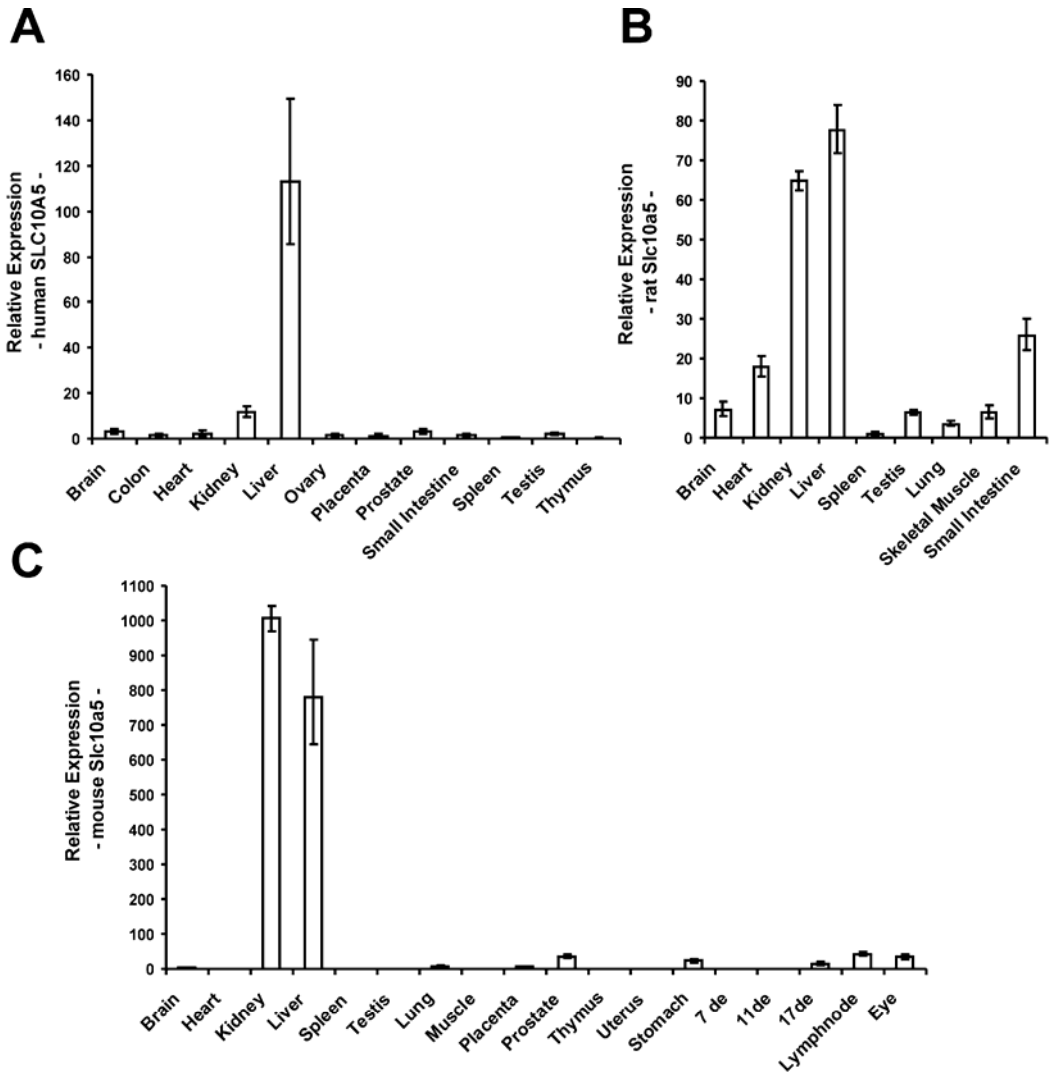

Figure 16. Expression pattern of (A) human SLC10A5, (B) rat Slc10a5, and (C) mouse Slc10a5, analyzed by real-time quantitative PCR. Template cDNAs were derived from multiple tissue cDNA panels, which have been normalized to the mRNA expression levels of four different housekeeping genes. Relative expression was calculated by $2^{-\Delta\Delta CT}$ transformation and represents x-fold higher SLC10A5/Slc10a5 expression in the respective tissue than in the spleen, which was the organ with the lowest SLC10A5/Slc10a5 expression. The data is presented as means ± SD of quadruplicate measurements.

Northern blot hybridization using a [^{32}P]Slc10a5 probe showed a specific band only in rat liver, which appeared at approximately 3 kb. No alternatively spliced transcription variants were found for rat Slc10a5 (Fig. 13).

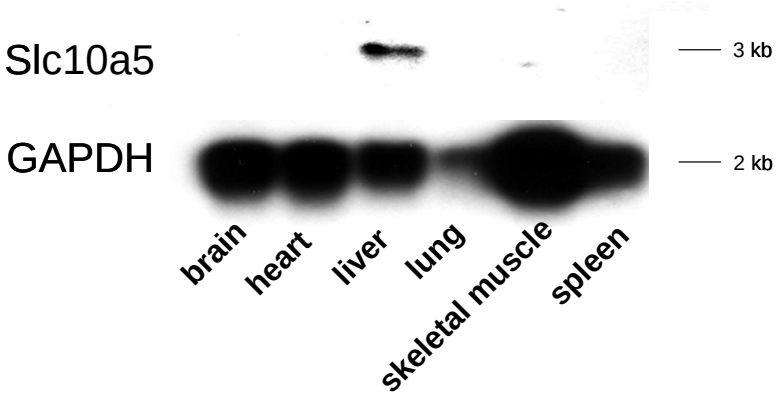

Figure 17. Northern Blot analysis of rat Slc10a5. Poly (A)$^+$ RNAs (3 µg) were separated by 1.6% agarose gelelectrophoresis and blotted to a nylon membran. [^{32}P]Slc10a5 cDNA probe was hybridized to a nylon membrane and exposure was performed for 6 days at -70°C. GAPDH Poly (A)$^+$ RNA was used as control.

Because of the high expression levels of human SLC10A5, mouse and rat Slc10a5 in liver and kidney, cellular localization of rat Slc10a5 was performed by *in situ* hybridization using specific digoxigenin-labeled Slc10a5 sense and antisense RNA probes. As shown in Fig. 18, rat Slc10a5 expression was detected in hepatocytes and renal proximal tubules.

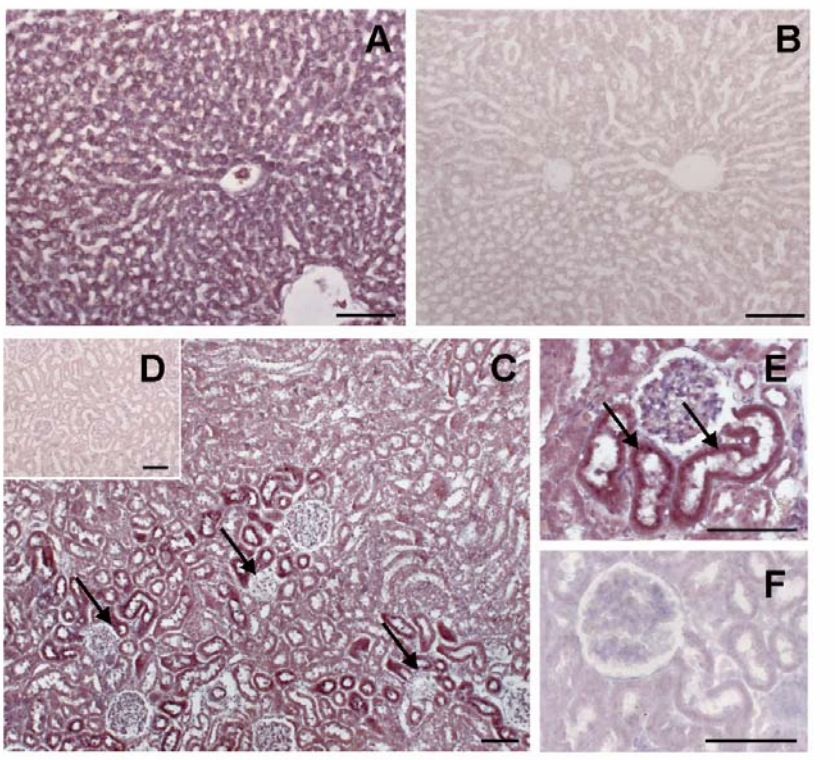

Figure 18. *In situ* hybridization analysis of Slc10a5 mRNA expression in (A-B) rat liver and (C-F) rat kidney. Liver and kidney sections were hybridized with digoxigenin-labeled Slc10a5 antisense (A,C,E) and sense (B,D,F) probes. Slc10a5 expression was detected in hepatocytes and renal proximal tubules (indicated by arrows). Scale bar: 100 µm.

4.2.3 Transport studies in *Xenopus laevis* oocytes

For functional characterization of the SLC10A5 protein, SLC10A5-cRNA injected *Xenopus laevis* oocytes were used and the transport of radiolabeled bile acids and sulfoconjugated steroid hormones was analyzed in comparison to water-injected oocytes. In contrast to NTCP-expressing oocytes, which were used as the positive control, no transport activity was detected for taurocholate, cholate, chenodeoxycholate, estrone-3-sulfate, pregnenolone sulfate or dehydroepiandrosterone sulfate in the SLC10A5-expressing oocytes (Table 6).

Table 6
Uptake studies with the human and mouse SLC10A5 proteins in *Xenopus laevis* oocytes.

Test compound	NTCP		Human SLC10A5	
	Uptake (fmol/oocyte/60 min)	*ratio*	Uptake (fmol/oocyte/60 min)	*ratio*
Taurocholate [6.4 µM]	11470 ± 7526	**468 ***	28.3 ± 6.8	**1.2**
Cholate [5 µM]	13132 ± 6612	**81 ***	202 ± 57	**1.2**
Chenodeoxycholate [5 µM]	17491 ± 5604	**2.9 ***	6341 ± 2500	**1.0**
Estrone-3-sulfate [20 nM]	134 ± 59	**50 ***	3.8 ± 1.6	**1.4**
PREGS [100 nM]	277 ± 140.5	**15 ***	28.2 ± 1.6	**1.6**
DHEAS [2 µM]	3061 ± 1454	**13 ***	285 ± 86	**1.2**
Test compound	**NTCP**		**Mouse Slc10a5**	
Taurocholate [5 µM]	1383 ± 568	**180 ***	8.7 ± 1.3	**1.1**
Estrone-3-sulfate [100 nM]	77.8 ± 12.8	**6.0 ***	17.8 ± 4.8	**1.4**

Note: Values represent means ± SD of 10 separate oocyte measurements. Ratio represents uptake into carrier-cRNA injected oocytes divided by uptake into water-injected oocytes. * Significantly higher uptake into carrier-cRNA injected oocytes compared with water-injected oocytes ($p < 0.001$). DHEAS: dehydroepiandrosterone sulfate.

4.2.4 Expression of SLC10A5 in *Xenopus laevis* oocytes and HEK293 cells.

In order to analyze whether the lack of transport activity of SLC10A5 in the oocytes resulted from insufficient protein synthesis or membrane insertion, the FLAG epitope was attached to the C-terminal end of human, rat, and mouse SLC10A5 proteins similarly as in the rat Slc10a4 protein and the appearance of the FLAG-tagged proteins in the oocytes was analyzed by immunofluorescence detection. As shown in Fig. 19A, human, rat, and mouse SLC10A5-FLAG proteins were clearly detected in the oocyte's plasma membrane. The SLC10A5-FLAG proteins were also expressed in HEK293 cells, but showed also no transport activity for taurocholate and estrone-3-sulfate in this expression system. HEK293 cells expressing the mouse SLC10A5-FLAG protein were also used for radioimmunoprecipitation experiments with an anti-FLAG antibody. A

specific band for the FLAG-tagged SLC10A5 protein was detected at 42 kDa which did not appear in the empty-vector transfected HEK293 cells. An additional faint band was visible at 84 kDa, which probably represents a dimeric form of the SLC10A5 protein (Fig. 19B).

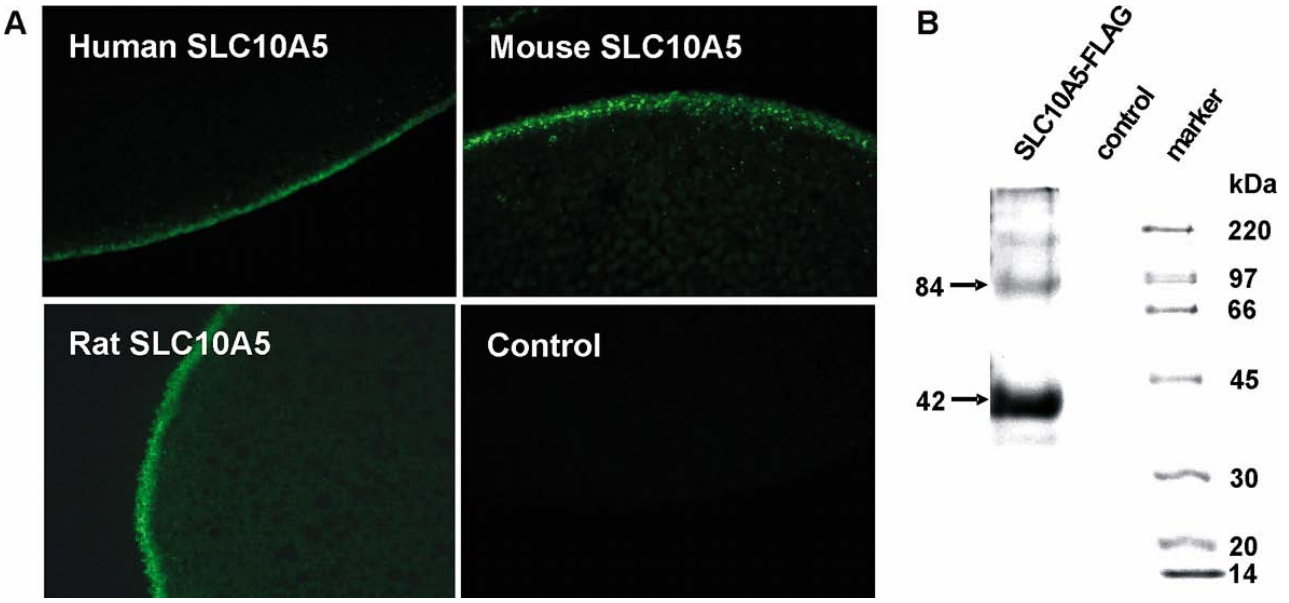

Figure 19. Expression of SLC10A5-FLAG fusion proteins in (A) *Xenopus laevis* oocytes and (B) HEK293 cells. (A) The human, mouse and rat SLC10A5-FLAG tagged proteins were detected in the plasma membrane of SLC10A5-FLAG-cRNA injected *Xenopus laevis* oocytes by immunofluorescence detection using an anti-FLAG antibody and Alexa Fluor 488. Water-injected oocytes were used as the negative control. (B) HEK293 cells transfected with the mouse Slc10a5-FLAG-pcDNA5 vector or empty vector (control) were used for radioimmunoprecipitation with an anti-FLAG antibody. The samples were separated by gel electrophoresis on a 12% SDS-polyacrylamide gel and exposed to standard x-ray film for visualization.

5. Discussion

5.1 The Complexity of the SLC10 Carrier Family

The former nomenclature of the SLC10 transporter family as the family of bile acid cotransporter (Hagenbuch and Dawson 2004) is not longer justified. None of the five new family members transports typical bile acids so far. Although SLC10A4 was originally introduced as new bile acid transporter (Splinter et al. 2006) neither this group nor we could confirm any bile acid transport via SLC10A4. Instead data in this thesis strongly suggest a functional, albeit yet unknown role in neurotransmission. This is discussed in the next chapter. SLC10A4 and the liver bile acid transporter NTCP (SLC10A1) originate from a common ancestor as do SLC10A3 and SLC10A5 (Fig.20). However, the latter belong to a separate clade of SLC10 genes (Clade II) setting them apart from the NTCP/SLC10A4 and ASBT/SLC10A6 transporters (Clade I). Within clade I only in case of ASBT/SLC10A6 the substrate spectrum is known: ASBT transport bile acids but not sulfated steroids, whereas SLC10A6 (SOAT) transports sulfated steroids but not unconjugated bile acids.

The 7th member of this family, SLC10A7 (Godoy et al. 2007) is unique and may represent an independent class of transporters. This carrier gene exhibits 12 exons, whereas the other members exhibit 1 (SLC10A3 and SLC10A5), 3 (SLC10A4) and 6 (SLC10A2 and SLC10A6) exons. Such heterogenecity in gene structure, however, is nothing extraordinary, as e.g. members of SLC2, SLC5, SLC7, SLC16, and SLC30.

5.2 The SLC10A4 Subfamily

5.2.1 Slc10a4 and the SLC10 Family

The rat Slc10a4 exhibits high mRNA expression levels in the brain (Geyer et al. 2006; Splinter et al. 2006). Here it was proven that Slc10a4 is expressed in cholinergic neurons throughout the rat CNS. Because the Slc10a4 protein was formerly assumed to be a novel bile acid carrier (Hagenbuch and Dawson 2004), its neuronal expression of Slc10a4 was unexpected and sheds new light on putative functions of the SLC10 carrier family.

Because Ntcp and Slc10a4 derived from a common ancestor gene, we assumed that Ntcp and Slc10a4 might share functional properties. In particular, the sulfoconjugated steroid hormones DHEAS and PREGS, which are transported by Ntcp, were prime candidates of Slc10a4 substrates. These steroids are present in the CNS at high concentrations and exert multiple effects on neuronal excitability, neuronal plasticity, and neuroprotection (Baulieu 1998; Rupprecht and Holsboer 1999; Wolf and Kirschbaum 1999; Schumacher et al. 2000; Mellon and Griffin 2002; Dubrovsky 2005). However, none of these compounds was transported by rat Slc10a4 when

expressed in *Xenopus laevis* oocytes or HEK293 cells. Detailed analysis of the amino acid sequences of Ntcp and Slc10a4 revealed some structural differences. E.g., the Slc10a4 protein does not contain the “ALGMMPL” signature motif of all NTCP/Ntcp, ABST/Asbt, and SOAT/Soat proteins (Geyer et al. 2006). However, it is not clear whether this motif is involved in substrate binding or transport activity. Also, the Slc10a4 protein consists of 437 amino acids and exceeds the length of the Ntcp protein (362 amino acid residues) by an additional N-terminal domain of about 60 amino acids. Nevertheless, Slc10a4 exhibits a secondary structure comparable to NTCP since it showed seven transmembrane domains and N_{exo}/C_{cyt} *trans*-orientation of the N-terminal and C-terminal domains.

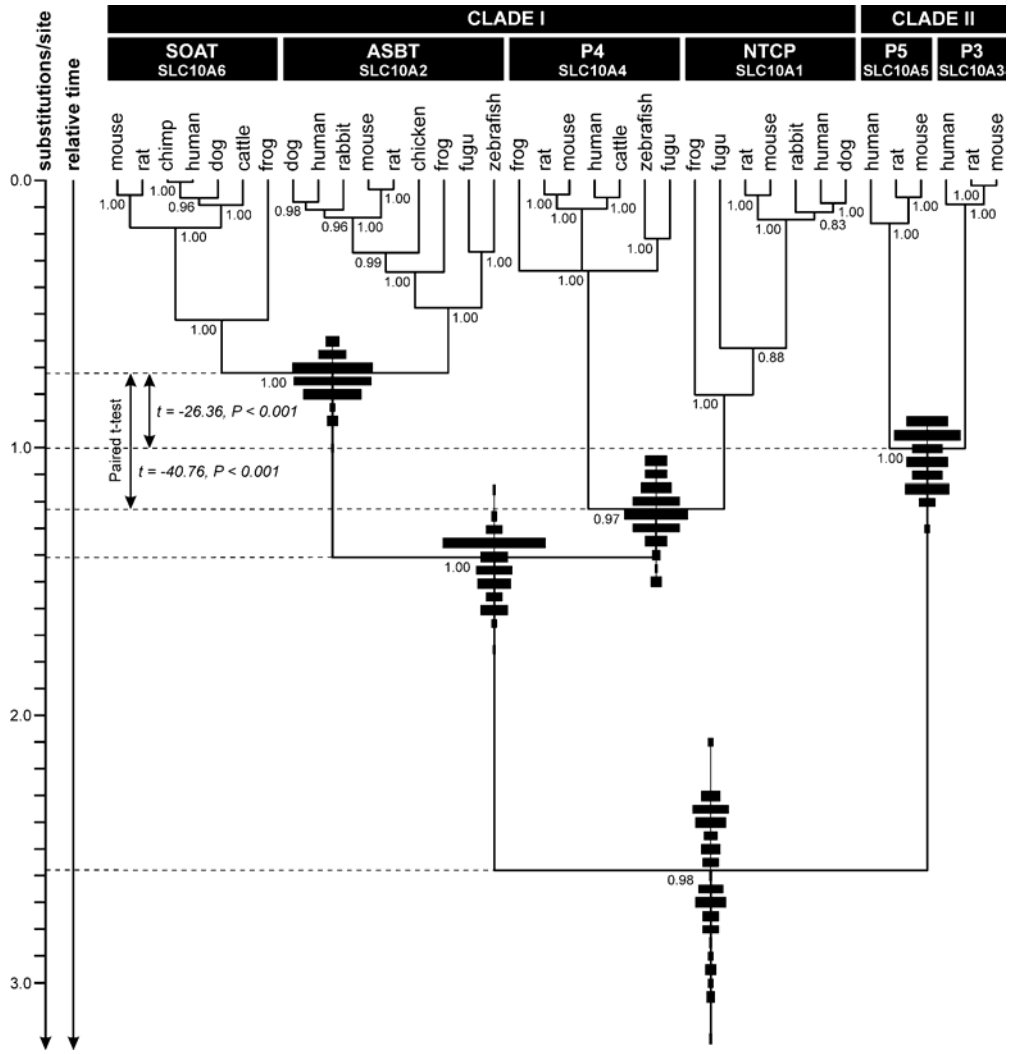

Figure 20. Clock-enforced Bayesian cDNA tree with lineages-through-time plot of selected mammalian and non-mammalian members of the SLC10 family according to Geyer et al. 2006. Respective cDNA sequences were aligned with Clustal W and truncated to the shortest sequence, resulting in 864 aligned nucleotide positions. As outgroup, a *Drosophila* sequence with high sequence similarity to the SLC10 familymembers was used. All major clades (i.e. protein subfamilies) are resolved with posterior probabilities greater than0.95 (plotted at nodes). Vertical branch lengths refect the substitutions per site (see scale on the left). In a clock-enforced tree, they also reflect coalescent time. However, as no clock rate is known for the SLC10 family, absolute times cannot be provided. Pairwise comparisons of node depths in the 100 best trees for the split of SOAT/ASBT on the one side and P4/NTCP and P5/P3 on the other side using paired *t*-tests indicated that the depth of the nodes (and therefore their age) differs significantly between both SOAT/ASBT and P4/NTCP as well as between SOAT/ASBT and P5/P3.

5.2.2 Expression of Slc10a4 in cholinergic neurons of the rat CNS

In contrast to Ntcp which shows tissue-specific and species-independent high expression in the liver (Hagenbuch et al. 1990; Ananthanarayanan et al. 1994; Stieger et al. 1994), Slc10a4 mRNA proved to be most highly expressed in the human, rat, and murine brain.

The cellular localization of Slc10a4 expression in the rat CNS was revealed by a polyclonal rabbit antiserum directed against the rat Slc10a4 protein. This antiserum showed specific Slc10a4 expression for all cholinergic cell groups (Fig.21) and their projection pathways in the rat brain, commonly identified by choline *O*-acetyltransferase (ChAT) expression (Eckenstein et al. 1982; Armstrong et al. 1983; Levey et al. 1983a,b) and immunoreactivities for VAChT (Gilmor et al. 1996; Weihe et al. 1996) or CHT1 (Misawa et al. 2001; Ferguson et al. 2003; Kus et al. 2003). Slc10a4-directed immunoreactivity was detected in perikarya and/or nerve terminals at varying degree in all of these cholinergic regions. Although Slc10a4-specific immunofluorescence staining clearly merged with VAChT-specific and CHT1-specific immunoreactivities in general, only a few specific regions were found where Slc10a4 expression was apparently higher (basolateral amygdaloid nucleus, ventral tegmental area, substantia nigra, nucleus of the solitary tract, and dorsal motor nucleus of vagus) or lower (nucleus of the vertical limb of the diagonal band, medial septal nucleus, caudate putamen, and basal nucleus of Meynert) than expression of VAChT and CHT1. The most apparent difference was observed within the substantia nigra (SN), where clear staining of Slc10a4-positive neuronal cell bodies, fibers and boutons was detected by immunohistochemistry. SLC10A4 mRNA proved to be strongly expressed also in the human SN, pointing to a particular importance of SLC10A4/Slc10a4 in this brain region. In contrast, immunostaining for VAChT and CHT1 was not observed within the SN. In earlier studies, expression of choline acetyltransferase (ChAT) was detected in neurons of the SN, and this enzyme showed an expression pattern very similar to that of Slc10a4 at the transition zone between the SN compact and reticular compartment (Martinez-Murillo et al. 1989). This prompted us to perform co-localization studies also with Slc10a4 and ChAT. In these studies we found co-localization of Slc10a4-specific and ChAT-specific immunoreactivities in neuronal cell bodies, confirming that also in the SN, Slc10a4 is expressed in cholinergic neurons. In a recent study, Jørgensen and coworkers (2006) found significant up-regulation of SLC10A4 mRNA expression during the development of the human ventral mesencephalon. The authors stated that SLC10A4 might be a candidate marker gene for dopaminergic progenitor neurons. However, based on the results of our co-localization studies with Slc10a4 and the catecholaminergic marker tyrosine hydroxylase, no co-expression of both proteins was observed throughout the rat brain. An exception was the dopaminergic regions ventral tegmental area and substantia nigra, where some neurons showed Slc10a4 protein also in dopaminergic cells. Its meaning is unclear but would not conflict with the general expression pattern in cholinergic neurons of the rat brain, as shown by VAChT, CHT1, and ChAT co-labeling studies from all other regions.

Very recently, Lein et al. (2007), published the expression pattern of ~ 20,000 genes in the adult mouse brain, including Slc10a4, using automated high-throughput *in situ* hybridization. The data were organized into the Allen Brain Atlas and are available online under http://www.brain-map.org. These experiments clearly confirmed Slc10a4 mRNA expression in all cholinergic cell groups where the Slc10a4 protein was detected in the present work.

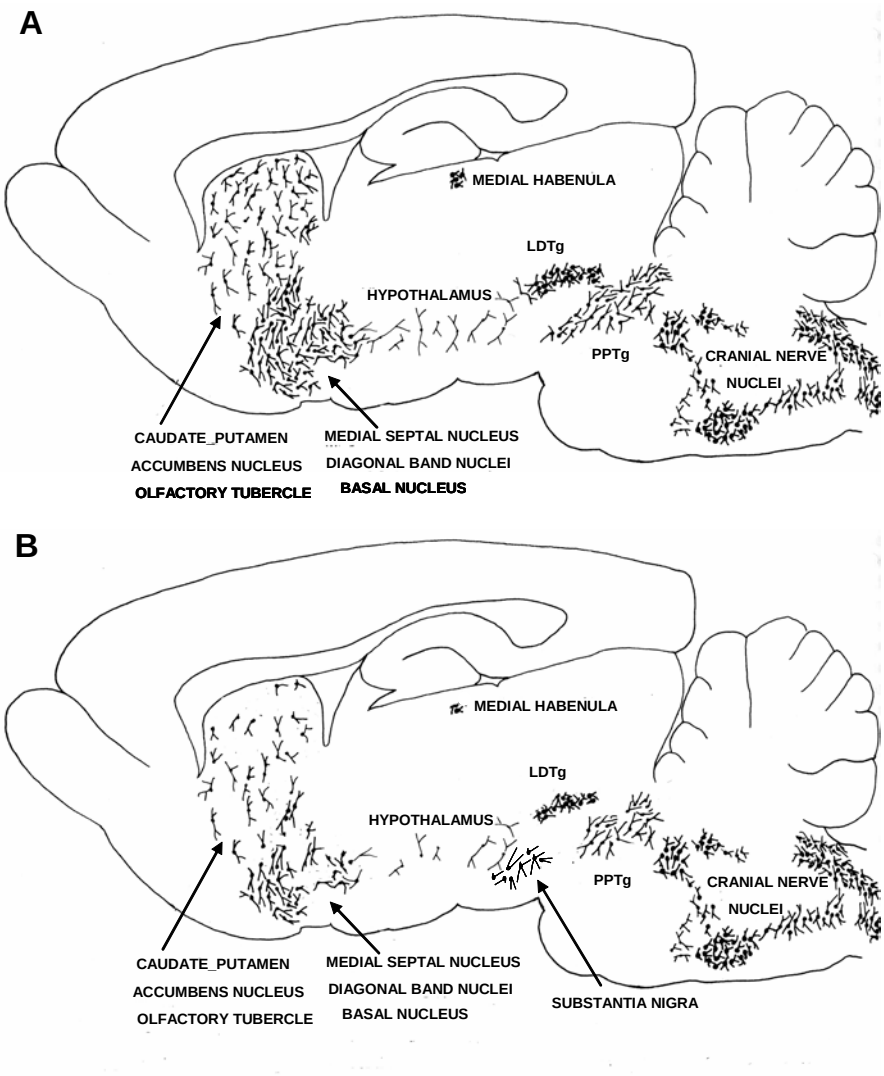

Figure 21.Schematic representation of the rostral-caudal organization of (A) cholinergic and (B) Slc10a4 cell groups in sagittal sections of rat brain. *A*, Continuous chain of cholinergic somata is distributed through the basal forebrain (caudate putamen, accumbens nucleus, olfactory tubercle, medial septal nucleus, diagonal band nuclei, and basal nucleus), medial habenula, mesopontine neurons (latero-dorsal tegmental nucleus-LDTg and pedunculopontine tegmental nucleus-PPTg), and the cranial nerve nuclei. *Adapted from Larry L. Butcher and Nancy J. Woolf in "The Rat Nervous System", 2004*. *B*, Reconstruction of Slc10a4 expression based on the data of the present study. Slc10a4 was observed in the basal forebrain complex, medial habenula, mesopontine cholinergic neurons, substantia nigra, and all cranial nerve nuclei. Whereas Slc10a4 expression seems to be weaker than the known cholinergic somata in the basal forebrain complex, in the substantia nigra the Slc10a4 protein appeared clearly stronger than other cholinergic marker proteins (CHT1, VAChT).

5.2.3 Subcellular localization of Slc10a4 and proposed function

Functionally, CHT1 serves to recapture choline from the synaptic cleft, in order to sustain new acetylcholine synthesis of cholinergic neurons (Haga 1971; Okuda et al. 2000; Okuda and Haga 2000). The CHT1 protein is not exclusively localized in the plasma membrane of presynaptic terminals though; instead, it was found mainly in intracellular vesicular structures that represent a reserve pool for this carrier (Ferguson and Blakely 2004; Sarter and Parikh 2005). CHT1 can be recruited from these vesicles to the plasma membrane by synaptic vesicle exocytosis in response to high neuronal activity (Ferguson et al. 2003; Ribeiro et al. 2003; Nakata et al. 2004). Several

recent studies examined the trafficking process of vesicles containing CHT1 or VAChT at the molecular level (Barbosa et al. 2002; Ferguson et al. 2003; Gates et al. 2004; Xie and Guo 2004; Ferreira et al. 2005; Ribeiro et al. 2005), but this process is still not completely understood (Ribeiro et al. 2006). It may be speculated that the Slc10a4 protein, which was localized at the plasma membrane when expressed in HEK293 cells and was partially present in intracellular compartments, might be involved in the docking and retrieval process of vesicles containing CHT1 or VAChT as outlined in Fig.22. Following another hypothesis, Slc10a4 could act as a synaptic reuptake carrier for acetate or any cotransmitter involved in the cholinergic transmission, i.e. ATP or VIP (Corthay et al. 1985; Willard 1990; Kupfermann 1991; Ribeiro et al. 1996; Burnstock 2006). Although there is no experimental evidence for this hypothesis until now, based on the data presented in this work Slc10a4 localization deserves closer attention regarding neurotransmission of cholinergic neurons.

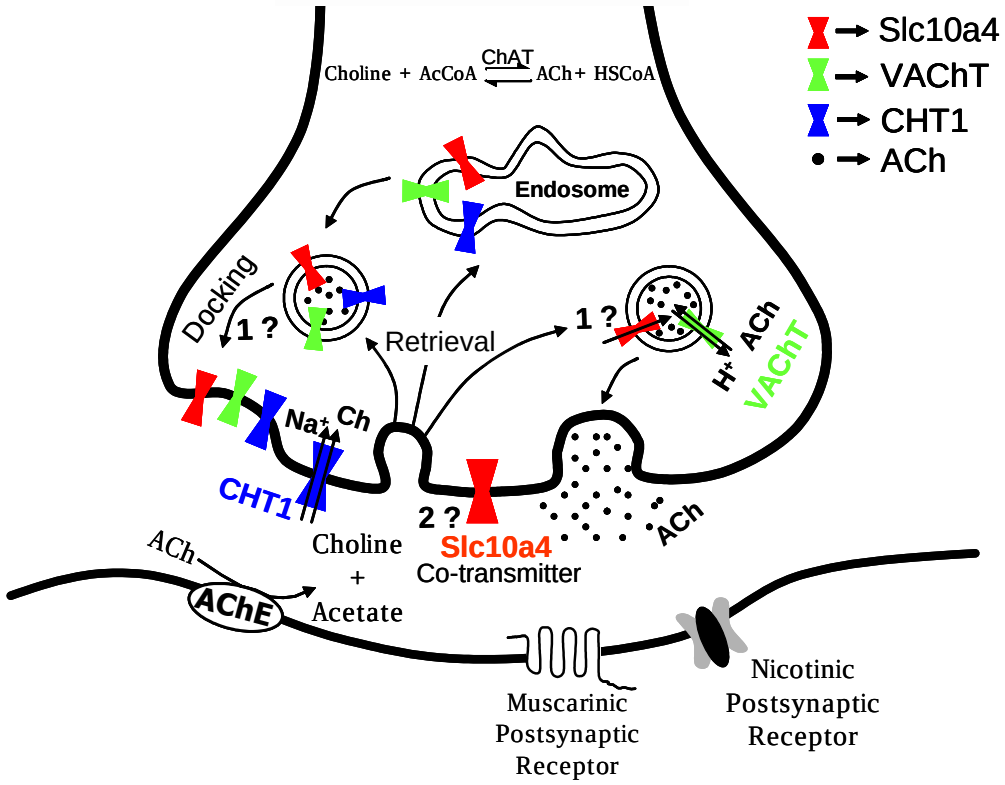

Figure 22. Hypothetical roles of Slc10a4 in cholinergic synapses. The cholinergic neurotransmission basically depends on three proteins: the choline O-acetyltransferase (ChAT), the enzyme that catalyses the synthesis of acethylcholine (ACh) from choline (Ch) and acetyl-coenzyme A (AcCoA), the proton-dependent vesicular acetylcholine transporter (VAChT), which transports newly synthesized ACh from cytoplasm into presynaptic vesicles, and the high-affinity sodium- and chloride-dependent choline transporter (CHT1), which mediates the reuptake of choline after breakdown of acetylcholine in the synaptic cleft by acetylcholinesterase (AChE). CHT1 is mainly expressed in presynaptic vesicles or endosomes that also contain VAChT. The trafficking of these proteins between the presynaptic vesicles and the plasma membrane is still not completely understood. Slc10a4 could participate in the docking and retrieval process of CHT or VAChT vesicles (hypothesis 1) or serves as a novel carrier for synaptic reuptake of acetate or any cotransmitter involved in the cholinergic synapse (hypothesis 2).

5.3 The SLC10A5 Subfamily

5.3.1 SLC10A5 and the SLC10 Family

The SLC10A5 proteins consist of 434-438 amino acids in human, rat, and mouse and show an overall amino acid sequence identity of >70%. Further SLC10A5-related sequences were identified by Ensembl orthologue predictions (Ensembl release 43) from cattle and chimp which exhibit high sequence identities to the human SLC10A5 protein (76% and 98%, respectively). Again, functional data of these proteins is lacking.

Bioinformatic programs showed membrane topologies with nine transmembrane domains and N_{exo}/C_{cyt} trans orientations of the N-terminal and C-terminal ends for SLC10A5/Slc10a5 proteins. This topology pattern is different from the potential seven transmembrane domains topology of the NTCP, ASBT, SOAT and SLC10A4 (Mareninova et al. 2005; Banerjee and Swan; 2006, Hussainzada et al. 2006; Geyer et al. 2007). Whether this structural difference directly influences the lack of bile acid and steroid sulfate transport function by SLC10A5 is not clear. On other hand a truncated ASBT, containing only 3 transmembrane domains exerted bile acid transport when expressed in cholangiocytes (Lazaridis et al. 2000).

5.3.2 Expression of Slc10a5 in the rat liver and kidney

As NTCP and ASBT, SLC10A5/Slc10a5 showed a distinct tissue-specific expression pattern in humans, rat, and mouse, with its highest expression in liver and kidney. In rats, Slc10a5 expression was further localized by *in situ* hybridization to hepatocytes and renal proximal tubules. If SLC10A5 is involved in the hepatic and renal transport of either rare bile acids or other solutes, it should be localized at the basolateral membrane of these cells. This needs to be established with an appropriate antibody.

5.3.3 SLC10A5 Protein Length

The bile acid carriers NTCP and ASBT in their deglycosylated forms showed apparent molecular weights of 33.5 kDa (Stieger et al. 1994) and 35 kDa (Wong et al. 1995), respectively, which is lower than the predicted molecular masses of the non-glycosylated proteins. Similar results were found for the FLAG-tagged mouse SLC10A5 protein that showed after radioimmunoprecipitation a specific band at 42 kDa which is 7 kDa smaller than its predicted mass of 49 kDa (48 kDa for the SLC10A5 protein + 1 kDa for the FLAG epitope). In addition to the 42 kDa band, we also found a faint band of higher molecular weight at 84 kDa that possibly represents a N^{96}-glycosylated form of the mouse SLC10A5 protein or a larger apparent protein aggregate, as was also reported for NTCP and ASBT (Shneider et al. 1995; Stieger et al. 1994, Kramer et al. 1997).

5.3.4 Potential Function of SLC10A5

Although expressed in the plasma membrane of *Xenopus laevis* oocytes, SLC10A5 did not mediate uptake of established substrates of the other SLC10 carriers NTCP, ASBT, and SOAT, i.e., bile acids such as taurocholate and cholate and sulfoconjugated steroid hormones such as estrone-3-sulfate and dehydroepiandrosterone sulfate (Craddock et al. 1998; Schroeder et al. 1998; Geyer et al. 2007). Although it was not proven in the present work that SLC10A5 transport any tested substrate, based on the liver-specific and kidney-specific expression pattern and the close phylogenetic relationship to NTCP and ASBT, it can be assumed that SLC10A5 is still a carrier protein but for other kinds of bile acids or other organic solutes. A recent working hypothesis is that it transports thyroid hormones such as the T3 and T4 and their sulfoconjugated forms (personal communication by Theo J Visser). Whereas transport of T3/T4 was previously shown for members of the OATP carrier family (Friesema et al. 1998; Abe et al.1998; Hagenbuch 2007), the sodium-dependent liver and kidney transporter for the sulfoconjugated forms is still undiscovered. Currently, studies are ongoing in which the transport activity for nine different bile acid molecules (TCDC, GCDC, GCD, TCD, GUDC, TUDC, GC, C, LC) as well as sulfoconjugated thyroid hormones is measured in a newly established SLC10A5-HEK293 cell line.

5.4 Future Prospects

Despite the restricted knowledge about the functional properties of the novel SLC10 members, this work will serve as a solid background to investigate the physiological role of SLC10A4 and SLC10A5.

To promote the untiring search for the functions of SLC10A4 and SLC10A5, the following studies are intended:

1. Generation of an anti-SLC10A5 antibody to define the cellular localization, in the liver and renal proximal tubules.
2. Stabile transfection of SLC10A4 and SLC10A5 into eukaryotic cell lines to complete transport measurements.
3. Unraveling trafficking of the rat Slc10a4 protein between intracellular compartments and the plasma membrane; the role of phosphorylation and dephosphorylation.
4. Transport measurements with choline and acethylcholine in Slc10a4-transfected cells and PC12 cells co-expressing CHT1 or VAChT to study the role of this protein in the cholinergic system.
5. Protein interactions between Slc10a4, CHT1 and VAChT by immunoprecipitation experiments and Fluorescence Resonance Energy Transfer (FRET).
6. Experiments using RNA interference (RNAi) or knockout mice to accomplish the biological function of the SLC10A4 and SLC10A5 proteins.

6 Summary

Over 10 years the solute carrier family SLC10 comprised two well established sodium-dependent bile acid transporters, i.e. the Na^+/taurocholate cotransporting polypeptide NTCP (SLC10A1) and the apical sodium-dependent bile acid transporter ASBT (SLC10A2). These carriers are essentially involved in the maintenance of the enterohepatic circulation of bile acids mediating the first step of active bile acid transport through the membrane barriers in the liver (NTCP) and the intestine (ASBT). Recently, two further members of this transporter family were identified in our group; they are referred to as sodium-dependent organic anion transporter SOAT (SLC10A6) and SLC10A7. While SOAT transports sulfoconjugated steroid hormones and sulfoconjugated bile acids, SLC10A7 remains an orphan carrier with yet unknown substrates.

In the present study, two novel members were discovered and referred to as Slc10a4 and SLC10A5 (GenBank accession nos. AY825924, AY825925, and DQ074435). This work describes molecular cloning, expression and molecular analysis as well as functional testing for these novel putative membrane transporters. Sequence lengths of the SLC10A4 and SLC10A5 proteins are between 434-438 amino acids in man, rat, and mouse which is much longer compared with other members this carrier family (i.e. 340-377 amino acids). However, sequence identity/similarity of SLC10A4 is quite high to NTCP, ASBT, and SOAT, being 29%/54%. In contrast, identity/similarity values of SLC10A5 are highest to SLC10A3 which is an orphan and hitherto uncharacterized member of the SLC10 family.

Slc10a4 exhibits a seven transmembrane domain topology with N_{exo}/C_{cyt} *trans*-orientation of the N- and C-terminal ends, whereas SLC10A5/Slc10a5 shows nine putative TMDs. Based on real time quantitative PCR and northern blot analyses SLC10A4 expression is predominant in the brain, whereas SLC10A5 is highest expressed in the liver and kidney. A polyclonal rabbit antibody was generated against the rat Slc10a4 protein and used for western blot and immunohistochemical analyses. Slc10a4-immunoreactivity was detected in cholinergic regions throughout the rat central nervous system. Co-localization studies with the cholinergic markers VAChT, ChAT, and CHT1 confirmed the presence of Slc10a4 in cholinergic neurons. Furthermore, the Slc10a4 protein is expressed in two dopaminergic regions: the substantia nigra and ventral tegmental area. Here, this protein was co-localized with ChAT and the catecholaminergic marker tyrosine hydroxylase. Slc10a5 expression was localized by *in situ* hybridization to hepatocytes and renal proximal tubules in rat liver and kidney sections, respectively.

For the functional characterization of Slc10a4 and SLC10A5/Slc10a5, these proteins were expressed in *X. laevis* oocytes and HEK293 cells. Thereby, the C-terminal end of the proteins was tagged by the FLAG epitope and plasma membrane expression was confirmed by immunofluorescence microscopy. However, up to now transport studies failed to show transport activity of Slc10a4 and SLC10A5/Slc10a5 for bile acids and steroid sulfates, which are the typical substrates for NTCP, ASBT, and SOAT. Regarding SLC10A5/Slc10a5, because similar expression

patterns to NTCP and ASBT and as these bile acid carriers are the most related carriers to SLC10A5 though, it's strongly supposed that SLC10A5 also has carrier function. Regarding Slc10a4, this carrier did not transport choline neither, which is a substrate of CHT1. Thus, in this study, the functional properties of Slc10a4 could not be completely elucidated, but Slc10a4 is assumed to be a new marker protein for cholinergic neurons. This unexpected finding for a novel member of the sodium/bile acid cotransporter family SLC10 sets Slc10a4 apart and needs further clarification.

7 Zusammenfassung

Die „Solute Carrier" Familie SLC10 besteht über 10 Jahre aus zwei sehr gut charakterisierten Mitgliedern: Dem „Na^+/Taurocholate Cotransporting Polypeptide" NTCP (SLC10A1) und dem „Apical Sodium-dependent Bile Acid Transporter" ASBT (SLC10A2). Diese Carrier haben eine essentielle physiologische Bedeutung in der Aufrechterhaltung des enterohepatischen Kreislaufs der Gallensäuren. Hierbei vermitteln sie den ersten Schritt der zellulären Aufnahme von Gallensäuren in Leber (NTCP) und Darm (ASBT).

Vor kurzem konnten zwei weitere Mitglieder dieser Familie in unserer Arbeitsgruppe identifiziert werden, welche als „Sodium-dependent Organic Anion Transport" SOAT (SLC10A6) und SLC10A7 bezeichnet wurden. Während SOAT sulfokonjugierte Steroidhormone und sulfokonjugierte Gallensäuren transportiert, konnte für den SLC10A7 bisher kein Substrat identifiziert werden.

In dieser Studie wurden zwei weitere Mitglieder der SLC10 Familie entdeckt und als SLC10A4 und SLC10A5 bezeichnet (GenBank accession nos. AY825924, AY825925 und DQ074435). Diese Arbeit beschreibt die molekulare Klonierung, Expression und molekulare Analyse sowie die funktionelle Testung dieser neuen möglichen Membrantransporter. Die Proteinsequenzen von SLC10A4 und SLC10A5 bestehen aus 434-438 Aminosäuren bei Mensch, Ratte und Maus und sind damit viel länger ist im Vergleich zu den Proteinlängen anderer Mitglieder dieser Transporterfamilie (340-377 Aminosäuren). Die Sequenzidentität/Sequenzähnlichkeit des SLC10A4 zu NTCP, ASBT und SOAT ist mit 29%/54% relativ hoch. Anderesseits ist die Identität/Ähnlichkeit des SLC10A5 am höchsten zu SLC10A3, welches ein bisher nicht charakterisiertes Mitglied der SLC10 Familie ist.

Der Slc10a4 der Ratte zeigt eine Membrantopologie mit sieben Transmembrandomänen und einer N_{exo}/C_{cyt} *trans*-Orientierung, wohingegen der SLC10A5/Slc10a5 neun mögliche TMDs hat. Basierend auf „real time quantitativer PCR" und Northern Blot Analysen lässt sich eine Expression von SLC10A4/Slc10a4 überwiegend im Gehirn feststellen, während SLC10A5/Slc10a5 in Leber und Niere stark exprimiert wird. Gegen den Slc10a4 der Ratte wurde ein polyklonaler Antikörper in Kaninchen generiert und mit diesem Western Blot und immunohistochemische Analysen durchgeführt. Eine Slc10a4-Immunoreaktivität wurde in den cholinergen Regionen des gesamten Zentralnervensystems der Ratte nachgewiesen. Co-Lokalisationsstudien mit den cholinergen Markern VAChT, ChAT und CHT1 bestätigen die Anwesenheit des Slc10a4 in den cholinergen Neuronen. Zusätzlich wurde das Slc10a4 Protein in zwei dopaminergen Regionen identifiziert: Substantia Nigra und Ventrales Tegmentales Areal. In diesen Regionen wird dieses Protein mit ChAT und dem catecholaminergen Marker Tyrosinhydroxylase co-exprimiert. Die Expression des Slc10a5 der Ratte wurde mit *in situ* Hybridisierung in den Hepatozyten und im proximalen Tubulus der Niere nachgewiesen.

Die funktionelle Charakterisierung des Slc10a4 und SLC10A5/Slc10a5 wurde in *X. laevis* Oozyten und HEK293 Zellen durchgeführt. Die Expression beider Proteine konnte durch Nachweis eines C-

terminalen FLAG Epitops mit Immunfluoreszenz-Mikroskopie in der Plasmamembran bestätigt werden. Bisher konnte in den Transportstudien allerdings keine Transportaktivität von Slc10a4 und SLC10A5/Slc10a5 für Gallensäuren und Steroidsulfate, welche die typischen Substrate des NTCP, ASBT und SOAT sind, festgestellt werden. Wegen seiner hoher Verwandtschaft zu den Gallensäuretransportern und der Lokalisation in Leber und Niere vermuten wir, dass auch SLC10A5 eine Transportfunktion aufweist, dessen Substrat noch identifiziert werden muss.

Hinsichtlich Slc10a4 konnte ich zeigen, dass dieses Protein auch kein cholin, ein Substrat des CHT1, transportiert. In dieser Arbeit konnten die funktionellen Eigenschaften des Slc10a4 nur teilweise geklärt werden. Allerdings scheint der Slc10a4 ein neues Markerprotein für cholinerge Neurone zu sein, welches ein unerwarteter Befund für ein Mitglied der „Sodium/Bile Acid Cotransporter“ Familie SLC10 ist.

8 References

Abe T, Kakyo M, Sakagami H, Tokui T, Nishio T, Tanemoto M, Nomura H, Herbert SC, Matsuno S, Kondo H, Yawo H. 1998. Molecular characterization and tissue distribution of a new organic anion transporter subtype (oatp3) that transports thyroid hormones and taurocholate and comparison with oatp2. *J Biol Chem 273*:22395-22401.

Alcalay M, Toniolo D. 1988. CpG islands of the X chromosome are gene associated. *Nucleic Acids Res 16*:9527-9543.

Alfonso A, Grundahl K, Duerr JS, Han HP, Rand JB. 1993. The Caenorhabditis elegans unc-17 gene: a putative vesicular acetylcholine transporter. *Science 261*: 617-619.

Ananthanarayanan M, Ng OC, Boyer JL, Suchy FJ. 1994. Characterization of cloned rat liver Na(+)-bile acid cotransporter using peptide and fusion protein antibodies. *Am J Physiol 267*:G637-G643.

Anwer MS. 2004. Cellular regulation of hepathic bile acid transport in health and cholestasis. *Hepatology 39*:581-590

Apparsundaram S, Ferguson SM, George AL, Jr., Blakely RD. 2000. Molecular cloning of a human, hemicholinium-3-sensitive choline transporter. *Biochem Biophys Res Commun 276*:862-867.

Apparsundaram S, Ferguson SM, Blakely RD. 2001. Molecular cloning and characterization of a murine hemicholinium-3-sensitive choline transporter. *Biochem Soc Trans 29*:711-716.

Armstrong DM, Saper CB, Levey AI, Wainer BH, Terry RD. 1983. Distribution of cholinergic neurons in rat brain: demonstrated by the immunocytochemical localization of choline acetyltransferase. *J Comp Neurol 216*:53-68.

Arrese M, Ananthanarayanan M. 2004. The bile acid export pump:molecular properties, function and regulation. *Pflügers Arch 449*:123-131.

Arvidsson U, Riedl M, Elde R, Meister B. 1997. Vesicular acetylcholine transporter (VAChT) Protein: A novel and unique marker for cholinergic neurons in the central and peripheral nervous systems. *J Comp Neurol 378*:454-467.

Barbosa J, Jr., Ferreira LT, Martins-Silva C, Santos MS, Torres GE, Caron MG, Gomez MV, Ferguson SS, Prado MA, Prado VF. 2002. Trafficking of the vesicular acetylcholine transporter in SN56 cells: a dynamin-sensitive step and interaction with the AP-2 adaptor complex. *J Neurochem 82*:1221-1228.

Banerjee A, Swaan PW. 2006. Membrane topology of human ASBT (SLC10A2) determined by dual label epitope insertion scanning mutagenesis. New evidence for seven transmembrane domains. *Biochemistry 45*:943-953.

Baulieu EE. 1998. Neurosteroids: a novel function of the brain. *Psychoneuroendocrinology 23*:963-987.

Benishin CD, Carrol PT. 1983. Multiple forms of choline-O-acetyltransferase in mouse and rat brain: Solubilization and characterization. *J Neurochem* 41:1030-1039.

Berrard S, Varoqui H, Cervini R, Israel M, Mallet J, Diebler MF.1995. Co-regulation of two embedded gene products, choline acetyltransferase and vesicular acetylcholine transporter. *J Neurochem 65*:939-942.

Berse B, Blusztajin JK. 1995. Coordinated up-regulation of choline acetyltransferase and vesicular acetylcholine transporter gene expression by the retinoic acid receptor α, cAMP, and leukemia inhibitory factor/ciliary neurotropic factor signaling pathways in a murine septal cell line. *J Bio Chem 270*: 101-122.

Bjorkhem I, Lund E, Rudling M. 1997. Coordinate regulation of cholesterol 7 alpha-hydroxylase and HMG-CoA reductase in the liver. *Subcell Biiochem 28*:23-55.

Brandon C, Wu JY. 1978. Purification and properties of choline acetyltransferase from Torpedo californica. *J Neurochem 30*:791-797.

Bravo DT, Kolmakova NG, Parsons SM. 2004. Choline is transported by vesicular acetylcholine transporter. *J Neurochem Int 91*:766-768.

Bravo DT, Kolmakova NG, Parsons SM. 2005. New transport assay demonstrates vesicular acetylcholine transporter has many alternative substrates. *Neurochem Int 47*:243-247.

Bruce G, Hersh LB. 1989. The phosphorilation of choline acetyltransferase. *Neurochem Res* 14:613-620.

Buongiorno-Nardelli M, Amaldi F. 1970. Autoradiographic detection of molecular hybrids between rRNA and DNA in tissue sections. *Nature 225*: 946-948

Burnstock G. 2006. Historical review: ATP as a neurotransmitter. *Trends Pharmacol Sci 27*:166-176.

Butcher LL, Oh JD, Woolf NJ, Edwards RH, Roghani A.1992. Organization of central cholinergic neurons revealed by combined *in situ* hybridization histochemistry and choline-O-acetyltransferase immunocytochemistry. *Neurochem Int 21*:429-445.

Cattori V, Eckhardt U, Hagenbuch B. 1999. Molecular cloning and functional characterization of two alternatively spliced Ntcp isoforms from mouse liver. *Biochem Biophys Acta 1445*:154-159.

Chen NH, Reith ME, Quick MW. 2004. Synaptic uptake and beyond: the sodium- and chloride-dependent neurotransmitter transporter family SLC6. *Pflügers Arch 447*:519-531.

Chiu KP, Ariyaratne P, Xu H, Tan A, Ng P, Liu ET, Ruan Y, Wei C, Sung WKK. 2007. Pathway aberrations of murine melanoma cell observed in Paired-End diTag transcriptomes. *BMC Cancer 7*: doi: 10.1186/1471-2407-7-109.

Clarkson ED, Bahr BA, Parsons SM. 1993. Classical noncholinergic neurotransmitters and the vesicular transport system for acetylcholine. *J Neurochem 61*:22-28.

Cohn MA, Rounds DJ, Karpen SJ, Ananthanarayanan M, Suchy FJ. 1995. Assignment of a rat liver Na^+/bile acid cotransporter gene to chromosome 6q24. *Mamm Genome 6*:60.

Colgan L, Liu H, Huang SY, Liu YJ. 2007. Dileucine motif is sufficient for internalization and synaptic vesicle targeting of vesicular acetylcholine transporter. *Traffic 8*:512-522.

Colman A. 1984. Translation of eukaryotic messenger RNA in Xenopus oocytes. In: Transcription and Translation. A Practical Approach (Hames BD and Higgins SJ, eds), pp 271-302 Oxford: IRL Press Limited.

Corthay J, Dunant Y, Eder L, Loctin F. 1985. Incorporation of acetate into acetylcholine, acetylcarnitine, and amino acids in the Torpedo electric organ. *J Neurochem 45*:1809-1819.

Craddock AL, Love MW, Daniel RW, Kirby LC, Walters HC, Wong MH, Dawson PA. 1998. Expression and transport properties of the human ileal and renal sodium-dependent bile acid transporter. *Am J Physiol 274*:G157-G169.

Dietsch JM, Turley SD, Spad DK. 1993. Role of liver in the maintenance of cholesterol and low density lipoprotein homeostasis in different animal species, including humans. *J Lipid Res 34*:1637-1659.

Dobransky T, Davis WL, Xiao GH, Rylett RJ. 2000. Expression, purification and characterization of recombinant human choline acetyltransferase: Phosphorilation of the enzyme regulates catalytic activity. *Biochem J 349*:141-151.

Dobransky T, Davis WL, Rylett RJ. 2001. Functional characterization of phosphorilation of 69-kDa human choline acetyltransferase at serine 440 by protein kinase C. *J Biol Chem 276*: 22244-22250.

Dubrovsky BO. 2005. Steroids, neuroactive steroids and neurosteroids in psychopathology. *Prog Neuropsychopharmacol Biol Psychiatry 29*:169-192.

Eckenstein F, Thoenen H. 1982. Production of specific antisera and monoclonal antibodies to choline acetyltransferase: Characterization and use for identification of cholinergic neurons. *EMBO J 1*:363-368.

Erickson JD, Varoqui H, Schäfer MKH, Modi W, Diebler MF, Weihe E, Rand J, Eiden LE, Bonner TI, Usdin TB. 1994. Functional identification of a vesicular acetylcholine transporter and its expression from a "cholinergic" gene locus. *J Biol Chem 269*:21929-21932.

Ferguson SM, Savchenko V, Apparsundaram S, Zwick M, Wright J, Heilman CJ, Yi H, Levey AI, Blakely RD. 2003. Vesicular localization and activity-dependent trafficking of presynaptic choline transporters. *J Neurosci 23*:9697-9709.

Ferguson SM, Blakely RD. 2004. The choline transporter resurfaces: new roles for synaptic vesicles? *Mol Interv 4*:22-37.

Fernandes CF, Godoy JR, Döring B, Cavalcanti MCO, Bergmann M, Petzinger E, Geyer J. 2007. The novel putative bile acid transporter SLC10A5 is highly expressed in liver and kidney *Biochem Biophys Res Commun 361*:26-32.

Ferreira LT, Santos MS, Kolmakova NG, Koenen J, Barbosa J, Jr., Gomez MV, Guatimosim C, Zhang X, Parsons SM, Prado VF, Prado MA. 2005. Structural requirements for steady-state localization of the vesicular acetylcholine transporter. *J Neurochem 94*:957-969.

Friesema ECH, Docter R, Moerings EPCM, Stieger B, Hagenbuch B, Meier PJ, Krenning EP, Hennemann G, Visser TJ. 1998. Identification of thyroid hormone transporters. *Biochem Biophys Res Commun 254*:497-501.

Gall JG, Pardue ML. 1969. Formation and detection of RNA-DNA hybrid molecules in cytological preparations. *Proc Natl Acad Sci USA 2*: 378-383.

Gardiner-Garden M, Fromer M. 1987. CpG islands in vertebrate genomes. *J Mol Biol 196*:261-282.

Gates J, Jr., Ferguson SM, Blakely RD, Apparsundaram S. 2004. Regulation of choline transporter surface expression and phosphorylation by protein kinase C and protein phosphatase 1/2A. *J Pharmacol Exp Ther 310*:536-545.

Gether U, Andersen PH, Larsson OM, Schousboe A. 2006. Neurotransmitter transporters: molecular function of important drug targets. *Trends Pharmacol Sci 27*:375-383.

Geyer J. 2004. Ouabaintransporter in Leber und Nebenniere von Ratte und Rind: Klonierung, Gewebeexpression, Substratcharakterisierung und funktionelle Bedeutung ISBN 3-89687-456-X

Geyer J, Godoy JR, Petzinger E. 2004. Identification of a sodium-dependent organic anion transporter from rat adrenal gland. *Biochem Biophys Res Commun 316*:300-306.

Geyer J, Wilke T, Petzinger E. 2006. The solute carrier family SLC10: more than a family of bile acid transporters regarding function and phylogenetic relationships. *Naunyn Schmiedeberg's Arch Pharmacol 372*:413-431.

Geyer J, Döring B, Meerkamp K, Ugele B, Bakhiya N, Fernandes CF, Godoy JR, Glatt H, Petzinger E. 2007. Cloning and functional characterization of human sodium-dependent organic anion transporter (SLC10A6). *J Biol Chem 282*: 19728-19741.

Gilmor ML, Nash NR, Roghani A, Edwards RH, Yi H, Hersch SM, Levey AI. 1996. Expression of the putative vesicular acetylcholine transporter in rat brain and localization in cholinergic synaptic vesicles. *J Neurosci 16*:2179-2190.

Godoy JR, Fernandes C, Döring B, Beuerlein K, Petzinger E, Geyer J. 2007. Molecular and phylogenetic characterization of a novel putative membrane transporter (SLC10A7), conserved in vertebrates and bacteria. *Eur J Cell Biol 86*:445-460.

Green RM, Ananthanarayanan M, Suchy FJ, Beier DR. 1998. Genetic mapping of the Na^+-taurocholate cotransporting polypeptide to mouse chromosome 12. *Mamm Genome* 9:598.

Haga T. 1971. Synthesis and release of (14C)acetylcholine in synaptosomes. *J Neurochem 18*:781-798.

Hagenbuch B, Lubbert H, Stieger B, Meier PJ. 1990. Expression of the hepatocyte Na^+/bile acid cotransporter in *Xenopus laevis* oocytes. *J Biol Chem 265*:5357-5360.

Hagenbuch B, Stieger B, Foguet M, Lubbert H, Meier PJ. 1991. Functional expression cloning and characterization of the hepatocyte Na^+/bile acid cotransport system. *Proc Natl Acad Sci U S A 88*:10629-10633.

Hagenbuch B, Meier PJ. 1994. Molecular cloning, chromosomal localization, and functional characterization of a human liver Na+/bile acid cotransporter. *J Clin Invest 93*: 1326-1331.

Hagenbuch B, Scharschmidt BF, Meier PJ. 1996. Effect of antisense oligonucleotides on the expression of hepatocellular bile acid and organic anion uptake systems in *Xenopus laevis* oocytes. *Biochem J 316*:901-904.

Hagenbuch B, Meier PJ. 1996. Sinusoidal (basolateral) bile salt uptake systems of hepatocytes. *Sem Liver Dis 16*: 129-136.

Hagenbuch B, Dawson P. 2004. The sodium bile salt cotransport family SLC10. *Pflügers Arch 447*:566-570.

Hagenbuch B. 2007. Cellular entry of thyroid hormones by organic anion transporting polypeptides. *Best Pract Res Clin Endocrinol Metab 21*:209-221.

Hediger MA.1994. Structure, function and evolution of solute transporters in prokaryotes and eukaryotes. *J exp Biol 196*:15-49.

Hediger MA, Romero MF, Peng JB, Rolfs A, Takanaga H, Bruford EA. 2004. The ABCs of solute carriers: physiological, pathological and therapeutic implications of human membrane transport proteinsIntroduction. *Pflügers Arch 447*:465-468.

Higaki J, Hara S, Takasu N, Tonda K, Miyata K, Shike T, Nagata K, Mizui T. 1998. Inhibition of ileal Na^+/bile acid cotransporter by S-821 reduces serum cholesterol and prevents atherosclerosis in rabbits. *Aterioscler Thromb Vasc Biol 18*:1304-1311.

Hussainzada N, Banerjee A, Swaan PW. 2006. Transmembrane domain VII of the human apical sodium-dependent bile acid transporter ASBT (SLC10A2) lines the substrate translocation pathway. *Mol Pharmacol. 70*:1565-1574.

Ichihashi T, Izawa M, Miyata K, Mizui T, Hirano K, Takagishi Y. 1998. Mechanism of hypocholesterolemic action of S-8921 in rats: S-8921 inhibits ileal bile acid absorption. *J Pharmacol Exp Ther 284*:43-50.

John HL, Birnstiel ML, Jones KW. 1969. RNA-DNA hybrids at the cytological level. *Nature 223*:582-7.

Jørgensen JR, Juliusson B, Henriksen KF, Hansen C, Knudsen S, Petersen TN, Blom N, Seiger A, Wahlberg LU. 2006. Identification of novel genes regulated in the developing human ventral mesencephalon. *Exp Neurol 198*:427-437.

Kanai Y, Hediger MA. 2003. The glutamate and neutral amino acid transporter family: physiological and pharmacological implications. *Eur J Pharmacol 479*:237-247.

Kim JY, Kim KH, Lee JA, Namkung W, Sun AQ, Ananthanarayanan M, Suchy FJ, Shin DM, Muallem S, Lee MG. 2002. Transporter-mediated bile acid uptake causes Ca^{2+} -dependent cell death in rat pancreatic acinar cells. Gastroenterology 122:1941-1953.

Kramer W, Wess G, Schubert G, Bickel M, Hoffmann A, Baringhaus K-H, Ehnsen A, Glombik H, Müllner S, Neckermann G, Schulz S, Petzinger E. 1992. Liver-specific drug targeting by coupling to bile acids. *J Biol Chem 267*:18598-18604.

Kramer W, Wess G. 1996. Bile acid transport system as pharmaceutical targets. *Eur J Clin Invest 26*:715-732

Kramer W, Wess G, Bewersdorf U, Corsiero D, Girbig F, Weyland C, Stengelin S, Enhsen A, Bock K, Kleine H, Le Dreau MA, Schafer HL. 1997. Topological photoaffinity labeling of the rabbit ileal Na^+/bile-salt-cotransport system. *Eur J Biochem 249*:456-464.

Kramer W, Stengelin S, Baringhaus KH, Enhsen A, Heuer H, Becker W, Corsiero D, Girbig F, Noll R, Weyland C. 1999. Substrate specificity of the ileal and the hepatic Na(+)/bile acid cotransporters of the rabbit. I. Transport studies with membrane vesicles and cell lines expressing the cloned transporters. *J. Lipid Res 40*:1604-1617.

Kramer W, Girbig F, Glombik H, Corsiero D, Stengelin S, Weyland C. 2001a. Identification of a ligand-binding site in the Na+/bile acid cotransporting protein from rabbit ileum. *J Biol Chem 276*:36020-36027.

Kramer W, Sauber K, Baringhaus KH, Kurz M, Stengelin S, Lange G, Corsiero D, Girbig F, Konig W, Weyland C. 2001b. Identification of the bile acid-binding site of the ileal lipid-binding protein by photoaffinity labeling, matrix-assisted laser desorption ionization-mass spectrometry, and NMR structure. *J Biol Chem 276*:7291-7301.

Knniper M, Kahle C, Breer H. 1992. Regulation of hemicholinium binding sites in isolated nerve terminals. *J Neurobiol 23*:163-172.

König J, Cui Y, Nies AT, Keppler D. 2000. A novel human organic anion transporting polypeptide localized to the basolateral hepatocyte membrane. *Am J Physiol 278*:G156-G164.

König J, Cui Y, Nies AT, Keppler D. 2000. Localization and genomic organization of a new hepatocellular organic anion transporting polypeptide. *J Biol Chem 275*:23161-23168.

Kupfermann I. 1991. Functional studies of cotransmission. *Physiol Rev 71*:683-732.

Kus L, Borys E, Ping CY, Ferguson SM, Blakely RD, Emborg ME, Kordower JH, Levey AI, Mufson EJ. 2003. Distribution of high affinity choline transporter immunoreactivity in the primate central nervous system. *J Comp Neurol 463*:341-357.

Kullak-Ublick GA, Glasa J, Boker C, Oswald M, Grutzner U, Hagenbuch B, Stieger B, Meier PJ, Beuers U, Kramer W, Wess G, Paumgartner G. 1997. Chlorambucil-taurocholate is transported by bile acid carriers expressed in human hepatocellular carcinomas. *Gastroenterology 113*:1295-1305.

Kullak-Ublick GA, Stieger B, Meier PJ. 2004. Enterohepatic bile salt transporters in normal physiology and liver disease. *Gastroenterology 126*:322-342.

Lazaridis KN, Tietz P, Wu T, Kip S, Dawson PA, LaRusso NF. 2000. Alternative splicing of the rat sodium/bile acid transporter changes its cellular localization and transport properties. *Proc Natl Acad Sci USA 97*:11092-11097.

Lein ES, Hawrylycz MJ et. al. 2007. Genome-wide atlas of gene expression in the adult mouse brain. *Nature 445*:168-176.

Levey AI, Armstrong DM, Atweh SF, Terry RD, Wainer BH. 1983a. Monoclonal antibodies to choline acetyltransferase: production, specificity, and immunohistochemistry. *J Neurosci 3*:1-9.

Levey AI, Weiner BH, Mufson EJ, Mesulam M-M. 1983b. Co-localization of acetylcholinesterase and choline acetyltransferase in the rat cerebrum. *Neuroscience 9*:9-22.

Li H, Xu G, Shang Q, Pan L, Shefer S, Batta AK, Bollineni J, Tint GS, Keller BT, Salen G. 2004. Inhibition of ileal bile acid transport lowers plasma cholesterol levels by inactivating hepatic farnesoid X receptor and stimulating cholesterol 7 alpha-hydroxylase. *Metabolism 53*:927-932.

Liu Y, Edwards RH.1997. Differential localization of vesicular acetylcholine and monoamine transporters in PC12 cells but not CHO cells. *J Cell Biol 139*: 907-916.

Lowry OH, Rosebrough N J, Farr AL, Randall RJ. 1951. Protein measurement with the folin phenol reagent. *J Biol Chem 193*:265-275.

Mareninova O, Shin JM, Vagin O, Turdikulova S, Hallen S, Sachs G. 2005 Topography of the membrane domain of the liver Na+-dependent bile acid transporter. *Biochemistry 44*:13702-13712.

Martinez-Murillo R, Villalba R, Montero-Caballero MI, Rodrigo J. 1989. Cholinergic somata and terminals in the rat substantia nigra: an immunocytochemical study with optical and electron microscopic techniques. *J Comp Neurol 281*:397-415.

Masson J, Sagne C, Hamon M, El Mestikawy S. 1999. Neurotransmitter transporters in the central nervous system. *Pharmacol Rev 51*:439-464.

Meier PJ, Stieger B. 2002. Bile salt transporters. *Annu Rev Physiol 64*:635-661.

Mellon SH, Griffin LD. 2002. Neurosteroids: biochemistry and clinical significance. *Trends Endocrinol Metab 13*:35-43.

Misawa H, Nakata K, Matsuura J, Nagao M, Okuda T, Haga T. 2001. Distribution of the high-affinity choline transporter in the central nervous system of the rat. *Neuroscience 105*:87-98.

Montosi G, Donovan A, Totaro A, Garuti C, Pignatti E, Cassanelli S, Trenor CC, Gasparini P, Andrews NC, Pietrangelo A. 2001. Autosomal-dominant hemochromatosis is associated with a mutation in the ferroportin (SLC11A3) gene. *J Clin Invest 108*:619–623.

Nakata K, Okuda T, Misawa H. 2004. Ultrastructural localization of high-affinity choline transporter in the rat neuromuscular junction: enrichment on synaptic vesicles. *Synapse 53*:53-56.

Oda Y, Nakanishi I, Deguchi T. 1992. A complementary DNA for human choline acetyltransferase induces two forms of enzyme with different molecular weights in cultured cells. *Brain Res Mol Brain Res 16*:287-294.

Oelkers P, Kirby LC, Heubi JE, Dawson PA. 1997. Primary Bile Acid Malabsorption Caused by Mutations in the Ileal Sodium-dependent Bile Acid Transporter Gene (*SLC10A2a*). *J Clin Invest 99*:1880.

Oh JD, Woolf NJ, Roghani A, Edwards RH, Butcher LL. 1991. Cholinergic neurons in the rat central nervous system demonstrated by *in situ* hybridization of choline acetyltransferase mRNA. *Neuroscience 47*: 807-822.

Okuda T, Haga T, Kanai Y, Endou H, Ishihara T, Katsura I. 2000. Identification and characterization of the high-affinity choline transporter. *Nat Neurosci 3*:120-125.

Okuda T, Haga T. 2000. Functional characterization of the human high-affinity choline transporter. *FEBS Lett 484*:92-97.

Paxinos G, Watson C. 2004. The rat brain in stereotaxic coordinates, fifth edition. San Diego, London: Elsevier Academic Press.

Petzinger E, Nickau L, Horz JA, Schulz S, Wess G, Ehnsen A, Falk E, Baringhaus K-H, Glombik H, Hoffmann A, Müllner S, Neckermann G, Kramer W. 1995. Hepatobiliary transport of hepatic 3-hydroxy-3-methylglutaryl coenzyme A reductase inhibitors conjugated with bile acids. *Hepatology 22*:1801-1811.

Petzinger E, Wickboldt A, Pagels P, Starke D, Kramer W. 1999. Hepatobiliary transport of bile acid, bile acid peptide, and bile acid oligo nucleotide conjugates in rats. *Hepatology 30*: 1257-1268.

Prado VF, Martins-Silva C, de Castro BM, Lima RF, Barros DM, Amaral E, Ramsey AJ, Sotnikova TD, Ramirez MR, Kim HG, Rossato JI, Koenen J, Quan H, Cota VR, Moraes MFD, Gomez MV, Guatimosim C, Wetsel WC, Kushmerick C, Pereira GS, Gainetdinov RR, Izquierdo I, Caron MG, Prado MAM. 2006. Mice deficient for the vesicular acethylcholine transporter are myasthenic and have deficits in object and social recognition. *Neuron 51*: 601-612.

Ribeiro JA, Cunha RA, Correia-de-Sá P, Sebastião AM.1996. Purinergic regulation of acetylcholine release. *Prog Brain Res 109*:231-241

Ribeiro FM, Alves-Silva J, Volknandt W, Martins-Silva C, Mahmud H, Wilhelm A, Gomez MV, Rylett RJ, Ferguson SS, Prado VF, Prado MA. 2003. The hemicholinium-3 sensitive high affinity choline transporter is internalized by clathrin-mediated endocytosis and is present in endosomes and synaptic vesicles. *J Neurochem 87*:136-146.

Ribeiro FM, Black SA, Cregan SP, Prado VF, Prado MA, Rylett RJ, Ferguson SS. 2005. Constitutive high-affinity choline transporter endocytosis is determined by a carboxyl-terminal tail dileucine motif. *J Neurochem 94*:86-96.

Ribeiro FM, Black SA, Prado VF, Rylett RJ, Ferguson SS, Prado MA. 2006. The "ins" and "outs" of the high-affinity choline transporter CHT1. *J Neurochem 97*:1-12.

Rius M, Nies AT, Hummel-Eisenbeiss J, Jedlitschky G, Keppler D. 2003. Cotransport of reduced glutathione with bile salts by MRP4 (ABCC4) localized to the basolateral hepatocyte membrane. *Hepatology 38*:374-384.

Root C, Smith CD, Winegar DA, Brieaddy LE, Lewis MC. 1995. Inhibition of ileal sodium-dependent bile acid transport by 2164U90. *J Lipid Res 36*:1106-1115.

Rupprecht R, Holsboer F. 1999. Neuroactive steroids: mechanisms of action and neuropsychopharmacological perspectives. *Trends Neurosci 22*:410-416.

Ryan RL, McClure WO. 1979. Purification of choline acetyltransferase from rat and cow brain. *Biochemistry 18*: 5357-5365.

Saeki T, Matoba K, Furukawa H, Kirifuji K, Kanamoto R, Iwami K. 1999. Characterization, cDNA cloning, and functional expression of mouse ileal sodium-dependent bile acid transporter. *J Biochem (Tokyo) 125*:846-851.

Sarter M, Parikh V. 2005. Choline transporters, cholinergic transmission and cognition. *Nat Rev Neurosci 6*:48-56.

Seward DJ, Koh AS, Boyer JL, Ballatori N. 2003. Functional complementation between a novel mammalian polygenic transport complex and an evolutionarily ancient organic solute transporter, OSTalpha-OSTbeta. *J Biol Chem 278*:27473-27482

Schäfer MKH, Eiden LE, Weihe E. 1998a. Cholinergic neurons and terminal fields revealed by immunohistochemistry for the vesicular acetylcholine transporter. I.Central nervous system. *Neuroscience 84*:331-359.

Schäfer MKH, Eiden LE, Weihe E. 1998b. Cholinergic neurons and terminal fields revealed by immunohistochemistry for the vesicular acetylcholine transporter. II. The peripheral nervous system. *Neuroscience 84*:361-376.

Schroeder A, Eckhardt U, Stieger B, Tynes R, Schteingart CD, Hofmann AF, Meier PJ, Hagenbuch B. 1998. Substrate specificity of the rat liver Na(+)-bile salt cotransporter in Xenopus laevis oocytes and in CHO cells. *Am J Physiol 274*: G370-G375.

Schumacher M, Akwa Y, Guennoun R, Robert F, Labombarda F, Desarnaud F, Robel P, De Nicola AF, Baulieu EE. 2000. Steroid synthesis and metabolism in the nervous system: trophic and protective effects. *J Neurocytol 29*:307-326.

Shneider BL, Dawson PA, Christie DM, Hardikar W, Wong MH, Suchy FJ. 1995. Cloning and molecular characterization of the ontogeny of a rat ileal sodium-dependent bile acid transporter. *J Clin Invest 95*:745-754.

Simon DB, Nelson-Williams C, Bia MJ, Ellison D, Karet FE, Molina AM, Vaara I, Iwata F, Cushner HM, Koolen M *et al.*. 1996a. Gitelman's variant of Bartter's syndrome, inherited hypokalaemic alkalosis, is caused by mutations in the thiazide-sensitive Na-Cl cotransporter. *Nat Genet 12*:24–30.

Simon DB, Karet FE, Hamdan JM, DiPietro A, Sanjad SA, Lifton RP 1996b. Bartter's syndrome hypokalaemic alkalosis with hypercalciuria is caused by mutations in the Na-K-2Cl cotransporter NKCC2. *Nat. Genet. 13*:183–188.

Soroka CJ, Lee JM, Azzaroli F, Boyer JL. 2001. Cellular localization and up-regulation of multidrug resistance-associated protein 3 in hepatocytes and cholangiocytes during obstructive cholestasis in rat liver. *Hepatology 33*:783-791.

Splinter PL, Lazaridis KN, Dawson PA, LaRusso NF. 2006. Cloning and expression of SLC10A4, a putative organic anion transport protein. *World J Gastroenterol 12*:6797-6805.

Stengelin S, Apel S, Becker W, Maier M, Rosenberger J, Bewesdorf U, Girbig F, Weyland C, Wess G, Kramer W. 1996. The rabbit ileal lipid-binding protein. Gene cloning and functional expression of the recombinant protein. *Eur J Biochem 239*:887-896.

Stieger B, Hagenbuch B, Landmann L, Hochli M, Schroeder A, Meier PJ. 1994. In situ localization of the hepatocytic Na^+/taurocholate cotransporting polypeptide in rat liver. *Gastroenterology 107*:1781-1787.

Trauner M, Boyer JL. 2003. Bile salt transporters: molecular characterization, function, and regulation. *Physiol Rev 83*:633-671.

Tremont SJ, Lee LF, Huang HC, Keller BT, Banerjee SC, Both SR, Carpenter AJ, Wang CC, Garland DJ, Huang W, Jones C, Koeller KJ, Kolodziej SA, Li J, Manning RE, Mahoney MW, Miller RE, Mischke DA, Rath NP, Fletcher T, Reinhard EJ, Tollefson MB, Vernier WF, Wagner GM, Rapp SR, Beaudry J, Glenn K, Regina K, Schuh JR, Smith ME, Trivedi JS, Reitz DB. 2005. Discovery of potent, nonsystemic apical sodium-codependent bile acid transporter inhibitors (Part1). *J Med Chem 48*:5837-5852.

Varoqui H, Diebler MF, Meunier FM, Rand JB, Usdin TB, Bonner TI, Eiden IE, Erickson JD. 1994. Cloning and expression of the vesamicol binding protein from the marine ray Torpedo. Homology with the putative vesicular acetylcholine transporter UNC-17 from Caenorhabditis elegans. *FEBS Lett 342*:97-102.

Varoqui H, Erickson JD. 1996. Active transport of acetylcholine by the human vesicular acetylcholine transporter. *J Biol Chem 271*:27229-32.

Vlahcevic ZR, Pandak WM, Stravitz RT. 1999. Regulation of bile acid biosynthesis. *Gastroenterol Clin North Am 28*:1-25.

Wang W, Seward DJ, Li L, Boyer JL, Ballatori N. 2001. Expression cloning of two genes that together mediate organic solute and steroid transport in the liver of a marine vertebrate. *Proc Natl Acad Sci USA 98*:9431-9436.

Weinman SA. 1997. Electrogenicity of Na^+-coupled bile acid transporters. *Yale J Biol Med 70*:331-340.

Weinman SA, Carrut MW, Dawson PA. 1998. Bile acid uptake via the human apical sodium-bile acid cotransporter is electrogenic. *JBiol Chem 273*:34691-34695.

Weihe E, Tao-Cheng JH, Schafer MK, Erickson JD, Eiden LE. 1996. Visualization of the vesicular acetylcholine transporter in cholinergic nerve terminals and its targeting to a specific population of small synaptic vesicles. *Proc Natl Acad Sci U S A 93*:3547-3552.

West KL, Ramjiganesh T, Roy S, Keller BT, Fernandez ML. 2002. 1-[4-[4-[(4R, 5R)-3,3-Dibutyl-7-(dimethylamino)-2,3,4,5-tetrahydro-4-hydroxy-1,1-dioxido-1-benzothiepin-5-yl]penoxy]butyl]-4-aza-1-azoniabicyclo[2.2.2]octane methanesulfonate(SC-435), an ileal apical sodium-

codependent bile acid transporter inhibitor alters hepatic cholesterol metabolism and lowers plasma low-density lipoprotein-cholesterol concentrationsin guinea pigs. *J Pharmacol Exp Ther 303*:293-299.

Willard AL.1990. A vasoactive intestinal peptide-like cotransmitter at cholinergic synapses between rat myenteric neurons in cell culture. *J Neurosci 10*:1025-1034.

Wolf OT, Kirschbaum C. 1999. Actions of dehydroepiandrosterone and its sulfate in the central nervous system: effects on cognition and emotion in animals and humans. *Brain Res Brain Res Rev 30*:264-288.

Wong MH, Oelkers P, Craddock AL, Dawson PA. 1994. Expression cloning and characterization of the hamster ileal sodium-dependent bile acid transporter. *J Biol Chem 269*:1340-1347.

Wong MH, Oelkers P, Dawson PA. 1995. Identification of a mutation in the ileal sodium-dependent bile acid transporter gene that abolishes transport activity. *J Biol Chem 270*:27228-27234.

Xie J, Guo Q. 2004. Par-4 inhibits choline uptake by interacting with CHT1 and reducing its incorporation on the plasma membrane. *J Biol Chem 279*:28266-28275.

Yang Chou J, Mansfield BC. 1999. Molecular genetics of type 1 glycogen storage diseases. *Trends Endocr Metab 10*:104-113

9 Annex

9.1 SLC10A5 Sequences

Human SLC10A5

```
LOCUS       AY825924               1317 bp    mRNA    linear   PRI 06-DEC-2004
DEFINITION  Homo sapiens SLC10A5 (SLC10A5) mRNA, complete cds.
ACCESSION   AY825924
VERSION     AY825924.1  GI:56159720
KEYWORDS    .
SOURCE      Homo sapiens (human)
  ORGANISM  Homo sapiens
            Eukaryota; Metazoa; Chordata; Craniata; Vertebrata; Euteleostomi;
            Mammalia; Eutheria; Euarchontoglires; Primates; Haplorrhini;
            Catarrhini; Hominidae; Homo.
REFERENCE   1  (bases 1 to 1317)
  AUTHORS   Geyer,J., Fernandes,C. and Petzinger,E.
  TITLE     Direct Submission
  JOURNAL   Submitted (12-NOV-2004) Institute of Pharmacology and Toxicology,
            Justus-Liebig-University of Giessen, Frankfurter Str. 107, Giessen
            35392, Germany
FEATURES             Location/Qualifiers
     source          1..1317
                     /organism="Homo sapiens"
                     /mol_type="mRNA"
                     /db_xref="taxon:9606"
                     /chromosome="8"
                     /map="8q21"
                     /tissue_type="liver"
     gene            1..1317
                     /gene="SLC10A5"
     CDS             1..1317
                     /gene="SLC10A5"
                     /note="P5"
                     /codon_start=1
                     /product="SLC10A5"
                     /protein_id="AAV80707.1"
                     /db_xref="GI:56159721"
                     /translation="MIRKLFIVLLLLLVTIEEARMSSLSFLNIEKTEILFFTKTEETI
                     LVSSSYENKRPNSSHLFVKIEDPKILQMVNVAKKISSDATNFTINLVTDEEGETNVTI
                     QLWDSEGRQERLIEEIKNVKVKVLKQKDSLLQAPMHIDRNILMLILPLILLNKCAFGC
                     KIELQLFQTVWKRPLPVILGAVTQFFLMPFCGFLLSQIVALPEAQAFGVVMTCTCPGG
                     GGGYLFALLLDGDFTLAILMTCTSTLLALIMMPVNSYIYSRILGLSGTFHIPVSKIVS
                     TLLFILVPVSIGIVIKHRIPEKASFLERIIRPLSFILMFVGIYLTFTVGLVFLKTDNL
                     EVILLGLLVPALGLLFGYSFAKVCTLPLPVCKTVAIESGMLNSFLALAVIQLSFPQSK
                     ANLASVAPFTVAMCSGCEMLLIILVYKAKKRCIFFLQDKRKRNFLI"
ORIGIN
        1 atgattagaa aacttttat tgttctactt ttgttgcttg tgactataga agaagcaagg
       61 atgtcatcgc tcagttttct gaatatagag aagactgaaa tactattttt cacaaagact
      121 gaagaaacca tccttgtaag ttcaagctac gaaaataaac ggcctaattc cagccacctc
      181 tttgtgaaaa tagaagatcc taaaatacta caaatggtga atgtggccaa gaagatctca
      241 tcagatgcta caaactttac cataaatctg gtgactgatg aagaaggaga aacaaatgtg
      301 actattcaac tctgggattc tgaaggtagg caagaaagac tcattgaaga aatcaagaat
      361 gtgaaagtca aagtgctcaa acaaaaagac agtctactcc aggcaccaat gcatattgat
      421 agaaacatcc taatgcttat tttaccacta atactattga ataagtgtgc atttggttgt
      481 aagattgaat tacagctgtt tcaaacagta tggaagagac ctttgccagt aattcttggg
      541 gcagttacac agtttttct gatgccattt tgcgggtttc ttttgtctca gattgtggca
      601 ttgcctgagg cgcaagcttt tggagttgta atgacctgca cgtgcccagg agggggtggg
      661 ggctatctct ttgctctgct tctagatgga gatttcacat tggccatttt gatgacttgc
```

```
 721 acatcaacat tattggctct gatcatgatg cctgtcaatt cttatatata cagtaggata
 781 ttagggttgt caggtacatt ccatattcct gtttctaaaa ttgtgtcaac actccttttc
 841 atacttgtgc cagtatcaat tggaatagtc atcaagcata gaatacctga aaaagcaagc
 901 ttcttagaga gaataattag acctctgagt tttattttaa tgttcgtagg aatttatttg
 961 actttcacag tgggattagt gttcttaaaa acagataatc tagaggtgat tctgttgggt
1021 ctcttagttc ctgctttggg tttgctgttt gggtactcct ttgctaaagt ttgtacgctg
1081 cctcttcctg tttgtaaaac tgttgctatt gaaagtggga tgttaaatag tttcttagct
1141 cttgccgtta ttcagctgtc ttttccacag tccaaggcca atttagcttc tgtggctcct
1201 tttacagtag ccatgtgttc tggatgtgaa atgttactga tcattctagt ttacaaggct
1261 aagaaaagat gtatcttttt cttacaagat aaaaggaaaa gaaatttcct aatctaa
```

Mouse Slc10a5

```
LOCUS       AY825925                1305 bp    mRNA    linear   ROD 06-DEC-2004
DEFINITION  Mus musculus SLC10A5 (Slc10a5) mRNA, complete cds.
ACCESSION   AY825925
VERSION     AY825925.1  GI:56159722
KEYWORDS    .
SOURCE      Mus musculus (house mouse)
  ORGANISM  Mus musculus
            Eukaryota; Metazoa; Chordata; Craniata; Vertebrata; Euteleostomi;
            Mammalia; Eutheria; Euarchontoglires; Glires; Rodentia;
            Sciurognathi; Muroidea; Muridae; Murinae; Mus.
REFERENCE   1  (bases 1 to 1305)
  AUTHORS   Fernandes,C., Geyer,J. and Petzinger,E.
  TITLE     Direct Submission
  JOURNAL   Submitted (12-NOV-2004) Institute of Pharmacology and Toxicology,
            Justus-Liebig-University of Giessen, Frankfurter Str. 107, Giessen
            35392, Germany
FEATURES             Location/Qualifiers
     source          1..1305
                     /organism="Mus musculus"
                     /mol_type="mRNA"
                     /strain="C57BL/6J"
                     /db_xref="taxon:10090"
                     /chromosome="3"
                     /map="3A1"
                     /tissue_type="liver"
     gene            1..1305
                     /gene="Slc10a5"
     CDS             1..1305
                     /gene="Slc10a5"
                     /note="P5"
                     /codon_start=1
                     /product="SLC10A5"
                     /protein_id="AAV80708.1"
                     /db_xref="GI:56159723"
                     /translation="MSGNFFIFLLLLVTPGEAKKSFLSFLNIQNTEMLSFTRTEENIV
                     VRSSYKDKQPHSSYLLVKLEDPKVLQVVNVTKTSLAVTDFTVNLKTFPGETNVTLQLW
                     ESEGRQTTLIDELKNVRVRVFRQTDDSLLQAPIHVDSSIFLLVLSMILLNKCAFGCKI
                     EFQVLQTVWKRPLPILLGVVIQFFLMPFCGFLLSQILGLPKAQAFGFVMTCTCPGGGG
                     GYLFALLLEGDVTLAILMTCTSTSLALIMMPVNSYFYSRLLGLAGAFHVPVLKIVSTL
                     LFILMPMSTGVIIKHKMPAKAICLERVVRPLSLTLMFVGIYLAFRMGLVFLRMANLEV
                     FLLGLLVPALGLLFGYSLAKVYLLPLPVCKTVALETGMLNSFLALAIIQLSFSQPKAH
                     EASVAPFTVAMCSSCEMLLLLLVYKAKRRPSLSTEYEKTPLV"
```

```
ORIGIN
        1 atgtctggca attttttat atttctactt ttgttggtga ccccaggaga agcgaagaag
       61 tcatttctca gttttctgaa tatacaaaat acagaaatgc tgtcctttac aaggacggaa
      121 gaaaacatcg ttgtaaggtc cagctataaa gacaaacagc ctcactccag ctacctgctc
      181 gtgaagttag aggatcctaa agtgctgcag gtggtgaatg tgaccaagac ctccctggct
      241 gtcacagact ttaccgtcaa cctgaagact ttcccaggag agaccaatgt gaccctgcag
      301 ctctgggagt ctgaaggtag gcaaacaaca ctcatcgacg agctaaagaa tgtcagagtg
      361 agagtgttca gacagacgga cgacagcctc ctccaggcac caatccatgt cgatagctcc
      421 atcttcctgc ttgtcttatc gatgatcctt ttaaataaat gtgcctttgg ctgcaagatt
      481 gaattccagg tgcttcaaac agtgtggaag agacctttgc caatacttct tggggtggtt
      541 atacagtttt ttcttatgcc attctgtggc tttctcttgt ctcagatttt gggcttgcct
      601 aaggcacagg cttttggatt tgtaatgacc tgcacatgcc caggaggagg tgggggctat
      661 ctctttgctc tccttctgga aggggatgtc actttggcca ttttgatgac ttgcacatca
      721 acgtccctgg ccctcatcat gatgcctgtc aactcatact tttacagtcg gctactgggc
      781 ttagcaggtg catttcacgt ccctgtgtta aagattgtgt ctactcttct tttcatactt
      841 atgccaatgt cgactggtgt catcattaaa cacaagatgc ctgcgaaagc aatctgttta
      901 gagagagtag tgcggcctct gagcttgact ttaatgttcg tgggcatcta cttggctttc
      961 cggatgggac tagtgtttct gagaatggct aacctagagg tgtttctatt ggggcttctg
     1021 gttcctgcac tgggcctttt gtttggctat tccttggcta aagtctactt gctgcctctt
     1081 cctgtttgca agacggttgc tctcgaaact gggatgttga atagtttctt agctctggcc
     1141 atcattcagc tttccttttc ccagcccaag gcacacgaag cctccgtagc ccccttttaca
     1201 gtagccatgt gttccagctg tgaaatgtta ctgctccttc tggtctacaa ggctaagaga
     1261 aggccatccc ttagcacaga atatgaaaaa actcctctag tttaa
```

Rat Slc10a5

```
LOCUS       DQ074435               1305 bp    mRNA    linear   ROD 27-JUN-2005
DEFINITION  Rattus norvegicus SLC10A5 (Slc10a5) mRNA, complete cds.
ACCESSION   DQ074435
VERSION     DQ074435.1  GI:68131803
KEYWORDS    .
SOURCE      Rattus norvegicus (Norway rat)
  ORGANISM  Rattus norvegicus
            Eukaryota; Metazoa; Chordata; Craniata; Vertebrata; Euteleostomi;
            Mammalia; Eutheria; Euarchontoglires; Glires; Rodentia;
            Sciurognathi; Muroidea; Muridae; Murinae; Rattus.
REFERENCE   1  (bases 1 to 1305)
  AUTHORS   Fernandes,C., Geyer,J. and Petzinger,E.
  TITLE     Cloning of P5 from rat small intestine
  JOURNAL   Unpublished
REFERENCE   2  (bases 1 to 1305)
  AUTHORS   Fernandes,C., Geyer,J. and Petzinger,E.
  TITLE     Direct Submission
  JOURNAL   Submitted (25-MAY-2005) Justus-Liebig-University of Giessen,
            Institute of Pharmacology and Toxicology, Frankfurter Str. 107,
            Giessen 35392, Germany
FEATURES             Location/Qualifiers
     source          1..1305
                     /organism="Rattus norvegicus"
                     /mol_type="mRNA"
                     /strain="Wistar"
                     /db_xref="taxon:10116"
                     /chromosome="2"
                     /map="2q23"
                     /tissue_type="small intestine"
```

```
     gene            1..1305
                     /gene="Slc10a5"
     CDS             1..1305
                     /gene="Slc10a5"
                     /note="P5 protein"
                     /codon_start=1
                     /product="SLC10A5"
                     /protein_id="AAY85181.1"
                     /db_xref="GI:68131804"
                     /translation="MSGKLFIILLLLVTPGEARKSFLRFLNIQNPEMLSFTKPEETVI
                     VRSSYEGKRPHSSYLLVKLEDPTVLQVVNVTKTSLDFTDFTINLKTFPGETNLTMQLW
                     ESEGRQTRLIEEITNIRVSVFRQTEDSLFQEPIHVNSSVFLLVLLMILLNKCAFGCKI
                     ELQVLQTVWKRPLPILLGAVTQFFLMPFCGFLLSQILGLSKAQAFGFVMTCTCPGGGG
                     GYLFALLLEGDVTLAILMACTSTSLALIMMPVNSYLYSCLLGLAGVFHVPVLKIVSTL
                     LFILTPVSIGIVIKHRMPKKAVCLERVVQPLSLTLMLVGVYLAFRMGLVFLRMANLEV
                     FLLGLLVPVLGFSFGYSFAKVYLLPLPVCKTVAIESGMLNSFLALAIIQLSFPQSKAY
                     EASVAPFTVAMCSSCEMLLLLLVYKAKKRPLLSTENEKAPLV"
ORIGIN
        1 atgtctggaa aacttttcat aattctcctt ttgttggtga ccccgggaga agcaaggaag
       61 tcatttctca gatttctgaa tatacaaaat ccagaaatgc tgtcgtttac gaagccagaa
      121 gaaaccgtca ttgtaaggtc cagctatgaa ggtaagcggc ctcactccag ctacctgctt
      181 gtgaagttgg aggatcctac agtgctgcag gtggtgaatg tgaccaagac ctccctggac
      241 ttcacagact tcaccatcaa cctgaagacg ttcccaggag agacaaacct caccatgcag
      301 ctctgggagt ctgaaggtag gcaaacaaga ctcatcgaag agataaccaa tatcagagtg
      361 agcgtgttca gacagacaga ggacagtctc ttccaggaac caatccacgt caacagctcc
      421 gtcttcctgc ttgtcttatt gatgatcctt ttaaataaat gcgcctttgg ctgcaagatt
      481 gaattacagg tgctccaaac agtgtggaag agacctttgc caatacttct tggggcggtt
      541 acacagtttt ttcttatgcc gttctgtggc tttctcttgt ctcagatttt gggcttgtca
      601 aaggcacagg cttttggatt tgtaatgacc tgcacatgcc caggaggggg tgggggctat
      661 ctctttgctc tccttctaga aggggacgtc actttggcca ttttgatggc ttgcacgtca
      721 acgtccctgg ccctcatcat gatgcctgtc aactcgtact tatacagttg cctactcggg
      781 ttagcaggtg tatttcacgt tcctgtctta aagattgtgt ctactcttct tttcatactt
      841 acgccagtat ccatcggcat agtcattaag cacagaatgc ctaaaaaagc agtctgtcta
      901 gagagagtgg tgcagcctct gagtttgact ttaatgttgg tgggagtcta cttggctttc
      961 aggatgggac tggtgtttct gagaatggct aacctagagg tgtttctttt ggggcttctg
     1021 gttcccgtac tgggcttttc atttgggtat tcctttgcta aagtctacct gctgccgctt
     1081 cctgtttgca aaacagtcgc aatcgaaagt gggatgttga atagtttctt agccctggcc
     1141 attattcagc tttcttttcc acagtccaag gcatatgagg cctccgtggc tccttttaca
     1201 gtagcgatgt gttctagctg tgaaatgttg ctgctccttc tggtctacaa ggctaagaag
     1261 aggccactcc ttagcacaga aaatgaaaag gctcctctcg tttaa
```

9.2 Alignment

SLC10A4

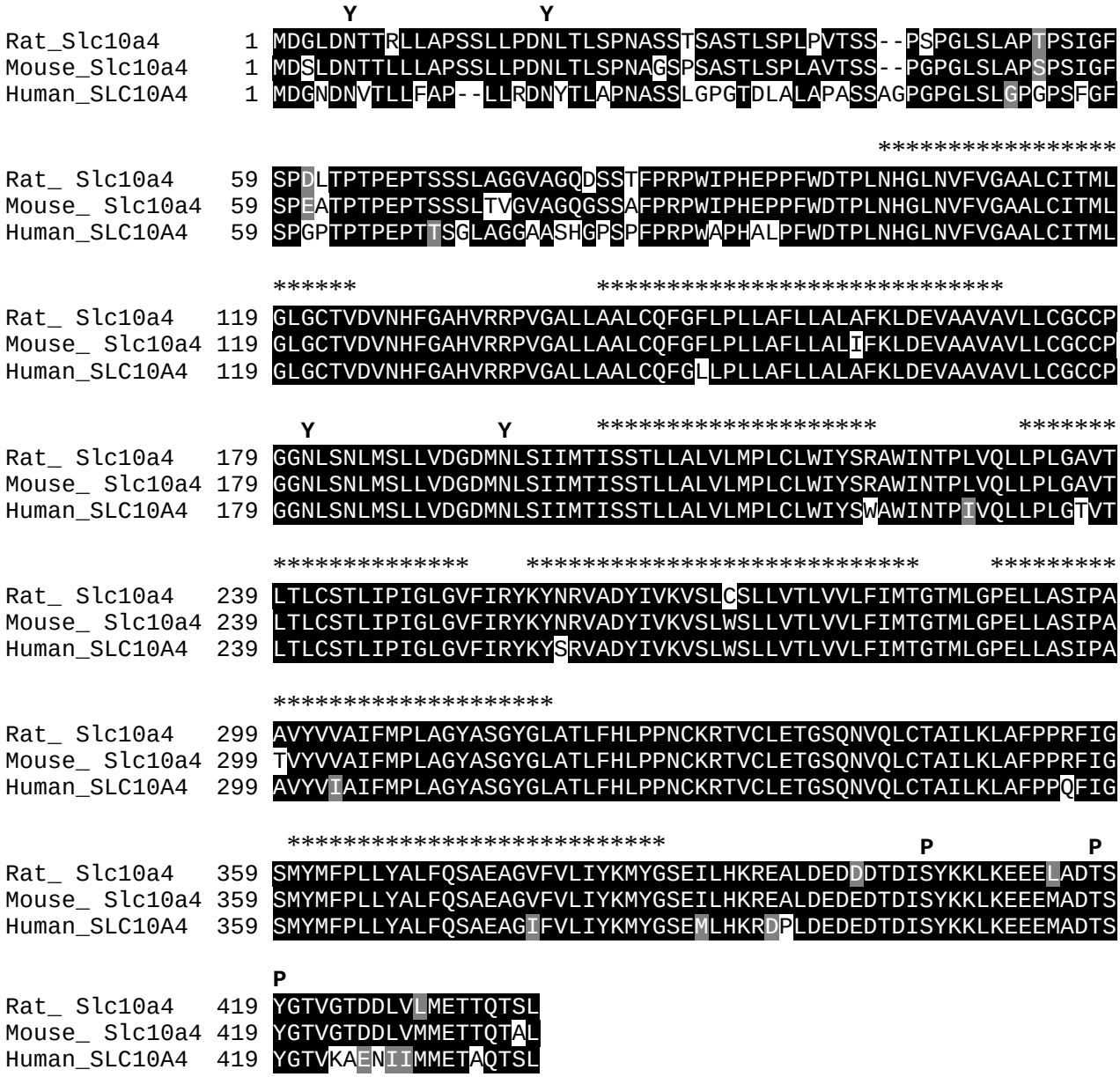

Amino acid sequence alignment of the human, rat, and mouse SLC10A4proteins. Multiple sequence alignment was conducted using the *ClustalW* algorithm and was visualized by BOXSHADE 3.21. Amino acid sequence identity is displayed with black shading; amino acid similarities are highlighted in grey. Gaps (-) are introduced to optimize alignment. Tansmembrane regions of SLC10A4 are indicated by asterisks (*), conserved putative N-glycosylation sites were marked by Y, and the putative phosphorylation sites are indicated by P.

9.3 Transmembrane Topologies

Transmembrane regions of SLC10A4 and SLC10A5 suggested by six topology prediction programs.

Species	Program	N-terminal	TMD1	TMD2	TMD3	TMD4	TMD5	TMD6	TMD7	TMD8	C-terminal
Human SLC10A4	HMMTOP	out	104-126	137-161	166-190	201-224	231-254	265-289	298-322	357-381	out
	TMpred	out	104-124	137-161	165-185	198-218	231-256	268-288	292-313	350-370	out
	TMHMM	out	107-129	136-158	168-190	202-224	234-256	268-290	300-322		in
	MEMSAT	out	107-124	137-161	168-190	198-219	231-254	268-288		350-370	in
	TMAP		102-124	142-170		202-222	232-252	257-284	290-318	360-386	
	PRED-TMR2		107-124	140-161		206-224	234-254	270-288	302-322	360-381	
Rat Slc10a4	HMMTOP	in	105-124	137-161	168-190	197-220	231-254	265-289	296-319	357-381	in
	TMpred	out	104-124	137-161	165-185	198-220	231-256	268-288	292-313	356-382	out
	TMHMM	in	105-127	137-159	166-188	198-220	232-254	264-286	293-315	360-382	in
	MEMSAT	out	107-124	137-161	168-190	198-219	231-254	268-288	298-322	360-382	out
	TMAP		102-124	142-170		197-225	227-255	257-284	290-318	360-386	
	PRED-TMR2		107-124	140-161		198-218	234-254	270-289	302-322	360-381	
Mouse Slc10a4	HMMTOP	in	105-124	137-161	168-190	197-220	231-254	265-289	296-319	356-380	in
	TMpred	out	104-124	137-161	165-185	198-220	231-256	268-288	292-313	356-382	out
	TMHMM	in	105-124	139-161	166-188	198-220	232-254	269-288	300-322	360-382	in
	MEMSAT	out	107-124	137-161	168-190	198-219	231-254	268-288	300-324	360-382	out
	TMAP		102-124	142-170		197-225	227-255	257-284	293-321	360-386	
	PRED-TMR2		107-124	140-161		198-218	234-254	270-288	302-322	360-381	

Species	Program	N-term.	SP	TMD1	TMD2	TMD3	TMD4	TMD5	TMD6	TMD7	TMD8	TMD9	C-term.
Human SLC10A5	HMMTOP	out		143-160	177-200	209-228	235-257	274-291	308-327	336-355	368-386	395-418	in
	TOPPRED	out		142-162	176-196	208-228	232-252	272-292	309-329	335-355	369-389	398-418	in
	TMpred	in	1-20	142-158	175-194	198-223	237-257	271-291	311-327	336-355	369-389	398-418	in
Rat Slc10a5	HMMTOP	out		141-158	175-194	207-226	243-265	272-289	306-325	334-353	370-387	396-415	in
	TOPPRED	out		134-154	174-194	204-224	230-250	270-290	303-323	333-353	367-387	396-414	in
	TMpred	in	1-19	135-156	175-194	202-223	235-255	269-289	309-325	334-353	367-387	396-416	in
Mouse Slc10a5	HMMTOP	out		139-158	175-194	207-226	233-252	267-289	306-325	334-353	370-387	396-415	in
	TOPPRED	out		138-158	174-194	204-224	230-250	269-289	307-327	333-353	367-387	396-416	in
	TMpred	in	1-18	139-158	175-194	204-220	235-255	269-287	309-326	334-350	367-387	397-415	in

SP: cleavage site predicted by SignalP 3.0 Server; TMD: transmembrane domain

9.4 SLC Transporters and Related Diseases

SLC Family	Protein name	Substrate	Transport type/ coupling ions	Link to disease	Tissue expression
SLC1A1	EAAC1/ EAAT3	L-Glu, D/L-Asp	C/ Na^+, H^+ and K^+	Dicarboxylic amino aciduria in knockout mice[G]	Brain (neurons), intestine, kidney, liver, heart
SLC1A2	GLT-1 /EAAT2	L-Glu, D/L-Asp	C/ Na^+, H^+ and K^+	Amyotrophic lateral sclerosis[A]	Brain (astrocytes), liver
SLC2A1	GLUT1	Glucose, Galactose, Mannose, glucosamine	F	developmental delay, acquired microcephaly, hypotonia	Erythrocytes, brain, blood brain barrier, Blood-tissue barrier
SLC2A2	GLUT2	Glucose, Galactose, Fructose, Mannose, glucosamine	F	Fanconi-Bickel syndrome	Liver, islet of Langerhans, intestine, kidney, brain
SLC3A1	rBAT	Heterodimerizes with light subunit $b^{0,+}$AT (SLC7A9): amino acid transport system $b^{0,+}$	E (see SLC7)	Classic Cystinuria type I[G]	Epithelial cells in kidney and small intestine, liver, pancreas, and brain. In epithelial cells of intestinal mucosa, and renal proximal tubule - apical plasma membrane
SLC4A1	AE1	Chloride Bicarbonate	E	Hemolytic anemia, distal renal tubular acidosis [G]	Erythrocytes, intercalated cells of renal collecting duct, heart and colon
SLC4A4	NBCe1	Sodium Bicarbonate (and/or Carbonate)	C	Severe proximal renal tubular acidosis, ocular abnormalities, short stature [G]	NBCe1-A: renal proximal tubule, eye NBCe1-B: widely distributed, pancreas, heart, eye. NBCe1-C: brain
SLC4A7	NBCn1	Sodium Bicarbonate	C	Blindness, Auditory Impairment [G]	Widely distributed: spleen, testes, brain, heart, lung, river.
SLC5A1	SGLT1	Glucose and Galactose (Urea and Water)	C/ Na^+ (H^+) F/ Na^+ (H^+) Channel Urea and Water	Glucose-glactose Malabsorption (GGM)[G]	Small Intestine, trachea, kidney and heart (Plasma membranes).
SLC5A2	SGLT2	Glucose	C/ Na^+	Renal Glucosuria[G]	Kidney cortex
SLC5A3	SMIT	Myoinositol (glucose)	C/ Na^+	Down's syndrome?	Brain, heart, kidney and lung (Plasma membranes).
SLC5A5	NIS	I^- (ClO_4^-, SCN^-, NO_3^-, Br^-	C/Na^+ / Uniporter Na^+ Channel Urea water	Hypothyroidism[G]	Thyroid, breast, colon and ovary (Plasma membranes).

SLC Family	Protein name	Substrate	Transport type/ coupling ions	Link to disease	Tissue expression
SLC6A1	GAT1	GABA	C/Na^+,Cl^-	epilepsy, schizophrenia	GABAergic neurons in central and peripheral nervous system, some non-neural tissues.
SLC6A2	NET	norepinephrine, dopamine	C/Na^+,Cl^-	depression, orthostatic intolerance, anorexia nervosa, cardiovascular diseases	central and peripheral nervous system, adrenal gland, placenta
SLC6A3	DAT	dopamine	C/Na^+,Cl^-	parkinsonism, Tourette syndrome, substance abuse, Attention deficit hyperactivity disorder (ADHD)	brain (dopaminergic neurons)
SLC6A4	SERT	serotonin	C/Na^+,Cl^-,K^+	anxiety, depression, autism, substance abuse, gastrointestinal disorders	central and peripheral nervous system, epithelial cells, platelets
SLC6A6	TAUT	taurine	C/Na^+,Cl^-	taurine deficiency diseases, retinal blindness, abnormal renal development	brain, retina, liver, kidney, heart, spleen, pancreas
SLC6A8	CT1	creatine	C/Na^+,Cl^-	X-linked creatine deficiency syndrome, mental retardation, musculo-skeletal disorders, cardio-myopathy	ubiquitous
SLC6A11	GAT3	GABA	C/Na^+,Cl^-	epilepsy	brain (GABAergic neurons, glia)
SLC6A19	B^0AT1	neutral amino acids	C/Na+	Hartnup disorder	intestine and renal proximal tubule. apical membrane
SLC7A7	y^+LAT1	Na^+ indep.: cationic amino acids; Na^+ depen.: large neutral L-amino acids (system y^+L)	E (preferen-tially intra-cellular cationic amino acid against extracellular neutral amino acid + Na^+)	Lysinuric protein intolerance (LPI)[G]:	small intestine, kidney, leucocytes, placenta, lung/ basolateral in epithelial cells
SLC7A9	$b^{0,+}$AT	cationic amino acids, large neutral amino acids (system $b^{0,+}$-like)	E (preferen-tially extra-cellular cationic amino acid against intracellular neutral amino acid)	Type B cystinuria (non-type I or type I phenotype)[G]	small intestine, kidney, lung, placenta, brain, liver/ apical in epithelial cells
SLC9A1	NHE1	Na^+, H^+, Li^+, NH_4^+	E: Na^+ / H^+ (1:1)	Ischemia / reperfusion injuries[A]; Essential hypertension[A];Diabetes-associated vascular hypertrophy[A]	Ubiquitous (plasma membrane; basolateral surface of epithelia)
SLC9A3	NHE3	Na^+, H^+, Li^+, NH_4^+	E: Na^+ / H^+ (1:1)	Congenital secretory diarrhea[G]	Intestinal tract, stomach. kidney, gall bladder, epididymis, brain; (apical surface and recycling endosomes of epithelia)

SLC Family	Protein name	Substrate	Transport type/ coupling ions	Link to disease	Tissue expression
SLC10A2	ASBT	Bile acids	C / Na^+	Primary Bile Acid Malabsorption (PBAM)[G]	Ileum, kidney, biliary tract
SLC11A1	NRAMP1	Mn^{2+}, Fe^{2+}, and other divalent metal ions	C / H^+	Polymorphisms linked to susceptibility[G] to bacterial infections (e.g. tuberculosis, leprosy), and to autoimmune diseases (e.g. Crohn's disease)	Phagolysosomes of phagocytes (macrophages, neutrophils)
SLC11A2	DMT1	Fe^{2+}, Cd^{2+}, Co^{2+}, Cu^{1+}, Mn^{2+}	C / H^+	Hereditary hemochromatosis[A]	Widespread, including intestine, erythroid cells, kidney, lung, brain, testis (Sertoli cells), thymus
SLC12A1	NKCC2	Sodium, Potassium, Chloride	C / Na^+/K^+/2Cl^-	Bartter syndrome type I[G]:	Kidney-specific (apical membrane of the thick ascending limb)
SLC12A3	NCC	Sodium, Chloride	C / Na^+/Cl^-	Gitelman's syndrome[G]	Kidney-specific (apical membrane of the distal convoluted tubule)
SLC12A6	KCC3	Potassium, Chloride	C / K^+/Cl^-	Peripheral neuropaty[G]	Widespread
SLC14A1	UT-B1(43)	Urea	F / -	Kidd antigen blood group[G]	- Kidney (vasa recta, papillary epithelia) - Erythrocytes, testes, brain, spleen
SLC14A2	UT-A1 (97, 117)	Urea	F / -	Orthostatic hypotension[G] (candidate gene)	- Kidney (luminal membrane of inner medullary collecting duct, IMCD)
SLC16A1	MCT1	Lactate, pyruvate, ketone bodies	C / H^+ or E / monocarboxylate	Muscle weakness (exercise intolerance)[G]	Ubiquitous
SLC17A5	sialin	Sialic acid	C/ H^+	Sialic acid storage disease (Salla disease)[G]	Heart, brain, liver, lung, pancreas, placenta, muscle, uterus, bladder, kidney, spleen.
SLC18A2	VMAT1	5HT Dopamine Adrenaline Noradrenaline Histamine	E / H^+	Cardio-vascular, Drug Addiction	Brain (neurons), adrenal gland (medulla), sympathetic ganglia (neurons, SIF cells), carotid body, small and large intestine (neurons), stomach (neurons and ECL-cells), endocrine pancreas, basophils, mast cells, dendritic cells and platelets Subcellular: large dense-core vesicles, smallll dense-core vesicles, tuberovesicular structures and small synaptic (dopaminergic) vesicles.
SLC18A3	VAChT	Acetylcholine	E / H^+	Myasthenic syndromes (ChAT only)[G]	Brain (neurons), peripheral nervous system (neurons), intestine (neurons) Subcellular: small synaptic vesicles
SLC19A1	RFT	N^5-methyltetrahydrofolate	E / OH^-	Methotrexate resistance	Ubiquitous / PM /MM

SLC Family	Protein name	Substrate	Transport type/ coupling ions	Link to disease	Tissue expression
SLC19A2	ThTr1	Thiamine	E / H^+	Thiamine-responsive megaloblastic anemia[G]	Ubiquitous / Plasma membrane
SLC19A3	ThTr2	Thiamine	E / H^+	Seizure susceptibility[G]?	Ubiquitous / Plasma membrane
SLC22A5	hOCTN2	L-carnitine, organic cations, polyspecific	C/Na^+ and L-carnitine, F (for organic cations)	Primary systemic carnitine deficiency[G]	Skeletal muscle, kidney (luminal membrane of proximal tubules), prostate, lung, pancreas, heart, small intestine, adrenal gland, thyroid gland, liver etc.
SLC22A8	hOAT3	Organic anions, polyspecific	E/organic anions	Osteosclerosis/osteopetrosis in mice[G]	Kidney, basolateral membrane of proximal tubules; brain, luminal membrane of choroid plexus; skeletal muscle, developing bone
SLC22A12	hURAT1	Urate	E/organic anions	Idiopathic renal hypo-uricaemia[G]	Kidney
SLC22A1L		not determined (transport of chloroquine- and quinidine-related compounds?)		Beckwith-Wiedemann syndro-me, Wilms tumor, rhabdomyo-sarcoma, adrenocortical carcinoma, and lung, ovarian, and breast cancer[G]	tumor suppressing gene
SLC25A4	AAC1	ADP, ATP	E/ ADP/ATP	Autosomal dominant progressive external ophtalmoplegia (AdPEO)[G], Senger syndrome	heart, skeletal muscle, much less in brain, pancreas, prostate, kidney, lung, thymus / inner mitochondrial membrane
SLC25A8	UCP2	H^+	F	obesity, type 2 diabetes	brain, lung, kidney, spleen, heart / inner mitochondrial membrane
SLC25A9	UCP3	H^+	F	obesity ?	skeletal muscle, lung / inner mitochondrial membrane
SLC25A13	AGC2	aspartate, glutamate	E / aspartate /glutamate + H^+	Citrullinemia type II (CTLN2)[G]	liver, kidney, pancreas, heart, skeletal muscle, brain / inner mitochondrial membrane
SLC25A15	ORC1	ornithine, citrulline, lysine, arginine	E / ornithine / citrulline + H^+;ornithine / H^+	HHH syndrome (Hyperornithinemia, Hyperammonemia, Homocitrullinuria)	liver, pancreas, lung, testis, small intestine, spleen, kidney, brain, heart / inner mitochondrial membrane
SLC25A19	DNC	dNDPs, dNTPs, NDPs, ATP, ddNTPs	E / dNDPs / ATP	Amish microcephaly (MCPHA)[G]	brain, testis, lung, kidney, liver, spleen, skeletal muscle, heart / inner mitochondrial membrane
SLC25A20	CAC	carnitine, acylcarnitines	E / carnitine /acylcarnitines F (at slow rate)	CACT deficiency[G] (carnitine/acylcarnitine carrier)	heart, skeletal muscle, liver (also in lung, kidney, brain, pancreas, lung, placenta) / inner mitochondrial membrane
SLC26A2	DTDST	SO_4^{2-}, Cl^-	E	Chondrodysplasias[G]	Widespread

SLC Family	Protein name	Substrate	Transport type/ coupling ions	Link to disease	Tissue expression
SLC26A3	DRA, CLD	SO_4^{2-}, Cl^-, HCO_3^-, OH^-, oxalate	E	Congenital Chloride-losing Diarrhea[G]	intestine, sweat gland, pancreas, prostate
SLC26A4	pendrin	Cl^-, HCO_3^-, I^-, formate	E	Pendred syndrome[G] Hereditary Deafness (DFNB4)[G]	inner ear, kidney, thyroid
SLC26A5	prestin	?	E	Deafness?	inner ear, brain, heart, spleen, and testis
SLC30A1	ZNT1	Zinc	Unknown	Embryonic lethal in mice	Widespread in rodents
SLC30A3	ZNT3	Zinc	Unknown	Seizures, Alzheimers in mice	Glutamatergic neurons
SLC30A4	ZNT4	Zinc	Unknown	Lethal milk (zinc-deficient milk) in mice	Widespread in rodents Secretory glands
SLC30A5	ZNT5	Zinc	Unknown	Bone abnormalities-osteopenia; heart failure in mice	Widespread; b cells
SLC34A1	NaPi-lla	inorganic phosphate	C / $Na/HPO_4^{=-}$	X-linked hypophosphatemia[G] Autosomal dominant hypophosphatemic rickets[G] Oncogenic hypophosphatemic osteomalacia[A]	kidney (proximal tubules; apical)osteoclasts, neurons
SLC35C1	GDP-Fuc transporte r	GDP-fucose	E/GMP	Leukocyte adhesion deficiency type II [G]/ Congenital disorder of glycosylation IIc [G]	Ubiquitous /Golgi
SLC37A4	SPX4	Glucose-6-phosphate	E/Inorganic phosphate	Glycogen storage disease non-1a (GSD)	Strongly expressed in liver, kidney and hematopoietic progenitor cells
SLC39A4	ZIP5	Zinc	Unknown	acrodermatitis enteropathica	Small intestine, stomach, colon, cecum, kidney / plasma membrane
SLC40A1	IREG1	Ferrous iron	Facilitated?	Type 4 haemochromato-sis	Basolateral membrane in duodenum, spleen red pulp macrophages plasma membrane, liver kupffer cells, Placenta, kidney
SLC42A1	RhAG (Rh50A)	NH_4^+	H^+	Rh_{null}-regulator	Red blood cells, (cell membrane)

Modified from Bioparadigms[TM] (www.bioparadigms.org), originally prepared by the authors of the SLC mini-review series published in *Pflügers Arch – Eur J Physiol (2004) 447:465-812*. A: Acquired defect; C: Co-transporter; E: Exchanger; F: Facilitated transporter; G: Genetic defect; MM: Mithochondrial Membrane; O: Orphan transporter; PM: Plasma Membrane.

Acknowledgements

The present work was performed at the Institute of Pharmacology and Toxicology of the Justus-Liebig University of Giessen during the years 2004-2007.

I want to thank Prof. Dr. Ernst Petzinger for the privilege given me to work at the Institute of Pharmacology and Toxicology and also for his professional guidance and supervision throughout this project. The overwhelming encouragement and support I received from him is gratefully acknowledged. Herr Petzinger danke für alles!!!

Thanks to Prof. Dr. Dr. Joseph Krieglstein for accepting to be my second supervisor and first referee as well as for his invaluable suggestions and significant contributions throughout this project.

I am also very grateful to the members of the examination committee Prof. Dr. Udo Bakowsky and Prof. Dr. Ulrich Matern.

I would like to express my gratitude and appreciation to my supervisor Dr. Joachim Geyer for his guidance and helpful suggestions throughout this study. Thanks for the critical observations, corrections and painstakingly reading through this thesis. I learnt a lot from him during my stay in Germany. Achim, I wish you all the best!

My sincere appreciation also goes to Dr. Jörg Alber who always found time to discuss many issues concerning the technicalities of my work and also to speak Portuguese with me. Special thanks go out to Dr. José Godoy for co-operation, criticism, encouragement and numerous discussions during my dissertation work. I found it very accommodating working with you.

Due acknowledgement also goes to Prof. Dr. Rüdiger Gerstberger and his team at the Institute of Veterinary Physiology of the Justus-Liebig University of Giessen for providing me the opportunity to work in his Laboratory. Special thanks to Dr. Thomas Hübschle, Dr. Sandra Rafalzik, and Doreen Marks for very good assistance and suggestions I received during development this work.

I also want to thank Barbara Döring who assisted me immensely in so many aspects of my work. Thanks also to my colleagues and friends Marcela Moncada, Kathrin Marschner, Olga Gavrilova, Kerstin Meerkamp, Stefanie Klintzsch, Garry Grosser, Simone Burger, Talah Kanbar, Emre Karakus, Hivda Mohyla, and Ebtisam Essid. It was indeed a great opportunity and pleasure working with you all.

I must acknowledge the assistance I received from Regina Leidolf, Klaus Schuh, Kurt Stumpf, Anita Neubauer, and Christoph Zimmermann. Thanks also to Birgit Kaus and Annelise Lotz.

I am also grateful to Dorothee von Schnakenburg, Dr. Knut Beuerlein, Dr. Daniel Zahner, Dr. Lauy Al-Anati, Prof. Dr. Christoph Lämmler, and Prof. Dr. Kornelia Ziegler.

A minha amiga Marcia Cavalcanti, mulher corajosa e determinada, agradeço pela força, otimismo e companheirismo durante estes anos, bem como pelas idéias e longas discussões...

Em especial quero agradecer aos meus amigos Cinthia Elim, Guilherme e Julian Lepski, Sabrina Pancera, Luiraima Salazar, André Messias, Roberto Portz, Eder Santos, Marcelo Bertazzo e Ester Serrano pela amizade, carinho e pelos bons momentos que passamos juntos na Alemanha.

Minha estimada amiga Gabi, Gilvan e Maria Júlia, agradeço por todas as maravilhosas risadas compartilhadas durante nossos fins de semana (hora em Frankfurt, hora em Giessen), bem como pelo total apoio e pela confiança depositada em minha pessoa.

Aos amigos Márcio Bruno, Geórgia, minha afilhada Tayná e Bruninho agradeço pela amizade e carinho, bem como por todo apoio durante nossos “pit stops” em Brasília.

A Mona Lisa e ao Danubio Andrade, amigos de todas as horas, ou melhor, irmãos, agradeço pela amizade, carinho, dedicação, compreensão e principalmente pela força no final desta etapa de vida. A vocês desejo muito sucesso e muitos filhos...

Aos meus queridos “avós” Sr. Raimundo e D. Antonia e a família de Freitas Fernandes agradeço pelo carinho e acolhimento de minha pessoa em vossa casa.

A minha família Freire Celedonio agradeço pelo apoio, confiança, amor e carinho demonstrados a minha pessoa. Vovós obrigada pela força e pelo carinho de vocês; tia Lila, minha segunda mãe, obrigada pelo amor e confiança depositados em minha pessoa; meus pais, obrigada pelo equilíbrio, segurança, simplicidade e pela imensa força que vocês sempre nos passaram; Carliza, minha irmã querida, agradeço por todo amor e dedicação e, principalmente, pela paciência em resolver todos os nossos pepinos enquanto eu estive fora de casa... e ao meu irmão e cunhada (Júnior e Paula), como também aos queridos sobrinhos (Carlos Neto, Ariane e Júlia), agradeço pela alegria, pelos momentos de descontração, e pela disposição de vocês. Aos meus tios e primos agradeço pelo apoio e por todos os bons momentos que passamos juntos. Principalmente ao tio Nanal pois sempre com excelente humor me levava e trazia todos os dias da faculdade.

E por último, eu não poderia deixar de agradecer o meu querido esposo Cléberson Fernandes pela correção desta tese e por todas as sugestões durante o desenvolvimento deste trabalho. Agradeço ainda por todos os momentos maravilhosos que compartilhamos juntos aqui na Europa, em Fortaleza ou em Porto Velho, como também por todo amor, carinho, atenção, paciência, apoio, companheirismo e dedicação. Muitas vezes estando longe, sempre esteve ao meu lado proporcionando a minha pessoa uma paz indescritível. Eu te amo!

This study was supported by the Brazilian-German CAPES/DAAD exchange program.

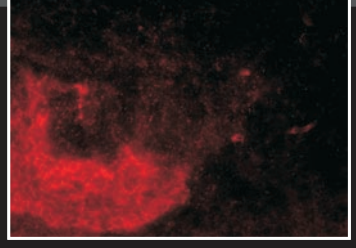
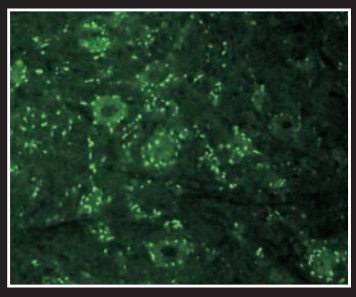

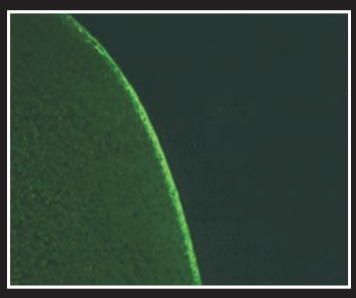
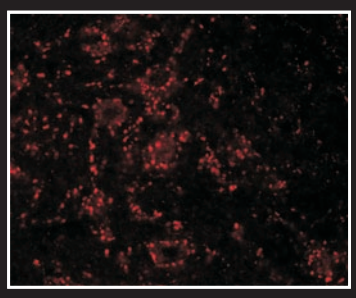
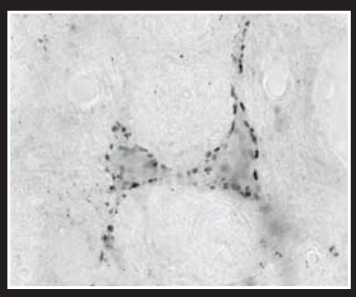
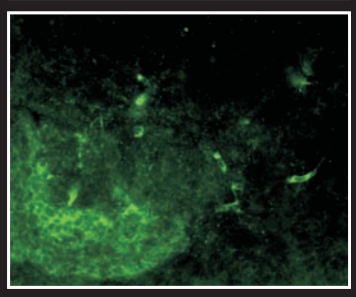
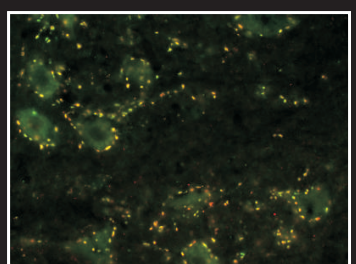

édition scientifique
VVB LAUFERSWEILER VERLAG

VVB LAUFERSWEILER VERLAG
ST AU FEN BER GRING 15
D-35396 GIESSEN

Tel: 0641-5599888 Fax: -5599890
redaktion@doktorverlag.de
www.doktorverlag.de

ISBN 3-8359-5230-7
9 783835 952300